MEASUREMENT OF SHIP RESISTANCE COEFFICIENT FROM SIMPLE TRIALS DURING A REGULAR VOYAGE

by

Gengshen Liu

B.S. Harbin Shipbuilding Engineering Institute
(1967)

M.S.(in NA & ME) Massachusetts Institute of Technology
(1984)

O.E. Massachusetts Institute of Technology
(1984)

M.S.(in OSM) Massachusetts Institute of Technology
(1985)

SUBMITTED IN PARTIAL FULFILLMENT
OF THE REQUIREMENTS FOR THE
DEGREE OF

DOCTOR OF SCIENCE

at the

MASSACHUSETTS INSTITUTE OF TECHNOLOGY
May 1988

Signature of Author _____
Department of Ocean Engineering
May 1988

Certified by _____
Martin A. Abkowitz, Thesis Supervisor

Accepted by _____
Chairman, Department Committee
on Graduate Students

MEASUREMENT OF SHIP RESISTANCE COEFFICIENT FROM SIMPLE TRIALS DURING A REGULAR VOYAGE

by

Gengshen Liu

Submitted to the Department of Ocean Engineering in
May 1988 in partial fulfillment of the requirement
for the degree of Doctor of Science

Abstract

The measurement of ship resistance is an important element in naval architecture and marine hydrodynamics research. The prediction of ship resistance from scaled model tests has been used for over a hundred years but the results suffer from "scale effect". The currently used sea trial method which is conducted before a ship is put into service is very costly and also suffers from the "scale effect" because it uses the wake fraction, thrust deduction factor and propeller thrust curves obtained from scaled model tests.

This thesis presents a new method of "measuring" the ship resistance of full size ships by applying identification technique to the mathematical model of ship surge motion. This method requires only a simple sea trial during a ship's regular voyage. Moreover, all the instruments needed for the data collection are already onboard except for a PC based data collector. A sea trial was conducted on the tanker EXXON PHILADELPHIA during a journey between Valdez, Alaska and San Francisco along the West Coast. By applying the extended Kalman filtering (EKF) technique to the data collected on this trip, and through the algorithms developed in this thesis to derive the resistance coefficient of the ship, not only was the ship resistance coefficient itself obtained with good accuracy, but also the wake fraction and the thrust deduction factor. The success of this method will not only benefit both the design of ship hulls and propellers but also the marine hydrodynamics research, especially at high Reynolds number. The recursive least-square technique and the recursive instrumental variable technique were also studied as alternative identification tools beside the EKF technique.

Thesis Supervisor: Dr. Martin A. Abkowitz
Title: Professor of Ocean Engineering

Acknowledgement

I wish to express my heartfelt gratitude to Professor Martin A. Abkowitz for his supervision and encouragement. Without his deep insight, rich experience and careful guidance, this work would not have been possible. His kindness, patience and friendship I shall always cherish.

My gratitude is also due the other thesis comittee members, Professors J. Kim Vandiver, Arthur B. Baggeroer and Michael S. Triantafyllou for their valuable suggestions and encouragement.

Appreciation is expressed to Professor Lennart Ljung of Linköping University of Sweden and to Dr. André Merab for many valuable discussions.

Special thanks go to Mr. David A. Bennett, staff engineer from Sperry Marine, to Mr. Bruce Easom from Exxon Shipping Company, to Captain Mitchell S. Stoller and the crew of EXXON PHILADELPHIA. Their enthusiastic attitude and hard work made the journey between Valdez, Alaska and San Francisco a very pleasant and fruitful one.

Thanks go to Dr. Tom Kosmeyer for his assistance in calculating the added-mass of the tanker EXXON PHILADELPHIA.

I also wish to extend my love and gratitude to my family and friends for their concern, understanding and support which have made my graduate life so much easier.

This research has been sponsored by the U.S. Maritime Administration. Support from the Exxon Shipping Company and the Sperry Coporation made the data measurement possible.

Contents

List of Figures

List of Tables

Chapter 1

Introduction

It is well known that reducing the resistance of ships and making their propulsion systems work efficiently has been one of the most important goals for naval architects. Choosing among the complicated body forms of ships and finding a good match between ship body and propulsion system is a major task during the design stage. However, because of the complexity of the geometric forms of ships and the complexity of the hydrodynamic forces existing between ships and the fluid they are moving in, it is still far beyond the ability of naval architects to meet these two goals with great success. In order to reduce the resistance forces, the measurement of the ship resistance and the exploration of their mechanics have been two topics of interest to scientists and engineers for more than a *century*. Although convincing explanations of the reasons behind the resistance for bodies moving in fluids have been provided from research results, and formulae

for the approximate calculation of the resistance forces on a simply formed body surface have been obtained, the complexity of the form of the bodies of ships still makes it very difficult to apply these theoretical formulae directly to the calculation of the resistance of ships. Even today, when high speed computer systems are routinely used in solving very difficult problems, the lack of a comprehensive theory has hindered the development of a numerical method. The resistance forces on ships are still predicted through conducting model tests in cooperation with sea trials rather than by numerical methods.

1.1 History of Ship Resistance Measurement

It has not been practical to measure the ship resistance directly. The conventional idea of measuring the resistance of a ship when she moves at a certain speed is to measure the towing force or propulsive force(exclusion of interference effects) which keeps her moving at that speed. Clearly, it is impossible to carry out this kind of measurement on large ships, not to mention supertankers with *hundreds of thousands* of *dead-weight tons*. Even for small ships, the towing method is not a choice since the mechanical system for the experiment is far too sophisticated (considering avoidance of towing ship wake). Besides, the equipment investment is expensive and the accuracy of the measurement results cannot be guaranteed. Another method of directly measuring ship resistance is to propel the ship by

means of aircraft jet engines mounted on deck and to measure the thrust of the engines (Lucy Ashton trials). These trials were very costly and time-consuming, and the results were of questionable accuracy, even though the ship was less than 200 *feet* long.

The use of smaller scaled models of ships to do the experiment is attractive. However, from dimensional analysis we know that the resistance acting on a body moving in a fluid is a function of three non-dimensional parameters:

$$R = f\left(\frac{UL}{\nu}, \frac{U}{\sqrt{gL}}, \frac{p-p_v}{\rho U^2}\right)$$

where R is the *resistance* or the *dragforce*, U is the velocity of the moving body relative to the fluid, L is the linear dimension of the moving body, ν is the *kinematic viscosity coefficient* of the fluid, g is the *gravitational acceleration*, ρ is the *density* of the fluid, p is the *pressure* in the fluid and p_v is the *vapor pressure*.

We call $\frac{UL}{\nu}$ the *Reynolds number*, $\frac{U}{\sqrt{gL}}$ the *Froude number*, and $\frac{p-p_v}{\rho U^2}$ is equivalent to a number called the *cavitation number*. (If we do not consider the free surface, R is only function of Reynolds number and cavitation number. That is the case for submersibles.) To maintain these parameters for both the ship model and the full scale ship is rarely possible. Although the idea of ship model tests originated with Leonardo da Vinci, it only became practical after the British naval architect William Froude first proposed the method of extending the model result to real ships, based on the

"Law of Comparison" stated by him in 1868.

Froude's idea is that besides the air resistance experienced by the above-water part of the main hull and the superstructure due to the motion of the ship through the air, the total resistance force on a ship moving in the water consists of three parts:

1. The *frictional resistance* due to the motion of the hull through the water which is a viscous fluid.

2. The *wave-making resistance* due to the lost of energy of the ship to the wave system created on the surface of the water.

3. The *eddy resistance* due to the energy carried away by eddies shed from the hull and appendages.

Froude took the latter two items together under the name "residuary resistance" and he mentioned in the "Law of Comparison": "The (residuary) resistance of geometrically similar ships is in the ratio of the cube of their linear dimensions, if their speeds are in the ratio of the square roots of their linear dimensions." That is, the residuary resistance is assumed independent of Reynolds number which we know is not the case. Based on this law, the method of extending the model results to the ship is as follows:

1. Once a real ship or its design has been chosen, its model is made to a

linear scale ratio of $\lambda\left(\lambda = \frac{L_s}{L_m}\right)$, and ran over a range of "corresponding speeds" such that

$$\frac{U_s}{\sqrt{L_s}} = \frac{U_m}{\sqrt{L_m}},$$

where L_m is the overall length of the model, L_s is the overall length of the real ship, U_m is the speed of the model and U_s is the speed of the real ship.

2. The *total model resistance* R_{tm} is measured in the towing tank.

3. The *model frictional resistance* R_{fm} is calculated assuming the resistance to be the same as that of a smooth flat plank of the same length and surface as the model.

4. The *model residuary resistance* R_{rm} is found by subtraction:

$$R_{rm} = R_{tm} - R_{fm}$$

5. The *ship residuary resistance* R_{rs} is calculated by the law of comparison:

$$R_{rs} = R_{rm} \times \lambda^3 \times \frac{\rho_s}{\rho_m}$$

where ρ_m is density of the fluid for model test, ρ_s is the density of the fluid the real ship sails in.

This applies to the ship at the corresponding speed given by the expression:

$$U_s = U_m\sqrt{\lambda}$$

6. The *ship frictional resistance* R_{fs} is calculated under the same assumption as in Step 3 by using the frictional coefficient for the ship length and speed. However, there is no reliable data on the resistance of a flat plank at high Reynolds number, hence this step always brings in errors.

7. The *total ship resistance* R_{ts} is then given by

$$R_{ts} = R_{fs} + R_{rs}$$

This method of extrapolation from model to ship has been used ever since William Froude set up the first model experimental tank at Torquay in 1870.

Although the Froude hypothesis is very helpful in reducing the scale effect on the estimation of the resistance coefficient, the big difference in Reynolds number between the model and the full scale ship still causes obvious errors. Furthermore, the model test method can only be used for the newly-designed or newly-constructed ships. Once the ships are put into service, it cannot be used for the prediction of the change of the condition of the ship hull and the propeller system due to fouling, corrosion or addition of appendages or hull alterations. Moreover, keeping the information about ship resistance coefficient during service is also of great importance. Since the available knowledge will help in judging the situation of the ship hull

and the propeller system and thereby help to determine the best time to put the ship into dry dock.

Efforts to minimize the "scale effect" over many years have resulted in the method currently used for estimating the resistance of the ship which consists of a combination of tests on both a model and on the full scale ship. The principle is to use the model test results to get the resistance curve of the ship through extrapolation and to acquire the *wake fraction* w and the *thrust deduction factor* t. Based on these results the sea trials of the full scale ship are conducted to measure the resistance of the ship by means of measuring the ship speed and the thrust. However, sea trials on the full scale ships in these procedures are very costly in equipment, personnel and time, since the ship has to be taken out of service and special instrumentation and qualified personnel have to be placed onboard. Moreover, sea conditions sometimes cause costly delays. Furthermore, the results are usually not satisfactory, because recording thrustmeters are not installed on most merchant ships, and consequently the resistance must be estimated from the power. Even for ships fitted with recording thrustmeters, the noisy measurements cause inaccuracies in measuring the *thrust force* T. The resistance force

$$R = (1 - t)T$$

depends on the thrust deduction factor t which is assumed to be the same as that of the model value. That assumption is incorrect. It has been

shown that the thrust deduction factor t also suffers from "scale effect" and so does the wake fraction w and the thrust coefficients of the propeller.

1.2 System Identification Method

As an alternative to the traditional methods, the method of applying system identification technique, which has been developed at MIT, has shown great potential in estimating the resistance coefficient of ships from relatively simple sea trials. The system identification method is based on a mathematical model of ship motion. Theoretically, with a mathematical model of the ship's surge motion at hand, measuring the *surge speed* u and the *propeller rotating rate* n, and using them as inputs into the mathematical model with a proper identification technique, satisfactory identified values of the resistance coefficient of the ship can be obtained. The success of the application of the *extended Kalman filter*(EKF) technique of system identification in the measurement of the main linear and nonlinear hydrodynamic coefficients in the maneuvering of the supertanker ESSO OSAKA, stimulated the research in this area at MIT. Using the tanker EXXON SAN FRANCISCO as the research object, simulated data of the surge speed u corresponding to the propeller rotating rate n for both the deceleration operation with a wind-milling propeller and the acceleration operation were used in the mathematical model. The results were very encouraging indicating good probability of successful identification of the

resistance from a ship trial. In May of 1987, real sea trials were carried out on the 75,000 *deadweight ton* tanker EXXON PHILADELPHIA which is a sister ship of the tanker EXXON SAN FRANCISCO, on a routine sailing between Valdez, Alaska and San Francisco. During the *five-day* voyage, a two hour period of calm weather was chosen. The sea trials took about 40 *minutes* with the ship generally headed in the desired direction of the voyage, the remainder of the time was used to conduct maneuvering trials which are not included as part of this thesis. Measurements were made of the ship's surge speed u, propeller rotating rate n, ship's heading angle ψ and the rudder angle δ. The surge speed u and propeller rotating rate n are to be used as inputs, the heading angle ψ and rudder angle δ are monitored to ensure that a straight course is maintained with negligible rudder action. Two kinds of planned sea trials were conducted: one in which the ship decelerated with a wind-milling propeller, while the other has the ship accelerating from *zero* speed to cruising(equilibrium) speed. The procedure for the sea trial is as follows:

- Maintain the ship in equilibrium state, while keeping straight course.
- Slow down the ship by cutting the power to the propeller, allowing the propeller to wind-mill.
- After the ship slows to half speed, reverse the propeller to bring the ship to a stop.

- After remaining at stop for a few minutes, speed up the ship by calling for cruising *rps* on the propeller to be obtained as quickly as possible.
- Maintain cruising speed long enough for collecting data. (several *minutes*)

The collected data u and n were used as inputs to identify the *ship resistance coefficient* C_R. The identified resistance coefficient is obtained with good accuracy(probably within 1%). In addition, the *full scale wake fraction* w_s and the *full scale thrust deduction factor* t_s were also determined from the identification procedure.

All the instruments required in the sea trials are standard instruments onboard except for a personal computer used as a digital data collector. The ship's routine voyage was little affected, only one extra person was needed, and in the future the data collection can be performed by a trained crew member, therefore keeping the expense low.

The success of the identification technique provides a new and very powerful method to get more accurate and reliable power prediction methods for ships during the design stage, accurate and timely description of the state of the resistance of the ships in service and accurate hydrodynamic data at extrmely large Reynolds number for use in boundary layer research. This constitutes the first time in the field of ship hydrodynamics that the resistance of a ship has been effectively measured through relatively simple and inexpensive sea trials with good accuracy. This is also the first

time that the wake fraction w and the thrust deduction factor t have been "measured" on a ship.

The identification method cannot completely replace model testing, not only because model test results constitute a reference for system identification, but also because when the ship is in the design stage, only model tests can be used to get the hydrodynamic coefficients in spite of the scale effects. However, the more accurate identified results from ship measurements can help improve the method now in use to extrapolate the model test results to full scale ships and to provide accurate wake fraction to improve propeller design with regard to efficiency, noise and cavitation.

In this thesis, a method of using system identification technique to estimate the resistance coefficient and the application of this method to the identification of the resistance coefficient of the EXXON PHILADELPHIA is presented.

In Chapter 2, the system equation is set up by applying hydrodynamic theory to ships and their propellers.

In Chapter 3, the design of the sea trials is determined both from the point of view of hydrodynamics and from the point of view of the theory of identification. The aims of the design of the sea trials are: getting "the most informative data" for the purpose of identification, collecting less noisy data, simplifying the sea trials and keeping the overall costs low. The instruments to be used onboard and their hook-up via a personal computer to form a data collecting system are also discussed. The procedure

for collecting data is briefly described and samples of measured data are presented.

Five hydrodynamic coefficients are involved in the surge equation: $-X_{\dot{u}}$ (the *added-mass of the ship corresponding to surge acceleration*), η_1, η_2, η_3(the *propeller thrust coefficients*) and C_R (the ship resistance coefficient). It is not possible to get all of them directly by identification. To get the resistance coefficient C_R, it is necessary to work several more steps after getting the results from the identification process.

In Chapter 4, it is shown how the added-mass coefficient $-X_{\dot{u}}$ was obtained through the numerical solution of the *Green theorem*, and how the resistance coefficient C_R was derived step by step. *Two* different procedures are discussed.

In Chapter 5, three different identification techniques are briefly discussed and compared. They are the *recursive least squares method*, the *recursive instrumental variable method* and the EKF method.

In Chapter 6, the identified results and the parameter values derived from these results are presented and discussed. To assess the results, the simulated surge motion of the tanker EXXON PHILADELPHIA is compared with the measured data.

Suggestions for future work in this area are made in Chapter 7 following a summary of the work that was carried out.

Chapter 2

Surge Equation

In ocean engineering, the object of study is the system consisting of the ocean vehicle or the offshore structure and the environment in which they exist. Besides the study of the dynamics of the fluid, an important topic of research is the behavior of vehicles and structures in the fluid, which includes the topics of maneuverability and sea-keeping. The complexity of ocean systems makes it very difficult to study them directly. Studying ocean systems with associated models is a commonly used method to avoid these difficulties.

Broadly speaking, models of systems are simplified, abstract constructs which are used to study the behavior of the systems. There are many kinds of models under this definition. In ocean engineering there are two kinds of models which are often used: one is the simplified scaled physical model which may not resemble the real system in all its details, but possesses

the most important characteristics of the system and hence behaves like the true system; the other is the mathematical model, usually a set of difference equations or differential equations, which are capable of describing the behavior of the system. Scaled models of ships used in towing tanks belong to the former category. As pointed out in the Introduction, they are commonly used but suffer from "scale effects" which limit their use. Mathematical models are also used in ocean systems research, especially in the study of ship motions. In contrast to the scaled models, a mathematical model generally can represent a certain type of ships by leaving a set of parameters undetermined. The selection of these parameters will specify a particular ship.

A mathematical model of a system is some mathematical relationship between a set of variables and the parameters mentioned above. The variables involved are used to describe the behavior of the system. For example, in maneuverability research for super tankers, despite differences of displacement, body form, engine horsepower etc., the structure of their mathematical models are the same, i.e. they consist of the same set of equations. Corresponding to any specific super tanker, the parameters have specific values. These parameters are called hydrodynamic coefficients which may be determined through different ways.

The complete setting up of the mathematical model can be accomplished in *two steps*. The first step is to find the structure of the model, and the second step is to determine the value of the coefficients. The first step

is critical. Since no system can be modeled exactly, a model developed in a suitable form can greatly reduce the complexity of actual study and may lead to reasonable results. An overly complex and detailed model may contain too many coefficients or parameters and make the second step virtually impossible. On the other hand, an overly simplified model may not be able to describe the behavior of the system properly. In this chapter we shall concentrate on setting up the mathematical model of ship systems for the study of the resistance and powering of ships.

Just as mentioned above, the mathematical model depends on both the type of the ship and the environment she is in. The only characteristics retained are the ones related to the object of this reseach. For the case of the study of ship resistance, only the motion of the ship in the surge direction is of interest, because the resistance of a ship is the drag force the ship suffers when she moves in straight ahead motion. That is, the model of a ship system for our study will only consist of the surge equation.

2.1 Resistance and Resistance Coefficient of Ships

The resistance force on a ship when she moves in water is the total force against her motion. The resistance has several components: the frictional resistance acting on the wetted surface of the ship body caused by the vis-

cosity of water; the eddy resistance or the form resistance directly caused by the energy lost due to the formation of eddies in the boundary layer; and the wave-making resistance caused by the energy lost in the wave made by surface ships when they are moving. The ship resistance is the function of her surge speed u, the Reynolds number and the Froude number. In a certain region of the Reynolds number and the Froude number, its amplitude is proportional to the square of the speed of the ship relative to the water. i.e.

$$R \propto u^2$$

So it can be written as

$$R = Cu^2$$

where C is a constant. This constant C can be non-dimensionalized and the corresponding non-dimensionalized constant C_R is defined as

$$C_R = \frac{C}{\frac{1}{2}\rho S u^2}$$

where S is the *wetted surface area* of the ship body.

Then the ship resistance R can be written as

$$R = \frac{1}{2}\rho S C_R u^2$$

C_R is called the ship resistance coefficient. Research on C_R has revealed that it is a function of the Reynolds number and the Froude number, and strictly speaking is not constant when the ship's speed is changing. Nevertheless, while the ship's speed varies within a narrow interval, correspond-

ingly the Reynolds number also varies in a narrow region, and the resistance coefficient of the ship varies very slightly, and therefore in such regions the ship resistance coefficient can be taken as a constant.

The resistance coefficient depends heavily on the characteristics of the ship: body form, wetted surface area, roughness of the surface, etc. When ships sail in the same environment, the value of the resistance coefficient can be changed by the change of the body condition: damage, fouling, corrosion and so on. The resistance coefficient value can increase significantly for the above reasons, and this will decrease the operational efficiency of ships drastically. The survey of the change of the resistance coefficient value is very important to the ship owners as well as the managers. And the resistance of a ship is of great importance to the ship designer.

2.2 Thrust and Thrust Coefficients, $\eta's$

From the derivation in Appendix A, the thrust force of the propeller can be expressed as

$$T = \eta_1 u^2 + \eta_2 un + \eta_3 n^2$$

With the characteristic that η_1 and η_2 are always negative, and η_3 is always positive, then it can be considered that the thrust force of a propeller is in fact the synthesis of *three* components with the physical meaning as some kind of hydrodynamic forces. And the thrust force is not necessarily

always positive.

These three components of propeller thrust force can be understood in the following way:

1. $\eta_3 n^2$ can be understood as a positive thrust source of the propeller. When the surge speed of the ship is *zero*, the thrust force of the propeller is from this part only. Because at $u = 0$, the thrust force provided by a propeller is the lifting force acting on its blades, $\eta_3 n^2$ can be referred to as the *lift-thrust* and the non-dimensional coefficient $\eta_{p3} = \frac{\eta_3}{\rho D^4}$ is then referred to as the *lift-thrust coefficient*.

2. $\eta_1 u^2$ has the same apparence as the drag of the locked propeller. When $n = 0$ and $u \neq 0$, the propeller provides a drag of this amount. Since this component of the propeller thrust is always negative and its value is proportional to the square of the forward speed, which is just the type of hydrodynamic drag force a body suffers while moving in the fluid with speed u. Hence $\eta_1 u^2$ can be referred to as the *drag-thrust* and the non-dimensional coefficient $\eta_{p1} = \frac{\eta_1}{\rho D^2}$ is referred to as the *drag-thrust coefficient*, even though it is not equal to the actual drag coefficient of a locked propeller.

3. $\eta_2 un$ exists only when both n and u are not *zero*. It is also some kind of drag, since it is always negative. It is the result of the correlation between u and n. Since it increases the value of the drag,

$\eta_2 un$ will be referred to as the *associated drag-thrust* and the non-dimensional coefficient $\eta_{p2} = \frac{\eta_2}{\rho D^3}$ is referred to as the *associated drag-thrust coefficient.*

These three coefficients will play important roles during the identification of the resistance coefficient of the ship, as will be seen in ensuing chapters.

2.3 Surge Equation of the Ship

When a ship keeps her straight course, the external forces acting on her consist of the thrust force provided by the propeller and the resistance force from the fluid. With the application of *Newton's law*, and without considering the interaction between the propeller and the ship hull,

$$(m - X_{\dot{u}})\dot{u} = \rho D^2 \eta_{s1} u^2 + \rho D^3 \eta_{s2} un + \rho D^4 \eta_{s3} n^2 - \frac{1}{2}\rho S C_R u^2 \qquad (2.1)$$

where $-X_{\dot{u}}$ is the added-mass of the ship in the surge direction as mentioned in Chapter 1, and D is the *ship propeller diameter.* From now on, $\eta_s's$ are used to represent the *ship propeller thrust coefficients* to be distinguished from its *model propeller thrust coefficients* represented by $\eta_p's$.

However, the interaction between the propeller and the ship hull is not negligible. To include this interaction, Equation(2.1) has to be modified. First, it is noticed that the speed of the flow in front of the propeller is

not the same as the ship's surge speed u, since the water in front of the propeller has been disturbed by the passage of the ship hull. The *advancing speed of the propeller* u_A, which is the velocity of the flow relative to the propeller, is usually lower than u.

$$u_A = (1 - w)u$$

where w is the wake fraction, which is usually less than one.

Second, because of the interaction between the propeller and the ship hull, the hydrodynamic pressure at the stern of the ship changes because of the presence of the propeller. The suction effect changes the flow past the ship hull and usually increases the resistance of the ship. There are *two* different ways to affect the modification:

- Introduce the *resistance augmentation fraction* a,

$$R = R_o(1 + a)$$

  where R_o is the resistance of the ship hull without considering the influence caused by the existence of the ship propeller.

- Accept the concept of the thrust-deduction factor t,

$$T = T_o(1 - t)$$

  where T_o is the thrust force provided by the ship propeller without the interaction between the ship hull and the ship propeller.

Both the thrust-deduction factor t and the resistance augmentation fraction a are used in this thesis.

After the modification, Equation(2.1) becomes

$$\dot{u} = \frac{(\rho D^2 \eta_{s1} {u_A}^2 + \rho D^3 \eta_{s2} u_A n + \rho D^4 \eta_{s3} n^2)(1-t) - \frac{1}{2}\rho S C_R u^2}{m - X_{\dot{u}}} \tag{2.2}$$

Using u instead of u_A and introducing new coefficients, the surge equation becomes

$$\dot{u} = \frac{\rho D^2 \eta_{t1} u^2 + \rho D^3 \eta_{t2} u n + \rho D^4 \eta_{t3} n^2 - \frac{1}{2}\rho S C_R u^2}{m - X_{\dot{u}}} \tag{2.3}$$

where

$$\begin{aligned} \eta_{t1} &= \eta_{s1}(1-t)(1-w)^2 \\ \eta_{t2} &= \eta_{s2}(1-t)(1-w) \\ \eta_{t3} &= \eta_{s3}(1-t) \end{aligned} \tag{2.4}$$

Combining the *two items* of u^2 into one,

$$\dot{u} = \frac{\rho D^2 (\eta_{t1} - \frac{S}{2D^2} C_R) u^2 + \rho D^3 \eta_{t2} u n + \rho D^4 \eta_{t3} n^2}{m - X_{\dot{u}}} \tag{2.5}$$

Now defining

$$\begin{aligned} {\eta_1}^* &= \eta_{t1} - \frac{S}{2D^2} C_R \\ {\eta_2}^* &= \eta_{t2} \\ {\eta_3}^* &= \eta_{t3} \end{aligned} \tag{2.6}$$

then the ship surge motion equation becomes

$$\dot{u} = \frac{\eta_1^* u^2 + \eta_2^* un + \eta_3^* n^2}{m - X_{\dot{u}}} \tag{2.7}$$

This is the system equation to be used in the system identification procedure which leads to the estimate of the ship resistance coefficient.

Chapter 3

Experiment Design and Measurement Data

3.1 Experiment Design

3.1.1 Sea trial pattern

Experiment design is an important stage in the overall identification procedure. A thoughtfully designed experiment is crucial, since the quality of the identification results, especially the accuracy of the identified parameters, depends on both the identification technique chosen and the quality of the data obtained in the experiment. A well designed experiment will produce sufficient relevant information about the dynamics of the system. Furthermore, in the event of failure in the identification due to an unsuit-

able choice of input signals, the whole experiment has to be repeated which is an expensive and time-consuming proposition. The case of the sea trial for collecting the data to be used in identification, which is now under discussion, is a good example. The sea trial is simple, and almost every ship can be submitted to it. However, since this technique is still in the stage of testing, it is necessary to convince the ship owners to lend their support. Before the voyage, it is necessary to prepare for the test by checking instruments onboard and rehearsing. This procedure is time consuming, and had the test failed, to carry it out again would have been very costly.

The goal of the experiment design is to maximize the information content of the data within the limits imposed by the given constraints and in the minimum time. To achieve this goal, the design of the experiment should include: choice of input variables, test signal design, choice of sampling rate, choice of experiment time length and presampling filters design. Each of these has a significant bearing on the information provided by an experiment and thus on the final identification result. At one extreme, a poorly chosen input may result in violent system disturbances with subsequent damage or loss to the system. At the other extreme, an input can be so conservative as to yield little or no information about the system's dynamic behavior. It would be a wasted effort even though a lot of (useless) data may have been collected. In most cases, the components of the experiment design are closely interrelated. Hence, the design of an experiment is generally an integrated problem. That is, in order to get an efficient ex-

periment or an optimal experiment, all the above mentioned factors should be considered simultaneously, although in the literature, these factors are usually discussed separately.

In practice, the experiment design cannot be accomplished by merely working with theories on optimal control and identification. Sometimes, a perfectly designed experiment plan based on the application of theoretical analyses may not be feasible due to the constraints existing in the experimental environment. Therefore, a priori knowledge of the system plays an important role. The limitations brought by constraints such as instrument availability, accuracy of equipment, etc. can affect all the components of the experiment design and sometimes leaves no room for flexibility. So in practice, once the goal of the identification has been set, the best thing to do is to first examine the environment of the experiment carefully to see what the constraints are and which part of the experiment as designed can be done under these constraints and how much room is left for the design flexibility etc. Then set up the design strategy and start to make the plan of the experiment.[8][10][16] [23]

For the identification of the resistance coefficient of ships, since the system equation is already established, the structure of the model is set and the only unknowns are the parameters which are assumed constant. The task of identification is therefore to estimate these parameters. The ship surge motion system, from the point of view of system theory, is a *single-input single-output system.* The input variable is the ship propeller

rotating rate n, and the output variable is the surge speed u of the ship. It is evident that to identify the resistance coefficient of the ship through a very simple maneuver of the ship and using instruments originally onboard ship, u and n automatically become the choice of variables to be measured in the experiment. Therefore the experiment design problem is reduced to a choice of suitable input signals for the input variable n and the choice of suitable sampling rate so that the desired parameter accuracy can be obtained in minimum time.

To get accurate values of the parameters through identification, the input signal n should possess two properties. One property is that it will guarantee that the results of the identification are consistent. This means that for the parameters η^**s* in the model, the input signal n should be able to discriminate between different groups of parameter values. In other words, if two different groups of values are assigned to the η^**s*, the same input signal n will correspondingly produce different values of output u. The other property is that the variance of the estimates of the parameters should be minimized. This, of course, depends on both the input signal shape and on the sampling rate. However, the choice of the input signal shape is the more important and difficult problem. The input signals possessing these characteristics are called the *persistent exciting signals*, and an experiment conducted with that class of input signals is called an *informative experiment.*

Starting from this principle, different criteria of optimal experiment de-

sign, both in the time domain and in the frequency domain, have been derived mainly from linear system theory. According to Goodwin et al, [9] for sensibly chosen criteria, the choice is often not critical, i.e. usually a good experiment according to one criterion will be deemed good by another criterion. Therefore one can pick any criterion which is meaningful and convenient. It is often preferable for the criterion to be posed in the frequency domain rather than in the time domain. The reason is that although the time domain analysis is carried directly on the signal itself, the frequency domain analysis gives more insight of the effects of the input signals on the system. Ljung[16] pointed out that very different input signals having the same spectrum can be equally good as far as input signal design is concerned. So one way the input signal design can be carried out is by first determining the best input spectrum and then selecting a realization of that spectrum by taking into consideration practical aspects of signal generation and input limits. To realize the signals, one can first choose an input signal which fits the physical system without conflicting with the constraints and then compare its spectrum with the best input spectrum. For the identification of the resistance coefficient of ships, the constraint for the design of the input signal for n is that the value of n should not be changed too rapidly. Also for the sake of the safety of the engine and propeller system, a high frequency change in n is to be avoided.

Based on these ideas, *two patterns* of simple maneuvering are considered. The first one is the accelerating maneuver or "speeding up", which is

to start the propeller from *zero rps* to full *rps*. It is hoped that through this procedure, the measurements of u and n can lead to the estimates of η_1^*, η_2^* and η_3^* simultaneously. The second one is the decelerating procedure or "wind-milling" maneuver. During this procedure, the ship is slowing down with the propeller in the wind-milling mode. The ship moves foward under its own inertia and is slowed down by the hydrodynamic resistance. Since the ratio of surge speed u and the propeller shaft rotating rate n keeps constant during this procedure, it can either be taken as a closed-loop identification or be taken as a new system, whose system equation is

$$\dot{u} = \frac{\frac{1}{2}\rho S \overline{C}_R u^2}{m - X_{\dot{u}}} + \varepsilon_n \tag{3.1}$$

where ε_n is the noise and $\overline{C}_R$ is the integrated resistance coefficient, which includes a part corresponding to the resistance of the wind-milling propeller. One reason to consider this maneuver, is that evidently $\overline{C}_R$ can be estimated very accurately from a system equation containing only one unknown parameter. Furthermore, from ship hydrodynamics it is known that in the wind-milling mode, the resistance of the propeller should be the order of 5% of that of the ship. So the result from this procedure can be used as a reference value to compare with the result identified from the acceleration maneuver. Since the ship is sailing under the equilibrium condition, the deceleration maneuver can be accomplished by bringing the ship to a stop for the initiation of the acceleration maneuver. Therefore adding a

deceleration maneuver (with wind-milling propeller) to the procedure consisting of the acceleration maneuver represents little additional effort. Since some ships cannot make the propeller wind-mill, this maneuver may not be applicable for a wide range of application to ships.

Experiment design is also based on the analysis of the covariance of the estimator which is used in the identification. However, since the exact covariance of a particular estimator is very difficult to ascertain, one proceeds with the assumption of the existence of an asymptotically efficient parameter estimator. The parameter covariance matrix is then approximated by the *Fisher information matrix* M which is defined as

$$M = \left(\frac{\partial \ln (\underline{y}|\underline{\theta})}{\partial \underline{\theta}}\right)^T \left(\frac{\partial \ln (\underline{y}|\underline{\theta})}{\partial \underline{\theta}}\right) \tag{3.2}$$

where $\underline{y}$ is the *output variable vector*, $\underline{\theta}$ is the *parameter vector*, the *index* ^{T} means the *transpose* of a matrix or a vector.[9]

Two particulars of the analysis have been addressed. One is whether the input signal is persistently exciting, which means that the input signal is sufficiently rich to excite all process modes of interest, so that the identifiability of the parameters can be guaranteed. According to Rothenberg, local parameter identificability is equivalent to non-singularity of the information matrix.[23] In the frequency domain analysis, Ljung has shown that this implies the minimum number of spectral lines of the input signal.[17] Zarrop has shown in his thesis, that for a linear single-input single-output system, the necessary condition for the input signal to be persistently ex-

citing, corresponding to the identification of N parameters, is that the spectrum of the input signal should have at least $\frac{N}{2}$ spectral lines.[23]

Though the model of ship surge motion is nonlinear in the variables u and n, it is linear in the parameters η_1^*, η_2^* and η_3^*. The analysis mentioned above can be applied to the ship surge motion system without too many difficulties. Checking the two experimental procedures: "speeding-up" and "wind-milling", it is evident that signals of n in both procedures are persistently exciting for the identification of $\eta^{*'}s$.

The other subject of analysis is to find an optimal input signal by minimizing $I = f(M)$—the *performance index of* M. One choice of I is

$$I = \ln(det\, M)$$

where $det\, M$ is the *determinant of* M.

The conclusion of studies by several authors is that the optimal signal can always be realized through carefully chosen binary signals. Examples for nonlinear systems given by Goodwin lead to the same conclusion.[8] However, for the ship system, since there is a limitation on the engine and propeller performance, binary signals of n are not practical.

3.1.2 Sampling rate and experiment length

Sampling rate is also a factor relating to the accuracy of the identification. Sampling rate is one of the components of the experiment design for general cases. For the identification of the resistance coefficient, one has to avoid

the aliasing phenomenon which occurs when the sampling interval is larger than the *time constant of the system.* In the experiment in which data for identifying the ship resistance is collected, the principle is to sample the data as fast as possible, since the increase in cost due to an increase of the sampling rate for such a simple problem is negligible. The time constant concept is used in linear system analysis. Although, the ship surge motion system is a nonlinear system, for a step input n, the response of u is an *exponential-like* function. Following the definition of the time constant of a linear system, the *pseudo time constant* τ for ship surge motion system can be defined as

$$\tau = \frac{u_e}{\dot{u}_0}$$

where u_e is the value of the u at the equilibrium state, and $\dot{u}_0$ is the value of $\dot{u}$ at time $t = 0$. For the tanker EXXON PHILADELPHIA, a pseudo time constant τ for the ship surge motion system of $\sim 410\,seconds$ has been obtained both by solving the equation analytically, and by the simulation of the ship motion based on the mathematical model.(see Appendix B) The sample interval of the measurement in the sea trial is 1 *second* which avoids aliasing. When the data are put into the estimator to estimate the coefficients in the identification stage, re-sampling on the measured data at a multiple of 1 *second* will be considered.

The duration of the experiment should be as long as possible for the sake of reliability of the data and of the accuracy of the results of identi-

fication. Insufficient time for an experiment may lead to a pitfall; in some instances, an accurate model that fits the data very well may be obtained through identification, however the model may be wrong. Data from another similar experiment may also lead to an "accurate" model but with quite different parameters obtained through the same identification procedure by the same identification method. Furthermore, the variance of the estimates is usually proportional to the inverse of the experiment length. Consequently, in order to improve the standard deviation of the estimates by a *factor of two*, the experiment has to be *four times* as long. Nevertheless, for the experiment duration, longer may not mean better, because extra disturbances are often introduced in a long time experiment, especially during a sea trial. According to Gustavsson[10], a rule of thumb is that the experiment should last at least *ten times* the major time constant. However, Zarrop in his thesis[23] cited an example where time duration is only *twice* the time constant in practice.

As mentioned above, the time constant for the ship surge motion system is about 410 *seconds* while the sea trial experiment length for each procedure was over 1000 *seconds*. It does not meet Gustavsson's rule. However, the identification on the simulated data showed that this time duration is good enough.

3.2 Instrument Layout

As mentioned earlier, some of the most important features of the method developed for estimating the resistance coefficient of ships is the simplicity of the sea trial, and the fact that all the necessary equipment is originally onboard. During the sea trial, to maintain the synchronization in the sampling of different variables, and to convert the measured data into digital records, a **PC** based datalogger was brought on board and connected with the onboard equipment through interface and ancillary units. A brief description of instruments follows.

1. The datalogger for data collecting is a Sperry Marine Data Acquisition System(**SMDAS**). It is based on a system developed by the Ship Performance Department(Code 1561) of **DTNSRDC**. A Sperry **PC** is augmented with additional hardware for the datalogging and display functions and uses the software developed by **DTNSRDC**. The time history data is converted into **ASCII** files. In its present configuration the **SMDAS** can collect up to 16 simultaneous channels of analog data in the *voltage* $\pm 10\, volts$ at sample rate up to 3 *samples per second.* Only 5 *channels* were used in the experiment. This system does not occupy large room, and the **PC** can be used for other performance as a micro computer besides datalogging.(see *Fig.* 3.1)

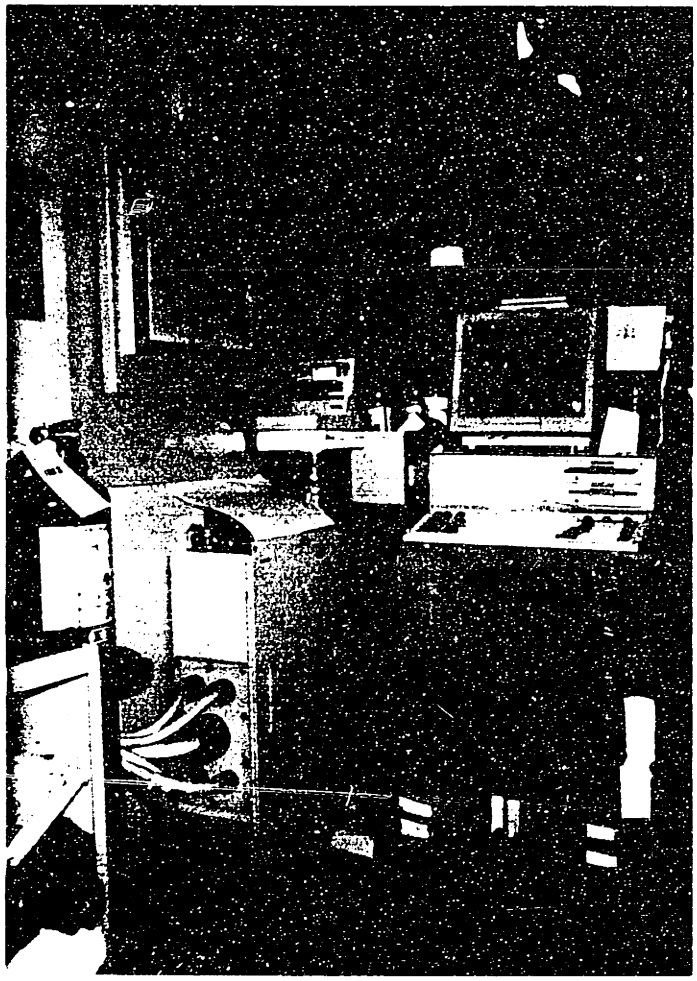

Figure 3.1: Sperry Marine Data Acquisition System

2. The Rudder Angle Indicator is made by SIEMENS Gmbh(Germany). It was originally onboard ship. It is a 50 *volt* 60 Hz synchro system with a three faced indicator on the ship's bridge. (see *Fig.* 3.2) A connected parallel synchro to analog converter has a sensitivity of 9.615 *degrees per volt*.(see *Fig.* 3.3) It is connected to the datalog-

ger through *channel* 1. This converter is small and very easy to be arranged on the bridge.

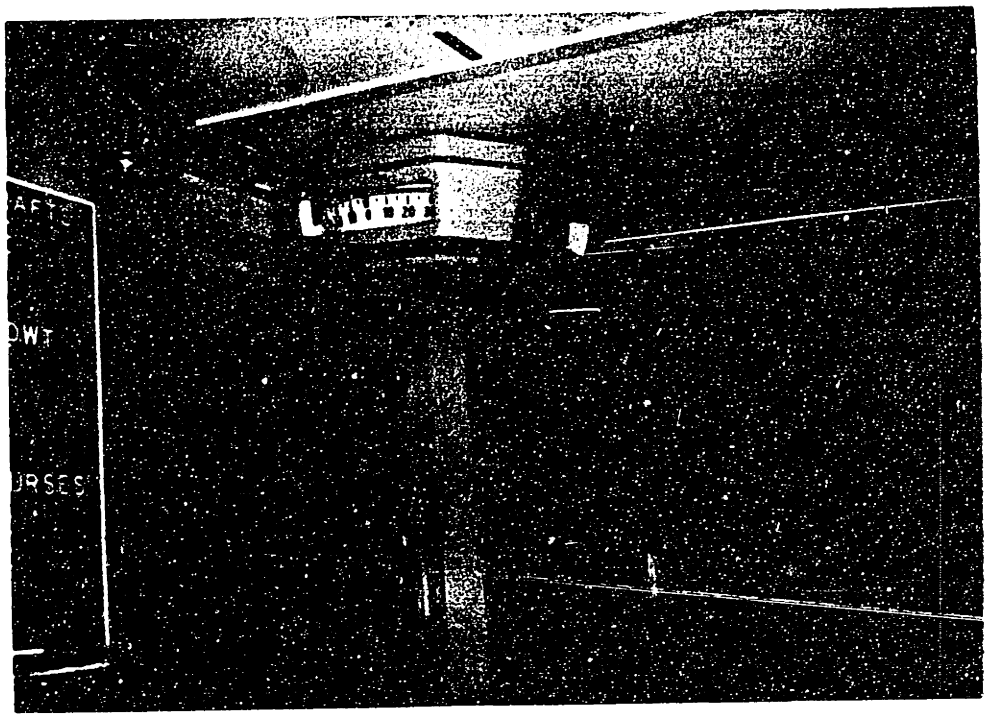

Figure 3.2: Rudder Angle Indicator

Figure 3.3: Signal Converter

3. The model **IC-8PR** Shaft Tachometer with remote meters is used to measure the *rpm*(*revolutions per minute*) of the propeller shaft. It is made by Electric Tachometer Corporation, (Philadelphia, Pa.). The high impedance monitor across the bridge meter has a sensitivity of 57.778 *revolutions per volt*. It is connected to the datalogger through *channel* 2. (see *Fig.* 3.4)

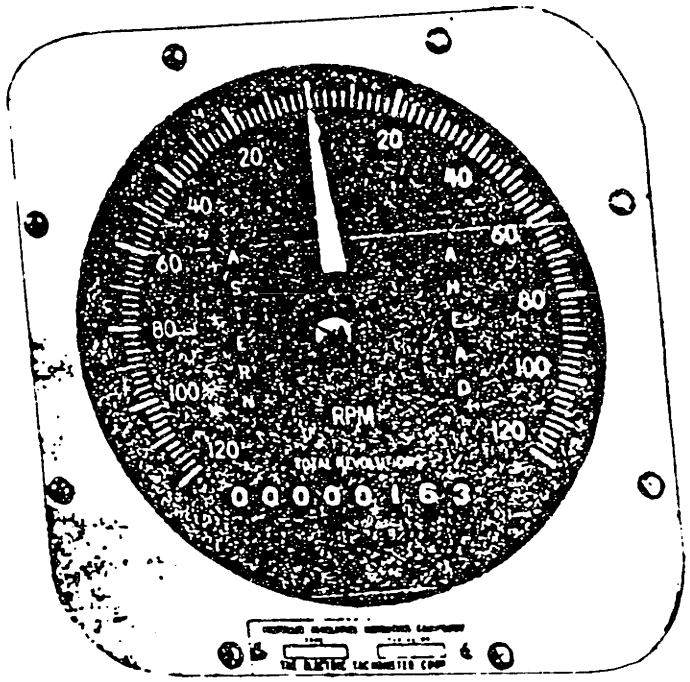

Figure 3.4: *RPM* Meter

4. The *MK* 227 Gyro-Compass is used for the measurement of the heading angles. It is made by Sperry Marine . It is connected to the datalogger through two channels: *channel* 3 and *channel* 4.(see *Fig.* 3.5)

   - Channel 3 records the heading angle within the range of $\pm 180°$. The $115\,volt$ $60\,Hz$ Synchro is geared at 1 : 1 to compass. Synchro to analog conversion gives $\pm 10\,volts$ for $\pm 180°$ of absolute heading.

   - Channel 4 records the heading angle change ranging from $-5°$ to $+5°$. The Synchro is geared to analog conversion gives $\pm 10\,volts$

for $\pm 5^{\circ}$ heading change.

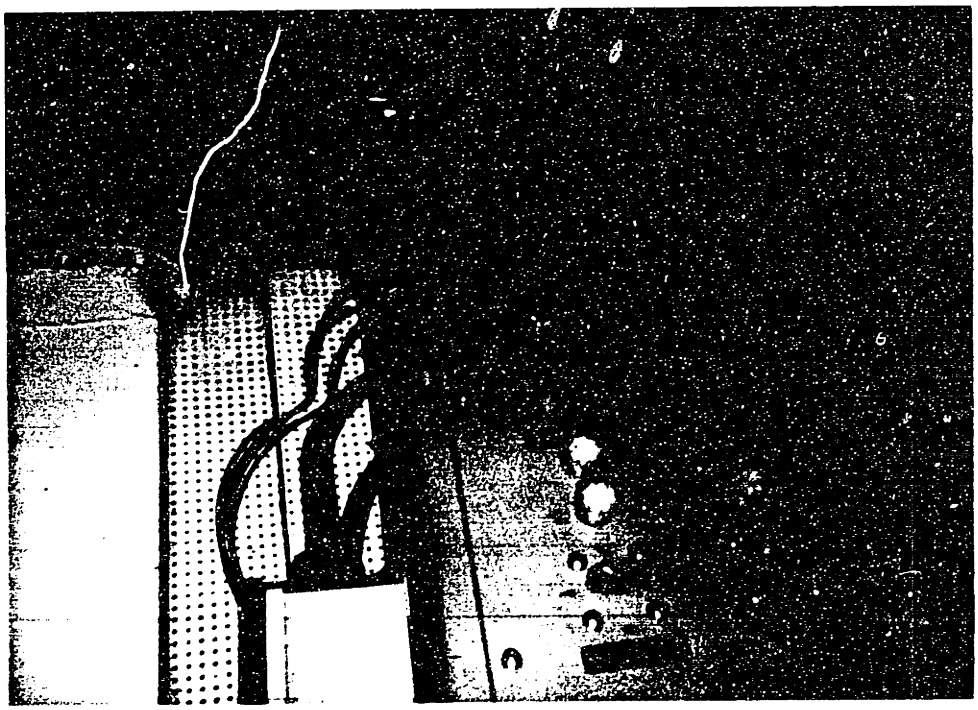

Figure 3.5: Gyro-Compass

5. The **SRD 301B** Sperry Marine Doppler Speed Log is used to measure the ship forward speed. The serial data to analog conversion gives 2.5 *knots per volt*. It is connected to the datalogger through *channel* 5. (see *Fig.* 3.6)

As mentioned before, the measurement of heading angle is only used to survey of the course of the ship; it is not necessary to record the heading angles and the rudder angles.

The whole network is shown in *Fig.* 3.7

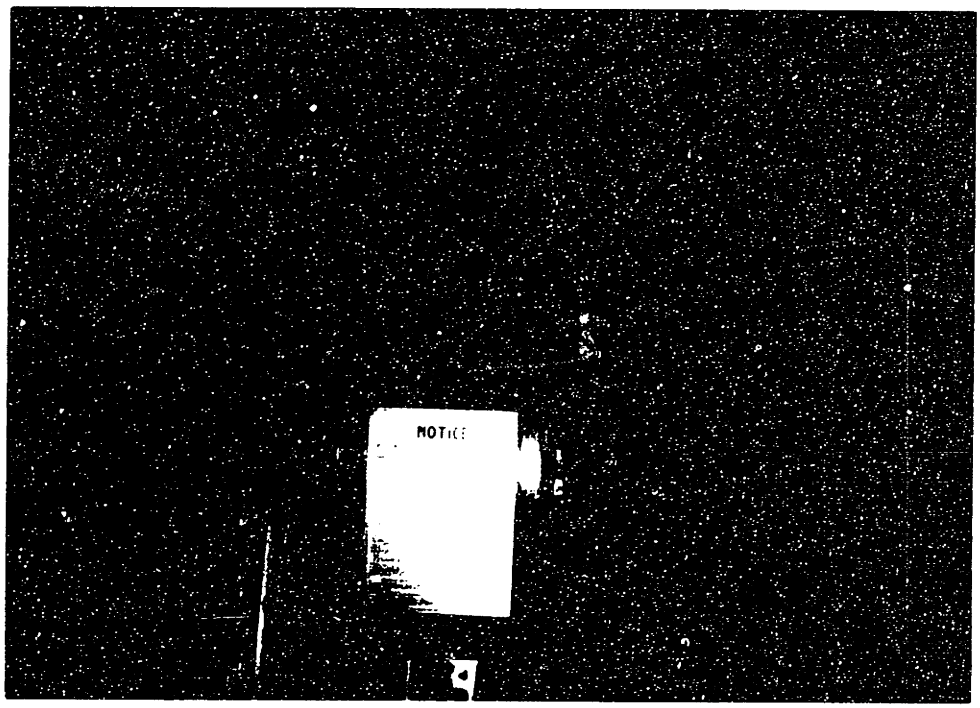

Figure 3.6: Doppler Speed Log

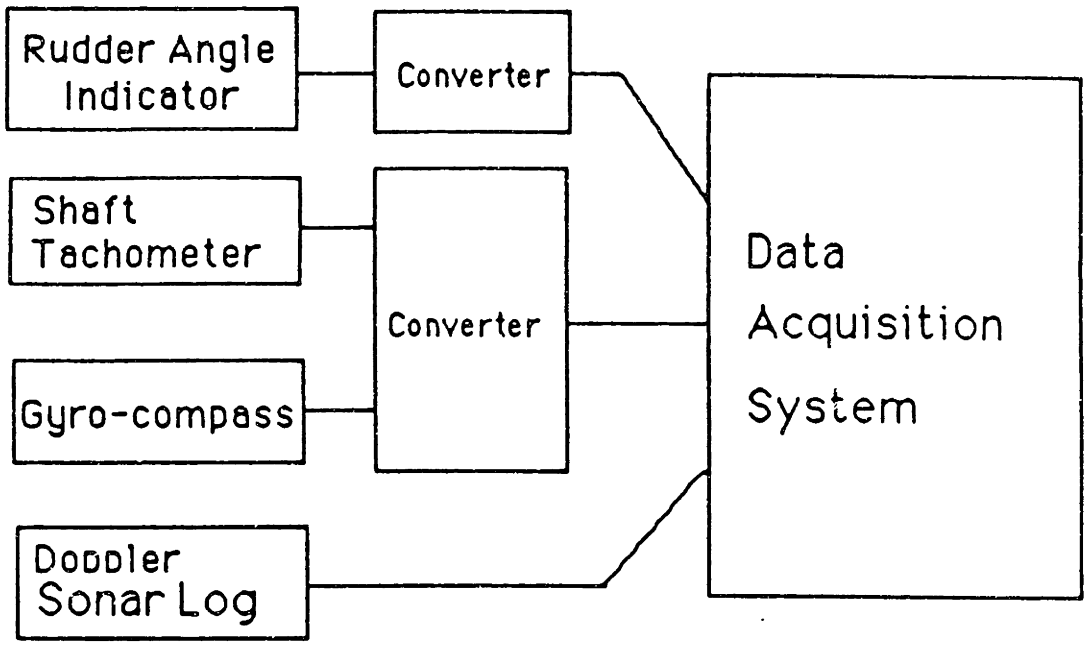

Figure 3.7: Network of Data Measurement

3.3 Results of Measurements

The sea trial for the measurement of u and n was conducted on May 12, 1987. On that day the 763 *feet* long, 76,000 *dead-weight ton* tanker EXXON PHILADELPHIA was on the way back from Valdez, Alaska to

San Francisco along the West Coast. The displacement of the tanker was $90,600\,tons$. The initial position of the sea trial was chosen in calm sea at $58°38.67'$ north and $143°29.25'$ west. At that time there was a slight swell of 1 to 2 $feet$ and no wind.

First, the deceleration procedure of the ship was conducted by cutting the steam to the engine and letting the propeller of the ship wind-mill. The ship kept moving straight foward. When the speed of the ship slowed down to half of the cruising speed, the engine was set in reverse which brought the speed of the tanker to *zero*. The acceleration procedure was then initiated by bringing the propeller rotating rate n to $70\,rpm$ as quickly as possible. The whole experiment took about $35\,minutes$ and went very smoothly.

The data measured during the experiment were directly recorded on floppy diskettes in ASCII form which are readable on any IBM compatible PC. The measurements of u and n from both acceleration and deceleration procedures are shown in *Fig.s* 3.8 $\sim$ 3.11. The noise analyses of these measurements are presented in Appendix C(*Fig.s*$C.2 \sim C.9$).

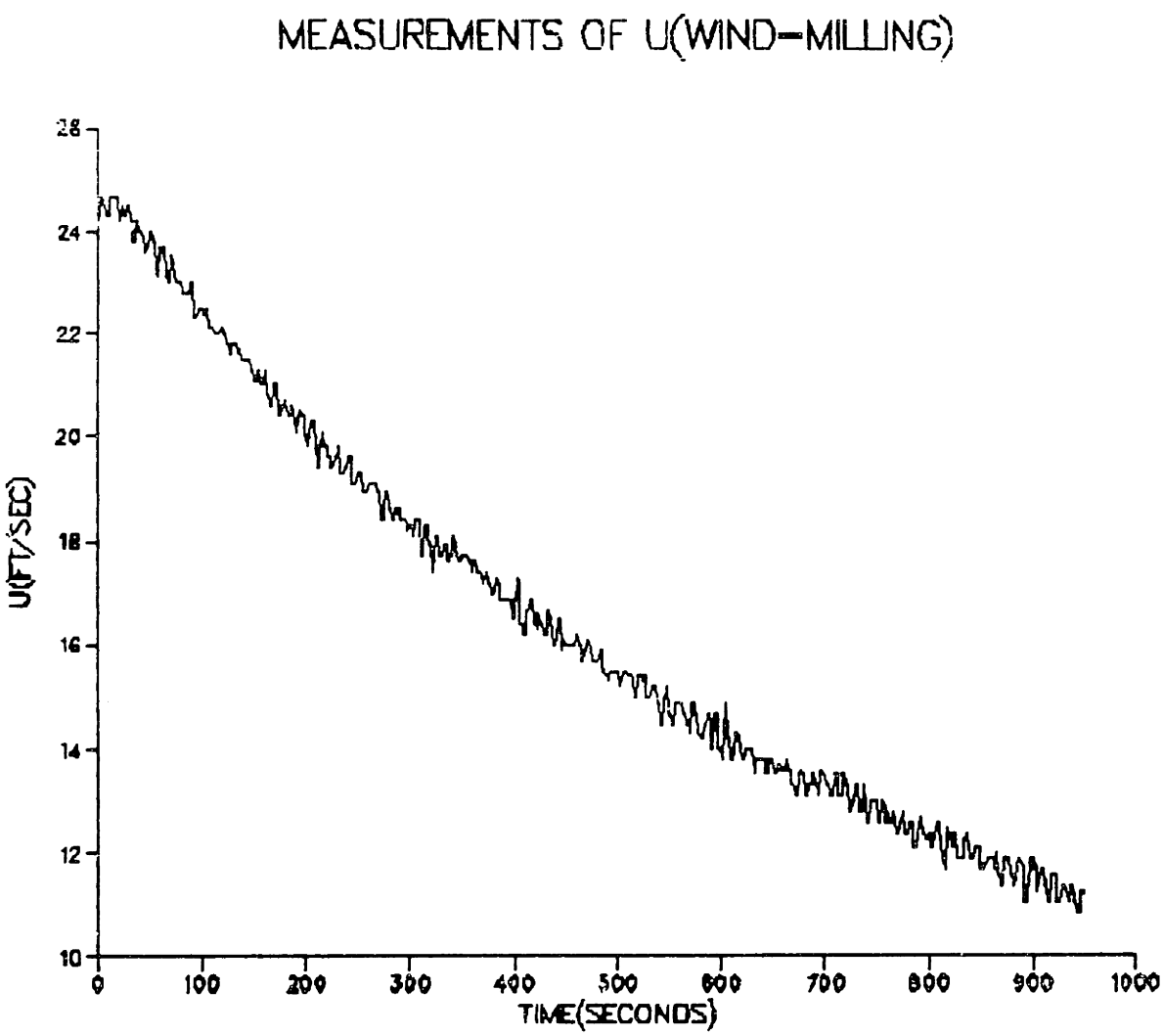

Figure 3.8: Measurement of u(Deceleration)

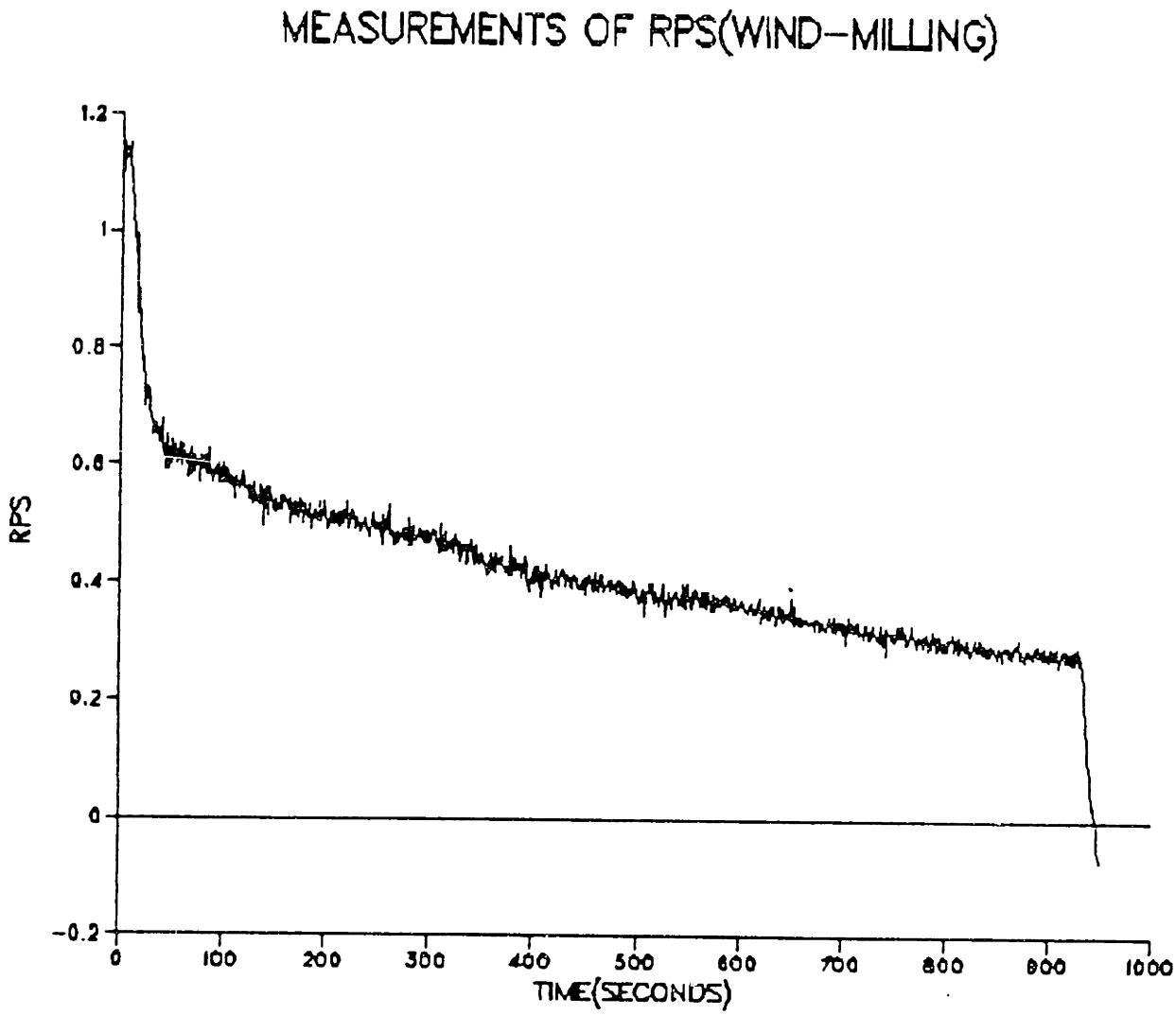

Figure 3.9: Measurement of *rps*(Deceleration)

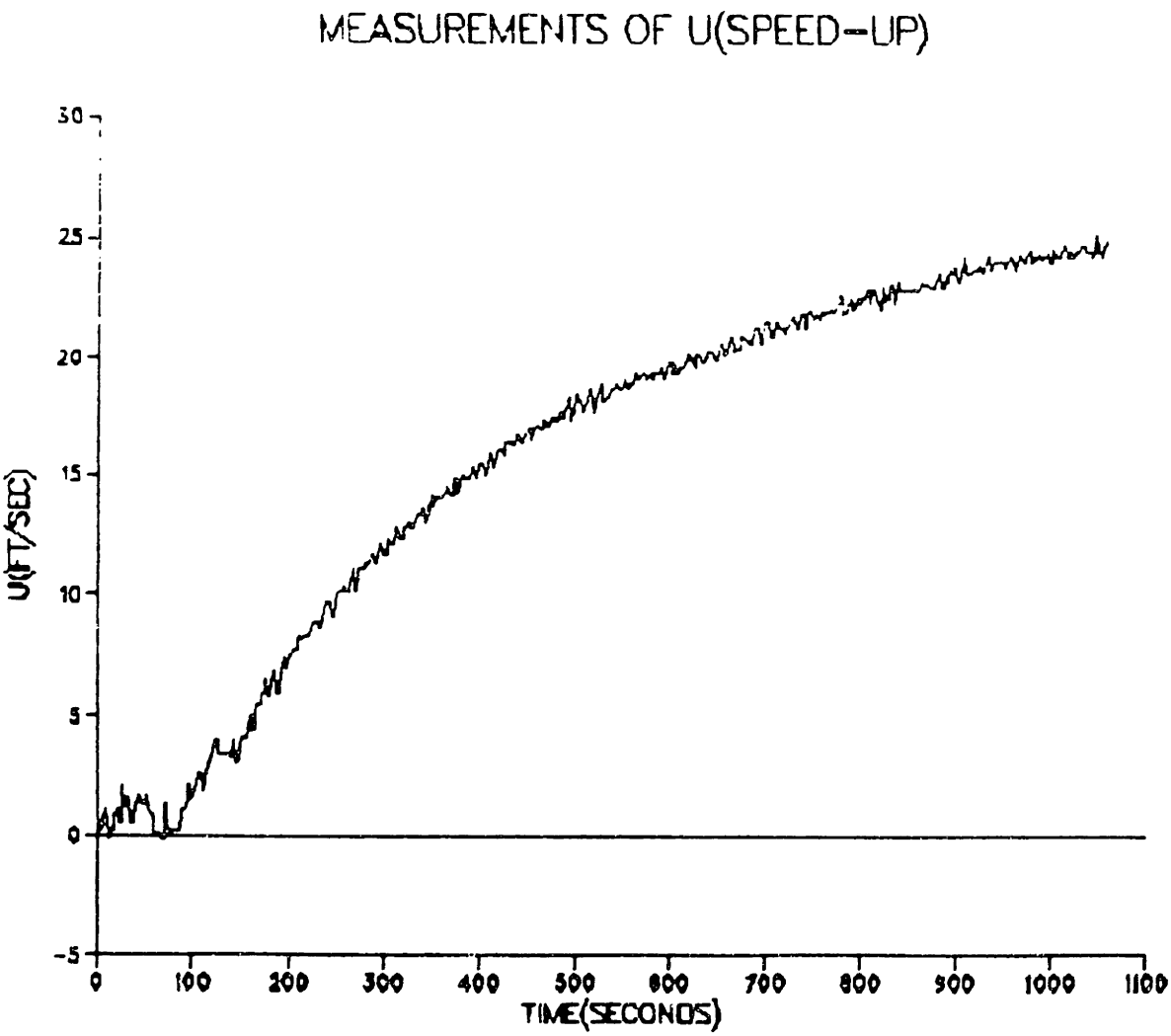

Figure 3.10: Measurement of u(Acceleration)

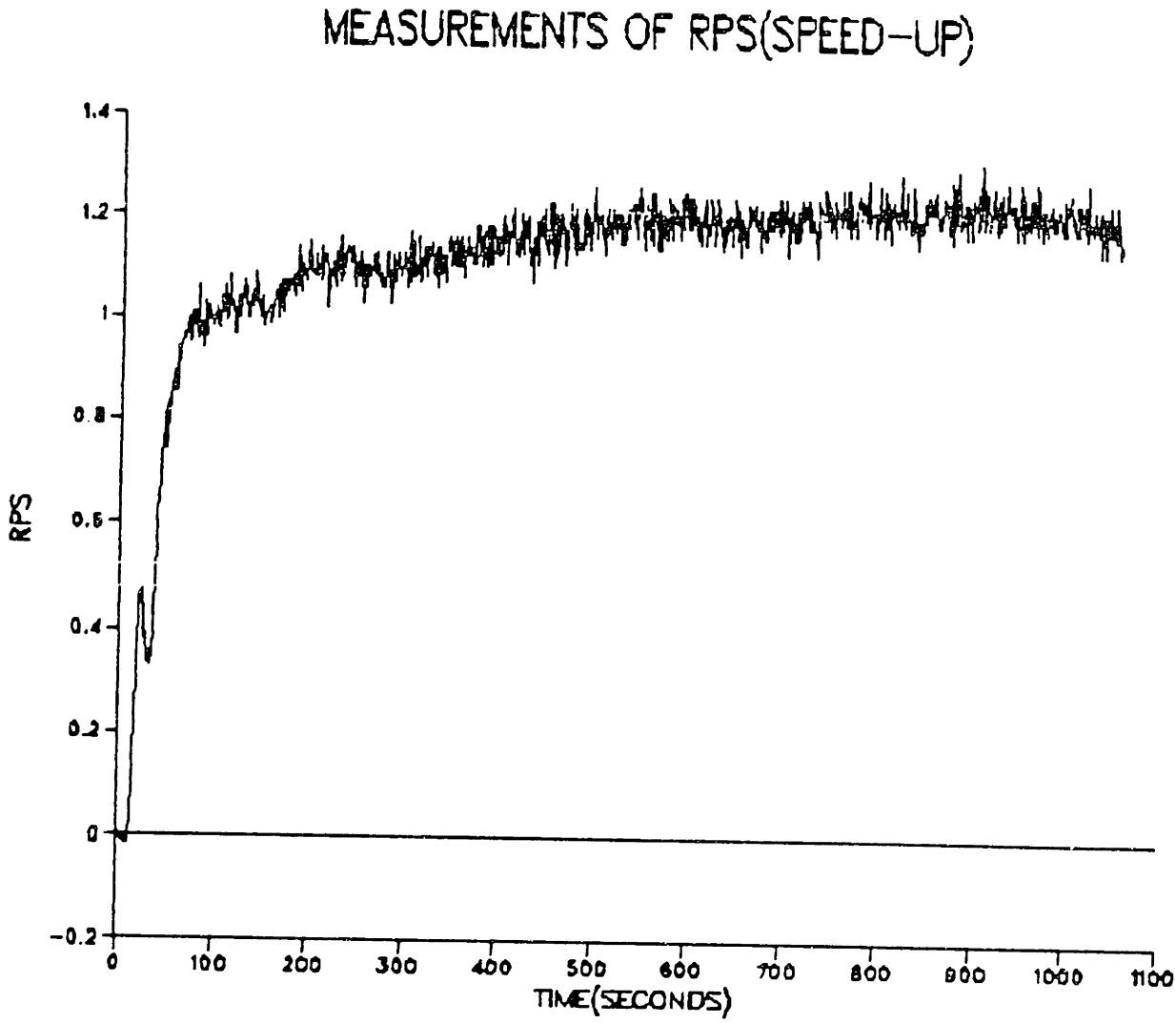

Figure 3.11: Measurement of *rps*(Acceleration)

Chapter 4

Strategy of Coefficient Estimation

Once the system equation has been derived, the next step is to find a way to estimate the parameters through an identification technique. System identification is part of system science. In system analysis, a major problem is the determination of the output signal based on the input time history and the properties of the system. The model of the system including its structure and the values of its parameters is already known. For the case of the surge motion of a ship, the object is to determine the signal u when the input signal n is given. System identification can be recognized as an "inverse problem" of system analysis, since it deals with the problem of determining the system model which describes the system behavior when both the input and output signals are known[17]. When the structure of the

system is known, the estimation of the parameters in the model becomes the main task of system identification. Different methods for parameter estimation, especially for the estimation of the parameters in linear systems, have been developed. Their common goal is to make the estimated values as accurate as possible. Methods such as the least squares method, maximum likelihood method, and the instrumental variable method have been extensively used. However, only those parameters which are identifiable can be estimated by the identification technique. Sometimes, because of the characteristic of the system model or because of lack of sufficient information, one or several parameters may not be estimated by any of the developed identification methods, especially for a system model with too many unknown parameters.

The examination on the ship surge motion Equation(2.5) shows that there are seven parameters to be estimated. They are $-X_{\dot{u}}$, η_{s1}, η_{s2}, η_{s3}, C_R, t and w. Their values, except for $-X_{\dot{u}}$, are usually obtained from model tests prior to the full scale ship trials. They suffer from the scale effect. From identification theory, it is evident that only three coefficients η_1^*, η_2^* and η_3^* can be estimated directly by the identification technique. Since the seven parameters mentioned above are combined into three identifiable parameters, it is not possible to get the resistance coefficient C_R of the ship directly through any identification technique. It is more practical to obtain the resistance coefficient C_R from the $\eta^{*}s$ after they have been estimated through identification. To achieve this goal, one needs to work by steps, and

before C_R is determined the other unknowns among the seven parameters mentioned above need to be determined first. The details of the approaches are discussed in the following sections.

4.1 Calculation of the Added-Mass Coefficient

It is known that $-X_{\dot{u}}$ has a physical meaning as the added-mass coefficient corresponding to longitudinal acceleration. Until now, it has generally been given a rough estimated value for a real ship by consulting the calculations for ellipsoids based on length-beam ratio and it is of the order of 5% of the displacement of the ship. The choice of the length-beam ratio is difficult but critical. For example, for a tanker, the difference between the width and the depth is obvious, so the equivalent ellipsoid will have two different length-beam ratios and consequently there should be two different values for its added-mass. Also, ship bows and sterns do not resemble ellipsoids. Although a small error in the value of $-X_{\dot{u}}$ would not cause a serious error in the identified result of the resistance coefficient, in the hope of improving the result as much as possible $-X_{\dot{u}}$ is calculated on the computer through the application of the Green theorem. In brief, from Green theorem, the distribution of hydrodynamic potentials on the wetted surface of the ship is a function of the shape of the surface, and the added-mass of the ship

corresponding to longitudinal acceleration is just

$$-X_{\dot{u}} = \rho \int\int_S \phi_1 \frac{\partial \phi_1}{\partial n} dS \tag{4.1}$$

where ϕ_1 represents the velocity potential due to a body motion with unit velocity in the surge direction and ϕ_1 is a function of $(\frac{1}{r})$[18]. Because of the complexity of the shape of the body surface of ships, this formula had not been used in practice, save for the simpler three dimensional bodies like spheroids and ellipsoids of revolution. However, the recently developed MIT Radiation and Refraction Program provides a numerical solution for the velocity potential and added-mass coefficient for arbitrary shapes. The program was used to calculate the added-mass $-X_{\dot{u}}$ for the tanker EXXON PHILADELPHIA. To perform the calculation, the first step is to divide the wetted surface of the ship into small quadrilateral panels. These panels do not have to be equal in size or shape. The coordinates of the vertices of each panel are collected in the clockwise direction and constitute the input for the computer program. Since the ship body is port-starboard symmetric, only half of the wetted surface of the ship is needed.

For the tanker, the wetted surface was divided in the following way: 20 *water planes* were used to divide the under water part of the ship body into layers, then 30 *transverse section planes* were used to cut the wetted surface between each two layers into panels. It is known that every tanker has a large parallel middle body, where the distances between each two transverse sections are larger than that at the bow and at the stern. As

shown in *Fig.* 4.1 and *Fig.* 4.2, half of the wetted surface of the ship is divided into 550 *panels*.(If both sides of the ship body are considered, there are 1,100 *panels* altogether.)

The procedure of obtaining the coordinates of the these panels is now briefly described:

First, all the coordinates of the vertices of the panels are collected from the layout of the ship hull and put into an input file.(See *Table* 4.1) Because these coordinates from the layout are in *feet*, *inches* and $\frac{1}{16}$*ths*, they need to be converted into *decimals* in *feet* to be used in the program. After the conversion, the coordinates of each panel are put into the order that the vertices of each panel are in the clockwise direction. (See *Table* 4.2). These data are then used as the input to the program calculating the added-mass coefficients of the ship. For the case involved in this thesis, $-X_{\dot{u}}$—the added-mass coefficient of the ship corresponding to longitudinal acceleration is to be calculated.

The calculated $-X_{\dot{u}}$ for EXXON PHILADELPHIA is 4.71% of the displacement of the tanker. The value of the added-mass for an equivalent ellipsoid is of the same order of magnitude. (see *Fig.* 4.3). The value of the added-mass coefficient of the ship corresponding to longitudinal acceleration obtained by this numerical method is reasonable and reliable.

```
20  29
 3   1   3     0   3   0     3   0   3     0   3   0     3   0
 3   0   3     0   3   0     3   0   3     0   3   0     3   0
 3   0   2     0   2   0     0   0   0     0   0   0     0   0
 0   2   4     6   8  10    12  14  16    18  20  22    24  26
28  30  32    34  36  38    40
  763.000     753.462     743.925     734.387     724.850     705.775
  686.700     648.550     610.400     572.250     534.100     495.950
  457.800     419.650     381.500     343.350     305.200     267.050
  228.900     190.750     152.600     114.450      76.300      57.225
   38.150      28.632      19.075       9.537       0.000
  736.333     738.333     739.667     740.667     742.000     743.000
  743.667     746.333     745.667     743.000     742.000     741.667
  741.333     741.667     742.667     744.333     751.667     767.000
  776.333     783.000     788.333
    1.500     -12.151     -15.401     -18.366     -19.698     -20.883
  -21.472     -21.263     -20.913     -19.785     -18.115     -16.196
  -13.331     -10.142      -7.250      -4.898      -2.968      -1.525
   -0.668      -0.256      -0.172
 1   1  13     2   3   8     5   4  13     9   9   4    20   7   4
33   2   0    45   0   0    54   5   9    59   8  12    60  11  10
62   6   0    62   6   0    62   6   0    62   6   0    62   6   0
60  11   6    59   5   0    53  11   6    43   6   2    29  11   3
22   3   5    14   7   1    11   2   5     8   5   3     6   5  11
 4  11   5
 1   6   4     3   2   6     7   3   0    12   2  12    24   5  14
38   0   8    49   3   2    57   3  15    61   6  14    62   1  14
62   6   0    62   6   0    62   6   0    62   6   0    62   6   0
62   1  13    61   0   0    56   5  15    47   7  13    34   6   4
26   8  12    18   5  14    14   2   5    10   9  13     8   4  14
 6   8   6
 1  10   0     3  10   2     8   5   6    13  10   7    27   3   3
41   7  13    52   3  14    59   3   7    62   2  11    62   6   0
62   6   0    62   6   0    62   6   0    62   6   0    62   6   0
62   6   0    61  10   1    58   1  11    50   5   3    37   6  10
```

Table 4.1: Input Data for Forming Panels(Part)

736.3330	0.0000	0.0000	734.3870	0.0000	0.0000
734.3870	1.1510	2.0000	738.3330	0.0000	2.0000
734.3870	0.0000	0.0000	724.8500	0.0000	0.0000
724.8500	2.2917	2.0000	734.3870	1.1510	2.0000
724.8500	0.0000	0.0000	705.7750	0.0000	0.0000
705.7750	5.4010	2.0000	724.8500	2.2917	2.0000
705.7750	0.0000	0.0000	686.7000	0.0000	0.0000
686.7000	9.7708	2.0000	705.7750	5.4010	2.0000
686.7000	0.0000	0.0000	648.5500	0.0000	0.0000
648.5500	20.6042	2.0000	686.7000	9.7708	2.0000
648.5500	0.0000	0.0000	610.4000	0.0000	0.0000
610.4000	33.1667	2.0000	648.5500	20.6042	2.0000
610.4000	0.0000	0.0000	572.2500	0.0000	0.0000
572.2500	45.0000	2.0000	610.4000	33.1667	2.0000
572.2500	0.0000	0.0000	534.1000	0.0000	0.0000
534.1000	54.4635	2.0000	572.2500	45.0000	2.0000
534.1000	0.0000	0.0000	495.9500	0.0000	0.0000
495.9500	59.7292	2.0000	534.1000	54.4635	2.0000
495.9500	0.0000	0.0000	457.8000	0.0000	0.0000
457.8000	60.9688	2.0000	495.9500	59.7292	2.0000
457.8000	0.0000	0.0000	419.6500	0.0000	0.0000
419.6500	62.5000	2.0000	457.8000	60.9688	2.0000
419.6500	0.0000	0.0000	381.5000	0.0000	0.0000
381.5000	62.5000	2.0000	419.6500	62.5000	2.0000
381.5000	0.0000	0.0000	343.3500	0.0000	0.0000
343.3500	62.5000	2.0000	381.5000	62.5000	2.0000
343.3500	0.0000	0.0000	305.2000	0.0000	0.0000
305.2000	62.5000	2.0000	343.3500	62.5000	2.0000
305.2000	0.0000	0.0000	267.0500	0.0000	0.0000
267.0500	62.5000	2.0000	305.2000	62.5000	2.0000
267.0500	0.0000	0.0000	228.9000	0.0000	0.0000
228.9000	60.9479	2.0000	267.0500	62.5000	2.0000
228.9000	0.0000	0.0000	190.7500	0.0000	0.0000
190.7500	59.4167	2.0000	228.9000	60.9479	2.0000
190.7500	0.0000	0.0000	152.6000	0.0000	0.0000

Table 4.2: Coordinates of Panels(Part)

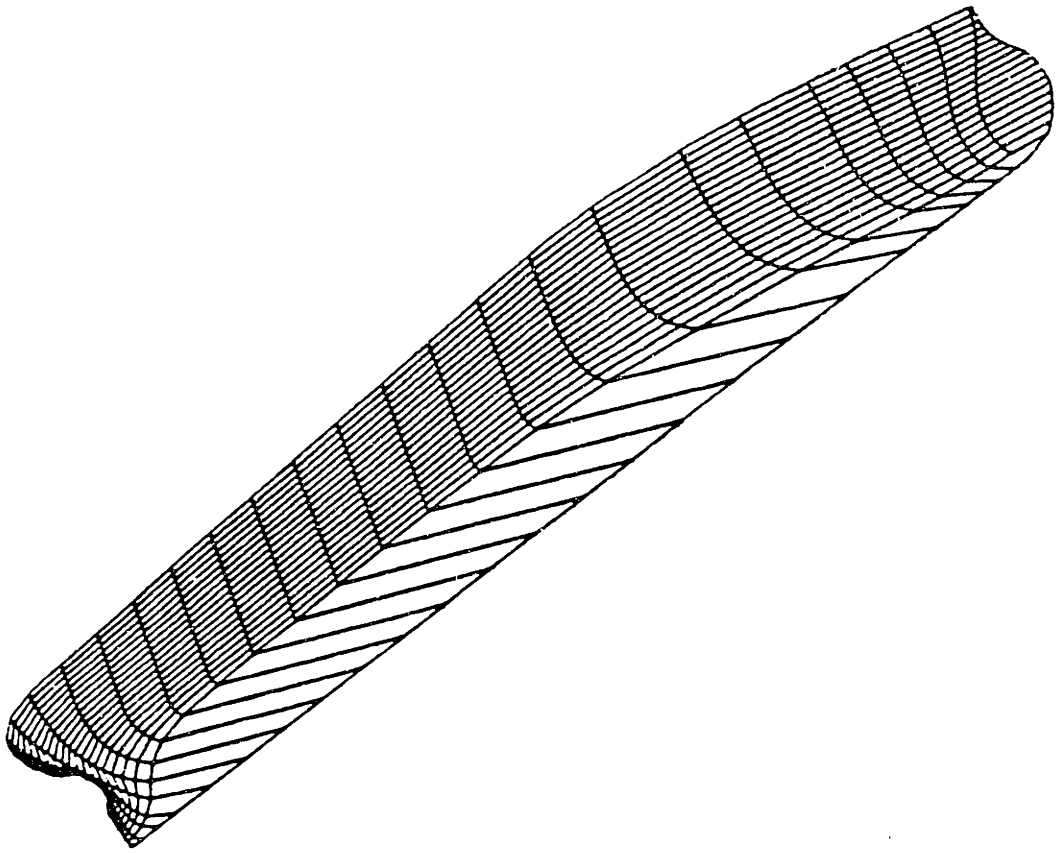

Figure 4.1: Panels of the Wetted Ship Surface(1)

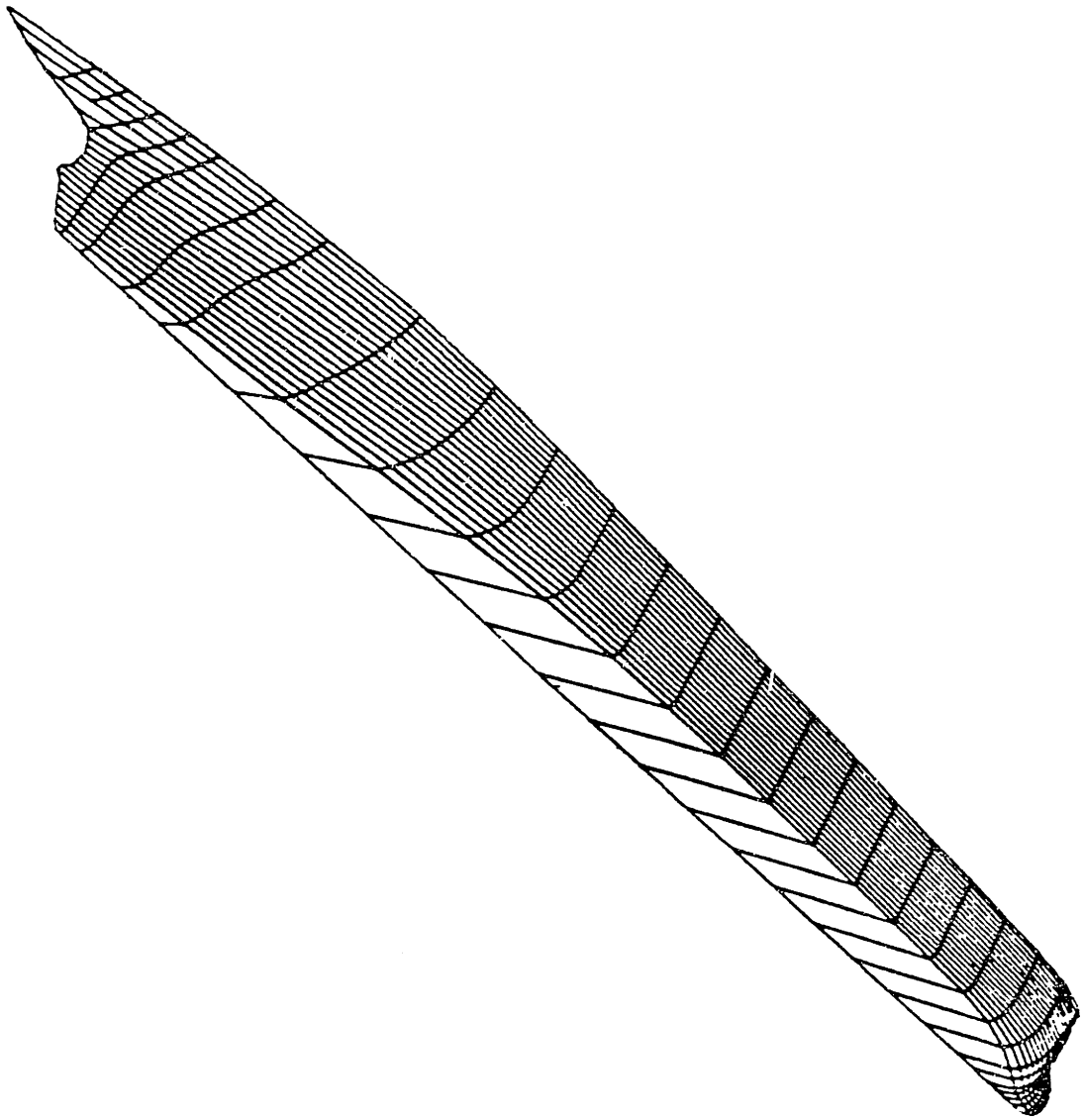

Figure 4.2: Panels of the Wetted Ship Surface(2)

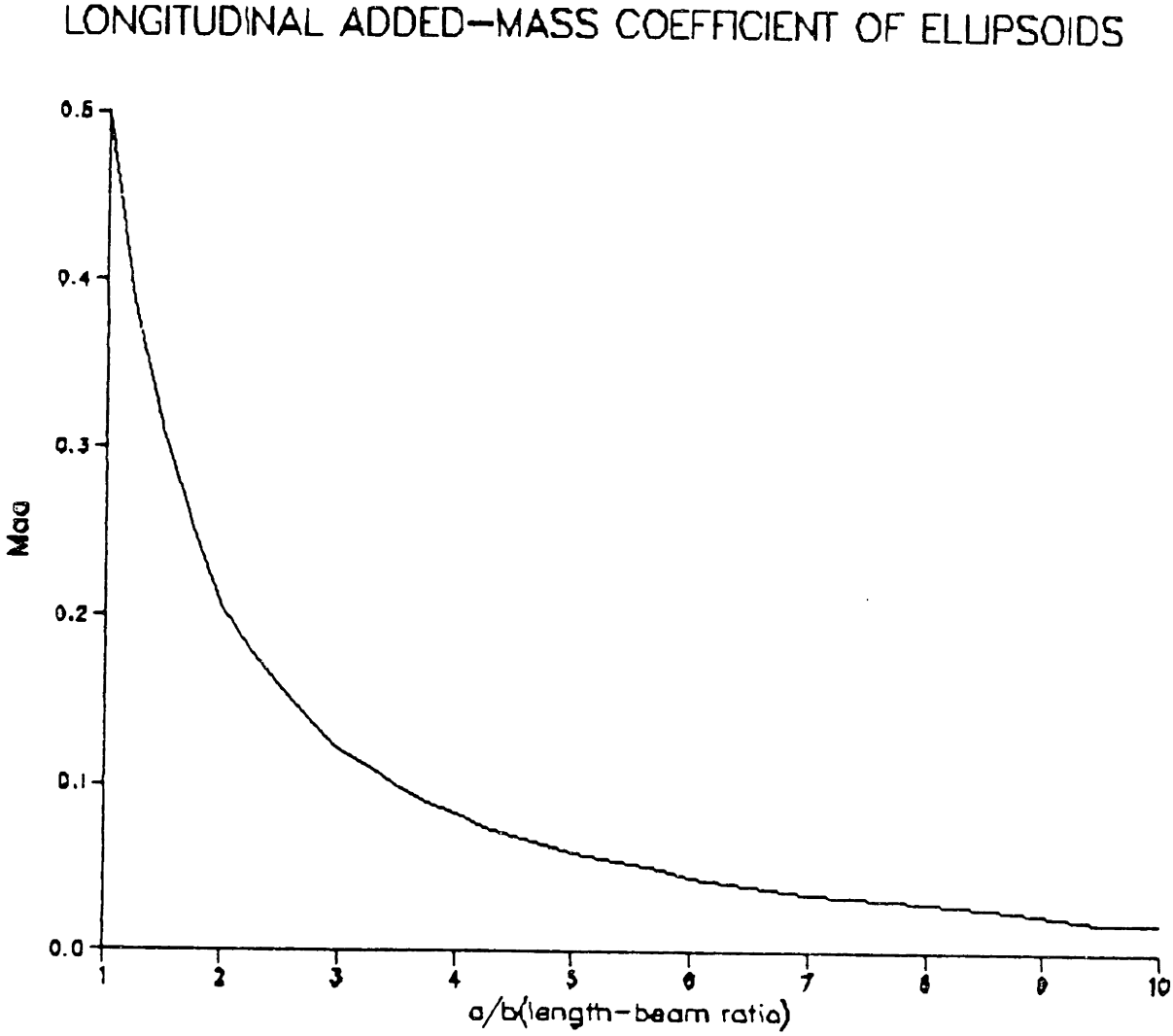

Figure 4.3: Curves of Added Masses for Ellipsoids

4.2 Propeller Coefficients

Although the added-mass coefficient $-X_{\dot{u}}$ of the ship is solved via a numerical method, to obtain the value of the ship resistance coefficient C_R, it is still necessary to know the values of η_{s1}, t and w first. There are two approaches with slight differences in solving for these three parameters. The starting point for both approaches is to make use of the thrust coefficient K_t curve of the model propeller from open water test.

4.2.1 Direct comparison method

This method is designed to get the ship resistance coefficient through direct comparison between identified values of η^**s* and those corresponding values from the model propeller K_t curve. Recall Equation(2.4) and Equation(2.6), the following relations hold:

$$\eta_{t1} = \eta_{s1}(1-t)(1-w)^2$$

$$\eta_2{}^* = \eta_{s2}(1-t)(1-w)$$

$$\eta_3{}^* = \eta_{s3}(1-t)$$

The differences in value between η_{t1}, $\eta_2{}^*$, $\eta_3{}^*$ and the η_s*s* of a propeller mounted on a ship is caused by the wake fraction w and the thrust deduction factor t. If η_s*s* are known then the resistance coefficient C_R as well as the wake fraction w and the thrust deduction factor t can be solved by steps from the above relations. Generally speaking, in comparison with ship

hulls, ship propellers suffer less from the "scale effect", because the scale ratio between a real propeller and its model is less than that between a real ship body and its model. The thrust coefficients of the model propeller $\eta_p's$ can be used for the derivation of the ship resistance coefficient C_R, the wake fraction w and the thrust deduction factor t, and then some adjustments will be made on t. $\overline{\eta}_3$ will help in the adjustment procedure as is shown later. Besides, $\overline{\eta}_3$ also helps to verify the condition of the ship propeller. Since $\overline{\eta}_3$ corresponds to a very low region of the advanced ratio J of the propeller, the mutual interaction between the ship hull and the ship propeller is negligible, so the thrust deduction factor t is near to zero. Consequently, $\overline{\eta}_3$ is close to η_{p3}. When the difference between $\overline{\eta}_3$ and η_{p3} is large and the estimated $\overline{\eta}_3$ is accurate, then most probably, the ship propeller is damaged. Investigation of the propeller condition should be made before the derivation of C_R is carried out. It should be remembered that when $\overline{\eta}_3$ is estimated through the identification techniques, the data used as input are corresponding to an interval with small but *non-zero* J values. Therefore $\overline{\eta}_3$ is not really equal to η_{p3}, and it cannot substitute η_{p3}. And because the input data set is small, to be sure the estimated value of $\overline{\eta}_3$ accurate, it should be checked carefully to see if its estimated value yields the surge speed simulation consistent with the measured data.

When the value of estimated $\overline{\eta}_3$ is very close to the value of η_{p3} from the propeller model test curve, combined with the identified $\eta^*'s$, C_R as well as w and t can be derived step by step as follows:

1. Take the model test value of lift-thrust coefficient η_{p3} as the first approximation of η_{s3}. From

$$1 - t = \frac{\eta_3^*}{\eta_{p3}} \tag{4.2}$$

the thrust deduction factor t is determined:

$$t = 1 - \frac{\eta_3^*}{\eta_{p3}} \tag{4.3}$$

The value of the thrust deduction factor t obtained here corresponds to the equilibrium state of the ship surge motion. Because the input data set used in the identification procedure corresponds to a surge speed interval close to the equilibrium state of the ship motion, during such an interval, the value of t converges to the expected value.

2. From

$$\begin{aligned} 1 - w &= \frac{\left(\frac{\eta_2^*}{\eta_3^*}\right)}{\left(\frac{\eta_{p2}}{\eta_{p3}}\right)} \\ &= \frac{\eta_2^* \eta_{p3}}{\eta_3^* \eta_{p2}} \end{aligned}$$

the wake fraction w is determined:

$$w = 1 - \frac{\eta_2^* \eta_{p3}}{\eta_3^* \eta_{p2}} \tag{4.4}$$

It is noticed that the value of w is directly calculated from the values of η_{p2} and η_{p3} without relying on the value of t obtained from the preceding step.

3. Based on the results from the first two steps, the value of $\eta_{\dagger 1}$ is obtained:

$$\eta_{\dagger 1} = \eta_{p1}(1-t)(1-w)^2 \tag{4.5}$$

$\eta_{\dagger 1}$ is an intermediate value for the calculation of the ship resistance coefficient C_R.

4. And then, the ship resistance coefficient can be determined through the following relation:

$$C_R = \frac{\eta_{\dagger 1} - \eta_1^*}{\frac{S}{2D^2}} \tag{4.6}$$

5. After the ship resistance coefficient C_R is obtained, make adjustment on the thrust deduction factor t and derive the ship propeller K_t based on the model propeller K_t curve as will be discussed in the following paragraphs.

The flow-chart of this method is shown in *Fig.* 4.4.

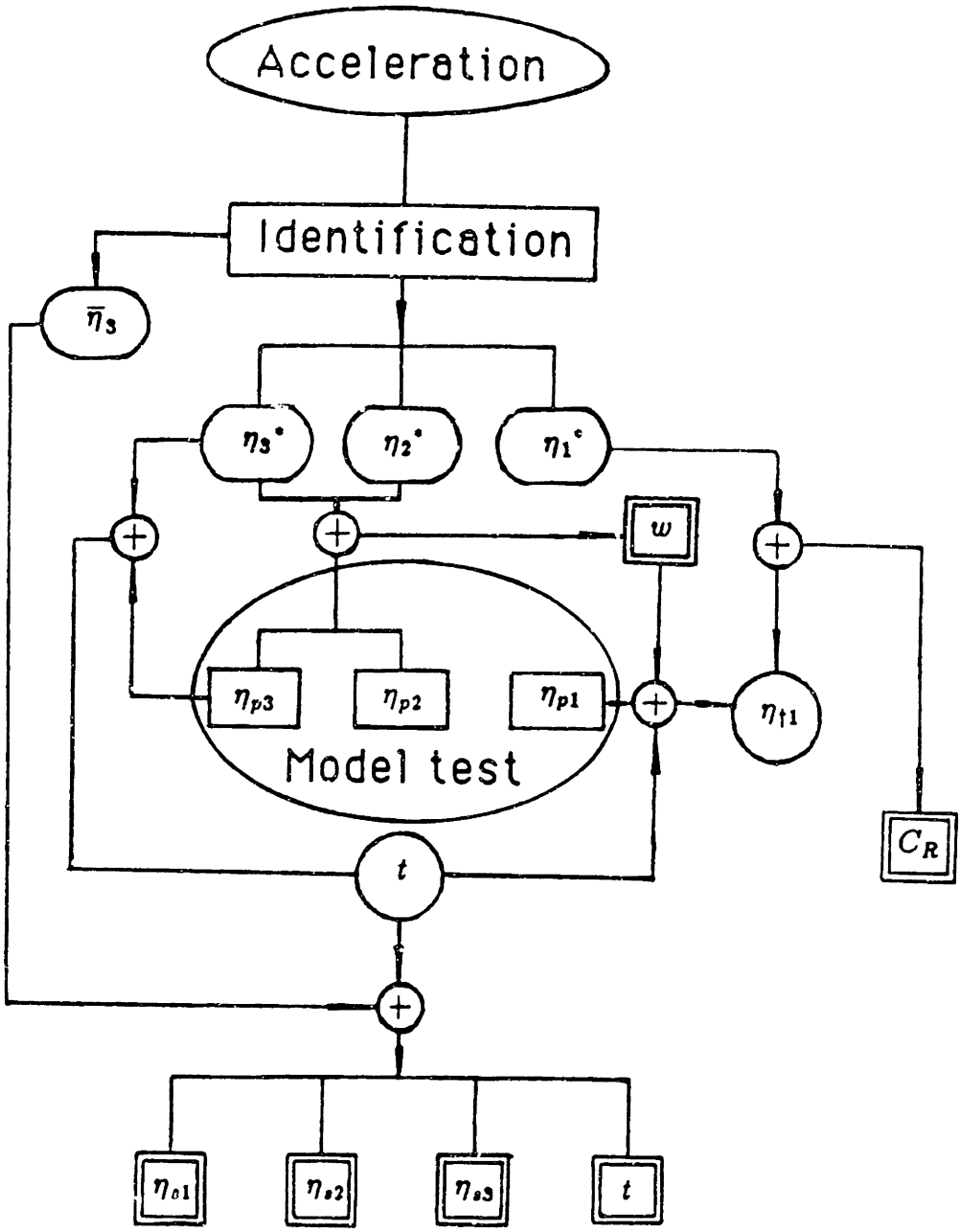

Figure 4.4: The Direct Comparison Method

Because of the aforementioned "scale effect", there is difference between the ship propeller K_t curve and its model test K_t curve. Moreover, the use of the model test values of the propeller thrust coefficients causes error in the derivation of t. The adjustment of the value of t can be made with the help from $\overline{\eta}_3$. To demonstrate how to make this adjustment, a property of t is first discussed. As written in articles and books on marine hydrodynamics, t is used to describe the effect on the propeller thrust forces by the mutual interaction between ship body and ship propeller. Originally, t is defined under the equilbrium condition of the ship surge motion. However, in ship motion research, t is used in the surge motion equation as presented in Chapter 2 of this thesis. The ship surge motion equation covers a large speed range from zero to the equilibrium. Hence, t should not be taken as a constant especially when the ship surge speed is very low, because the value of t changes drastically under that condition. Instead of considering the thrust deduction factor t directly, the study of the augmented resistance coefficient a provides an insight into the regularity of the variation of t. The augmented resistance coefficient a describes the interaction between the body of a ship and the propeller behind it. It says that the existence of the propller changes the distribution of the fluid field around the ship body, and therefore increases the hydrodynamic resistance on the ship. Comparing the two different forms of the ship surge equations:

$$\begin{cases} (m - X_{\dot{u}})\dot{u} &= (1-t)T - \frac{1}{2}\rho S C_R u^2 \\ (m - X_{\dot{u}})\dot{u} &= T - \frac{1}{2}\rho S C_R (1+a) u^2 \end{cases}$$

It follows that in general,

$$tT = \frac{1}{2}\rho S C_R a u^2$$

or

$$t = \frac{S C_R {J_p}^2}{2D^2 K_t (1-w)^2} a$$

where J_p is the advanced ratio of the ship propeller.

According to Abkowitz[4], modelling the propeller as an *actuator disk* and applying the momentum theorem, it follows that

$$a = 2\kappa(1-w)\left(\sqrt{1 + \frac{8K_t}{\pi {J_p}^2}} - 1\right) \tag{4.7}$$

where κ depends on the geometry of the ship(hull and propeller).

Hence

$$t = \frac{\kappa S C_R {J_p}^2}{D^2 K_t (1-w)}\left(\sqrt{1 + \frac{8K_t}{\pi {J_p}^2}} - 1\right) \tag{4.8}$$

or

$$\kappa = \frac{a_e}{2(1-w)\left(\sqrt{1 + \frac{8K_{te}}{\pi {J_e}^2}} - 1\right)} \tag{4.9}$$

where a_e, J_e and K_{te} are respectively the values of a, J_p and K_t at the equilibrium state.

Parameter κ can be determined by Equation(4.9) at the equilibrium state of the surge motion of the ship. Because at the equilibrium state the

value of t is derived from the identified results, and the advanced ratio J_e is also known, the only unknown is κ. By substituting for the determined value of κ in Equation(4.8), it follows that t is a function of the only variable J.

Now is the time to show how to adjust the t value with the help of $\overline{\eta}_3$ and the just established function of t. During the adjusting procedure, the ship propeller K_t curve can also be produced on the base of the model test K_t curve. The basic idea is that t_e—the value of the thrust deduction factor at the equilibrium state is obtained by assuming the ship propeller K_t curve being the same as the model test curve, but this is inaccurate. This inaccuracy leads to the inconsistency of the t value corresponding to $\overline{\eta}_3$ when it is obtained by the following two different ways:

1. By comparing $\overline{\eta}_3$ with the model test η_{p3}

$$\bar{t} = \frac{\overline{\eta}_3}{\eta_{p3}} \tag{4.10}$$

2. By using the formula just established

$$\bar{t} = \frac{\kappa S C_R \overline{J}_p^{\,2}}{D^2 \overline{K}_t (1-w)} \left(\sqrt{1 + \frac{8\overline{K}_t}{\pi \overline{J}_p^{\,2}}} - 1 \right) \tag{4.11}$$

In order to get rid of this inconsistency, starting from the equilibrium state t value t_e, the following steps are followed.

1. First obtain the value of $\bar{t}$ corresponding to $\overline{\eta}_3$ by plugging the values of $\overline{J}_p$ and $\overline{K}_t$ in Equation(4.11).

2. Then bring this $\bar{t}$ value back to Equation(4.10) to obtained an updated η_{s3} which is taken as the value of that ship propeller thrust coefficient.

3. Bring this updated η_{s3} into Equation(4.3), then an updated t_e will be obtained.

4. If the updated t_e is the same as before, then stop. Otherwise, repeat the whole procedure until the inconsistency disappears.

This iteration process will lead to a proper t_e value, and at the same time give a reasonable K_t curve for the ship propeller, by making an adjustment on the model test K_t curve. Iteration on the t_e value of the propeller of EXXON PHILADELPHIA following this principle is presented in Chapter 6.

4.2.2 Recurrence method

This method combines two procedures: the deceleration procedure with the propeller wind-milling and the acceleration procedure. The basic idea is as follows:

1. The data obtained from the deceleration procedure are used to identify the *integrated resistance coefficient* $\overline{C}_R$, which as mentioned before is the sum of a part corresponding to the resistance of the ship body and a part corresponding to the resistance caused by the wind-milling propeller. Since $\overline{C}_R$ is the only unknown parameter in the

equation for the deceleration maneuver, the result of identification should be accurate.

2. Using the measured data u_{wm} and n_{wm} during the deceleration procedure, the advanced ratio of the propeller mounted on the ship can be determined from the following relation:

$$J_{wm} = J_{awm}(1 - w)$$

where $J_a = \frac{u}{nD}$ is called the *apparent advanced ratio* because u is the speed of the ship not the speed of the flow approaching the propeller. It can be seen that when u is replaced by u_{wm}, then J_{awm} should be a constant and it can be identified from the measurements. w is obtained from Equation(4.4) based on the measured data in the acceleration procedure.

3. Similarly as in the direct comparison method, use the identified value of $\eta_3{}^*$ and the value of η_{p3} obtained from the model test K_t curve to calculate the value of the thrust deduction factor t at the equilibrium state of the surge motion of the ship.

4. Recall Equation(4.9), κ can be determined when the values of a, K_t and J at equilibrium state are known. And once κ is determined, a_{wm} is then obtained immediately.

5. The ship resistance coefficient C_R can be obtained through Equation (4.12) which is derived as follows:

$$(1+a_{wm})\frac{1}{2}\rho S C_R u^2 - \rho n^2 D^4 K_{twm} = \frac{1}{2}\rho S \overline{C}_R u^2$$

$$(1+a_{wm})\frac{1}{2}\rho S C_R u^2 = \frac{1}{2}\rho S \overline{C}_R u^2 + \rho n^2 D^4 K_{twm}$$

Then,

$$C_R = \frac{1}{1+a_{wm}}(\overline{C}_R + \frac{2D^2 K_{twm}}{{J_{awm}}^2 S})$$

or

$$C_R = \frac{1}{1+a_{wm}}(\overline{C}_R + \frac{2D^2 K_{twm}(1-w)^2}{{J_{wm}}^2 S}) \qquad (4.12)$$

6. Similarly, t_{wm} rather then a_{wm} can be used in solving C_R.

$$\frac{1}{2}\rho S C_R u^2 - \rho n^2 D^4 K_{twm}(1-t_{wm}) = \frac{1}{2}\rho S \overline{C}_R u^2$$

or

$$\frac{1}{2}\rho S C_R u^2 = \frac{1}{2}\rho S \overline{C}_R u^2 + \rho n^2 D^4 K_{twm}(1-t_{wm})$$

Then,

$$C_R = \overline{C}_R + \frac{2D^2 K_{twm}(1-t_{wm})}{{J_{awm}}^2 S}$$

or

$$C_R = \overline{C}_R + \frac{2D^2 K_{twm}(1-t_{wm})(1-w)^2}{{J_{wm}}^2 S} \qquad (4.13)$$

Since K_{twm} is small (of the order of 5% of $\overline{C}_R$), small errors in the estimation of K_{twm} and t_{wm} will not cause intolerable error in the estimation of C_R.

7. Following the procedure mentioned in the direct comparison method, identify the value of $\overline{\eta}_3$ through EKF technique by using the data measured during the acceleration procedure as the input. Based on the identified value of $\overline{\eta}_3$, calculate the corresponding $\bar{t}$ and check whether it is consistent with the value obtained through Equation(4.10). If it is consistent, then stop. Otherwise, make an adjustment on the K_t curve of the propeller of the ship. And then using the adjusted propeller thrust coefficients $\eta_s's$ as input, repeat the above steps until the inconsistency disappears.

Both methods are used in the estimation of the resistance coefficient for the tanker EXXON PHILADELPHIA, the results from these two different methods are consistent. From the previous discussion, it is clear that as the goal of identifying the ship resistance coefficient C_R is pursued, the ship propeller thrust coefficients η_{s1}, η_{s2} and η_{s3}, the wake fraction w and the thrust deduction factor t of the ship can also be obtained as by-products. From the results presented in Chapter 6, it will be seen that the resulting values are reasonable, and consistent with theory. This is the first time that the value of t and w of the real ship are "measured" through sea trial. This will benefit research in ship hydrodynamics, especially the research and design of ship propellers.

The flow-chart of this method is shown in *Fig.* 4.5.

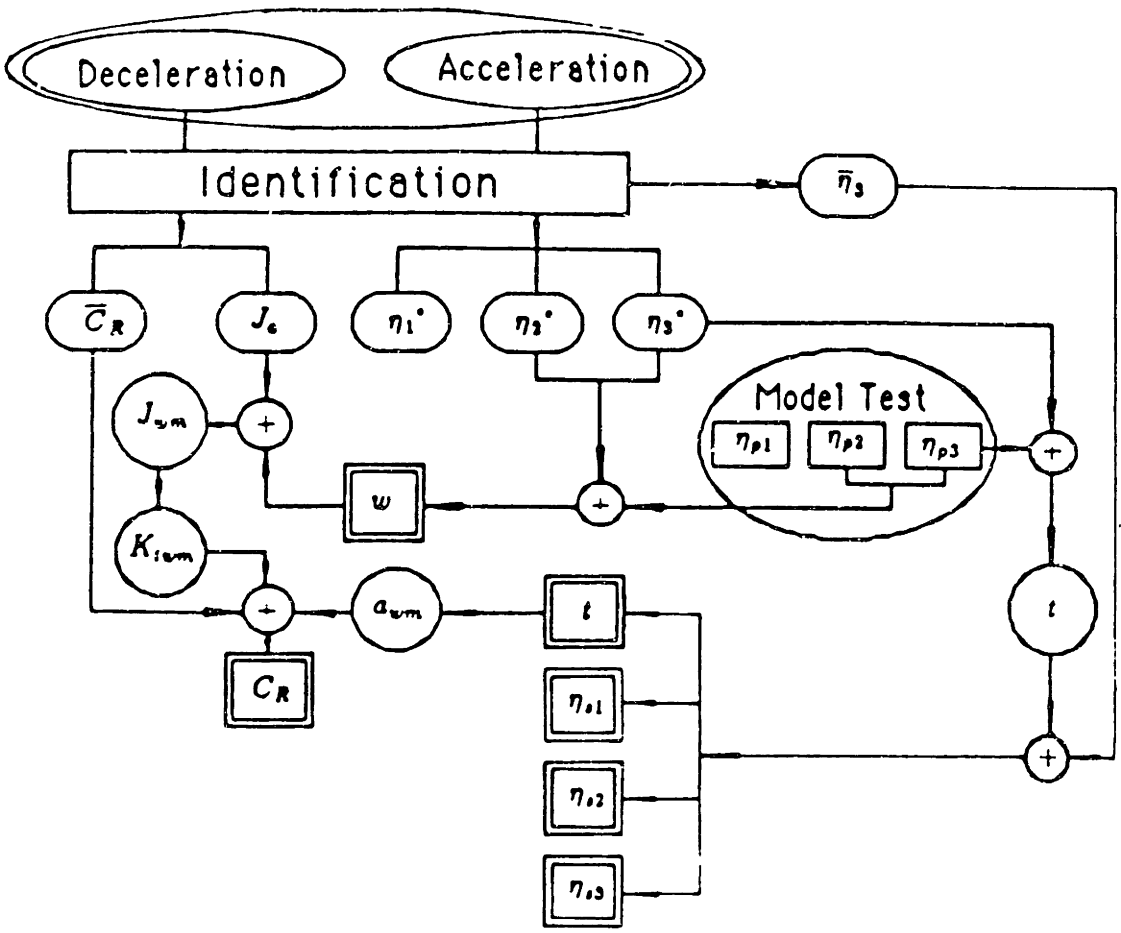

Figure 4.5: The Recurrence Method

Chapter 5

Identification Techniques

Once the sea trial is over and the necessary data have been collected, the next step is to apply these data to the surge motion model and to get the estimated value of the integrated ship resistance coefficient $\overline{C}_R$ in the deceleration procedure and of the coefficients η_1^*, η_2^* and η_3^* in the acceleration procedure. As mentioned before, to obtain satisfactory identification results, three important factors are

- A reasonable model which is able to appropriately describe the dynamic characteristics of interest in the system;
- A carefully designed and conducted experiment which leads to the collection of most informative data for the use in identification;
- An intelligently chosen identification technique which can effectively apply the collected data to the system model will produce accurate

estimations of the coefficients.

An improperly chosen identification technique in some instances will bring about unnecessary burden of calculations and in some other instances it will result in wrong or inaccurate estimation, even though the collected data are most informative.

For stochastic dynamic systems, identification techniques are, in the final analysis, algorithms developed for processing the measured data. When the structure of the system model is known, as in the case of the ship resistance coefficient estimation, the principle of algorithm development is either to make the error in the estimation minimum, or to maximize the likelihood function. To achieve this goal, the starting point of analysis is the index function of the covariance of the observed variables, or the likelihood function of the system which is the conditional probability function for the measurement at the given value of the coefficients. These functions depend upon both the system model structures and the choice of the identification technique. According to the difference in model structure, systems are divided into linear systems and nonlinear systems. For linear systems, all their system equations are linear in the state variables. All systems other than linear systems are nonlinear systems. A lot of research work has been done on linear systems. Because of the simplicity of the equation forms, algorithms of identification for linear systems have been fully developed and can be found in literature. However, for nonlinear systems, few

detailed algorithms have been developed, and a lot of preliminary analyses are needed when a specific system is dealt with.

Evidently, the system equation of ship surge motion is nonlinear. Therefore, when considering the estimation of the hydrodynamic coefficients in the ship surge equation, nonlinear identification techniques are naturally considered first. Among identification techniques for nonlinear systems, the EKF technique is one of the most widely used. The success of using EKF in estimating both linear and nonlinear hydrodynamic coefficients in the system model of ship maneuvering had been very encouraging for its application to the ship resistance coefficient estimation problem[3][12] [15]. Furthermore, the results of estimating the ship resistance coefficient by applying EKF to the system model with simulated data as the measurements were reasonably accurate. Consequently, EKF is the main identification technique in the practical estimation of the ship resistance coefficient.

However, unlike the nonlinear systems with complicated form, the ship surge motion equation is linear in the hydrodynamic coefficients $\overline{C}_R$ and η_1^*, η_2^* and η_3^*. As a try, the application of some linear system identification techniques with proper adjustment had been considered. In this chapter, besides EKF, two linear identification techniques— the recursive least squares technique and the recursive instrumental variable technique are discussed.

5.1 EKF Technique

5.1.1 Kalman filtering

The *Kalman filtering technique* is the most widely used optimal filtering technique for estimating the state of a linear system. Kalman filtering is a recursive algorithm for estimating the state variables of the linear systems with known system models. It gives the optimal estimation of the state variables in the sense that the variance of the estimated variables are minimized.

For a linear system with the following system model and measurement model:

$$\begin{cases} \dot{\underline{x}} &= A\underline{x} + \underline{\varepsilon} \qquad \underline{\varepsilon} \sim N(\underline{0}, Q) \\ \underline{y}_k &= H_k \underline{x}_k + \underline{v}_k \quad k = 1, 2, \ldots, \underline{v}_k \sim N(\underline{0}, R_k) \end{cases}$$

where $N(\underline{0}, Q)$ and $N(\underline{0}, R_k)$ represent the normal distributions with zero mean and variance matrices Q and R_k respectively; and k is the number of time steps for a discrete process.

The *continous-discrete Kalman filter* for this system is as follows:

$$\dot{\hat{\underline{x}}} = A\hat{\underline{x}} \tag{5.1}$$

$$\dot{P} = A\hat{\underline{x}}P + PA^T\hat{\underline{x}} + Q \tag{5.2}$$

$$\hat{\underline{x}}_{k(+)} = \hat{\underline{x}}_{k(-)} + K_k[\underline{y}_k - H_k\hat{\underline{x}}_{k(-)}] \tag{5.3}$$

$$P_{k(+)} = [1 - K_k H_k] P_{k(-)} \tag{5.4}$$

$$K_k = P_{k(-)} H_k{}^T [H_k P_{k(-)} H_k{}^T + R_k]^{-1} \tag{5.5}$$

where $\hat{\underline{x}}$ is the estimated state variable vector, $P_{k(-)}$ and $P_{k(+)}$ are the error covariance matrices before and after the kth time step. K_k is the *Kalman gain matrix* at the kth time step. And equations in (5.1) are referred to as the *Kalman filter propagation equations*[7][14].

The Kalman filter provides a simple and elegant solution to the problem of estimating the state variables in a linear finite-dimensional stochastic dynamic system, and is very convenient for computer programing. However, since the linearity of the system equations plays an important role in its derivation and performance as an optimal filter, the Kalman filter is not strictly applicable for nonlinear system state estimation. And even for linear systems, the Kalman filter technique can not be applied to the problem of parameter estimation and state variable estimation with unknown parameters. The reason is that in order to estimate the unknown parameters in a linear system, the unknown parameters have to be taken as augmented state variables and hence a new system is built up. This new system is generally nonlinear. To overcome this difficulty, the EKF technique has been developed.

5.1.2 Extended Kalman filtering technique

The derivation of the EKF is based on the same principle of minimizing the variance of the estimated state variables of a system. The linearity of the system equations is not a prerequisite.

For a nonlinear system with the following state model and measurement model:

$$\begin{cases} \dot{\underline{x}} &= \underline{f}(\underline{x},t) + \underline{\varepsilon} \qquad \underline{\varepsilon} \sim N(\underline{0},Q) \\ \underline{y}_k &= \underline{h}_k(\underline{x}(t_k)) + \underline{v}_k \quad k = 1,2,\ldots,\underline{v}_k \sim N(\underline{0},R_k) \end{cases}$$

the *continuous-discrete extended Kalman filter* for this system is

$$\dot{\hat{\underline{x}}} = f(\hat{\underline{x}},t) \tag{5.6}$$

$$\dot{P} = F(\hat{\underline{x}},t)P + PF^T(\hat{\underline{x}},t) + Q \tag{5.7}$$

$$\hat{\underline{x}}_{k(+)} = \hat{\underline{x}}_{k(-)} + K_k[\underline{y}_k - \underline{h}_k(\underline{x}(t_k))] \tag{5.8}$$

$$P_{k(+)} = [I - K_k H_k{}^T(\hat{\underline{x}}_{k(-)})]P_{k(-)} \tag{5.9}$$

$$K_k = P_{k(-)}H_k{}^T(\hat{\underline{x}}_{k(-)})[H_k(\hat{\underline{x}}_{k(-)})P_{k(-)}H_k{}^T(\hat{\underline{x}}_{k(-)}) + R_k]^{-1} \tag{5.10}$$

where

$$F(\hat{\underline{x}},t) = \frac{\partial \underline{f}(\underline{x},t)}{\partial \underline{x}}\Big\|_{\underline{x}=\hat{\underline{x}}}$$

$$H_k(\hat{\underline{x}}_{k(-)}) = \frac{\partial \underline{h}_k(\underline{x}(t_k))}{\partial \underline{x}(t_k)}\Big\|_{\underline{x}(t_k)=\hat{\underline{x}}_{k(-)}}$$

Comparing the propagation equations with that of the Kalman filter, their structures are similar, and that is the reason it bears the name of "Kalman". Generally speaking, since the matrix P_k in Equation (5.6) is only an approximation to the true covariance matrix, there is no guarantee that the actual estimate obtained will be close to the true optimal estimate. Note that for the ship surge motion equation, the measurement equation is exactly a linear function. And for a short time interval(compared with the system time constant), the solutions of the EKF propagation equations should be accurate enough for approximating the true results. Hence the results of estimation should be reasonably accurate. The results derived from the EKF to hydrodynamic coefficient estimation of ship maneuvering support this conclusion. Even so, the results of the estimation by using the reality.

5.2 Recursive Least Squares Method

As mentioned before, the ship surge motion equation is nonlinear in the state variable u and input variable n, but linear in parameters η_1^*, η_2^* and η_3^*. This special property inspires the idea of trying to apply identification algorithms for the linear systems to ship surge motion system with some adjustment. One of the linear identification techniques to be tried is the least squares technique.

The basic idea of the least squares technique is that for a discrete linear

system described by the following equation[9][16][22]:

$$\underline{y} = \underline{x}\underline{\psi} + \underline{\varepsilon} \tag{5.11}$$

where $\underline{\psi}$ is a parameter vector, $\underline{\varepsilon}$ is the noise of the system model and $\underline{\varepsilon} \sim N(\underline{0}, Q)$.

The estimated parameter vector by applying the least squares technique is in the following form:

$$\underline{\hat{\psi}} = (\underline{x}^T \underline{x})^{-1} \underline{x}^T \underline{y} \tag{5.12}$$

To apply this technique to the estimation of the hydrodynamic coefficients in ship surge motion equation, the procedure shown below is followed.

1. The ship surge motion equation is converted into discrete form as[1]

$$\Delta u_k = h(\eta_1^* u^2 + \eta_2^* un + \eta_3^* n^2) + \varepsilon_k \tag{5.13}$$

where h is the time interval between the kth and the $(k+1)$th time step, and Δu_k is the difference of surge speed u at the kth and the $(k+1)$th time step:

$$\Delta u_k = u_{k+1} - u_k$$

2. Introduce the expressions:

$$y_k = \Delta u_k$$

$$\underline{\hat{\eta}}_k = \begin{bmatrix} \hat{\eta}_1 \\ \hat{\eta}_2 \\ \hat{\eta}_3 \end{bmatrix}_k$$

Then the equation becomes

$$y_k = \underline{x}_k{}^T \underline{\hat{\eta}}_k \tag{5.14}$$

3. Apply the recursive least squares technique to it, the algorithm of calculating $\underline{\hat{\eta}}$ is as follows:[22]

$$\underline{\hat{\eta}}_k = \underline{\hat{\eta}}_{k-1} - P_{k-1}{}^* \underline{x}_k (\hat{Q} + \underline{x}_k{}^T P_{k-1}{}^* \underline{x}_k)^{-1} (\underline{x}^T{}_k \underline{\hat{\eta}}_{k-1} - y_k) \tag{5.15}$$

$$P_k{}^* = P_{k-1}{}^* - P_{k-1}{}^* \underline{x}_k (\hat{Q} + \underline{x}_k{}^T P_{k-1}{}^* \underline{x}_k)^{-1} \underline{x}_k{}^T P_{k-1}{}^* \tag{5.16}$$

where $P_k{}^* = QP_k$, $P_k = X^T X^{-1}$, and X is a $k \times 3$ matrix with $\underline{x}_k{}^T$ as its kth row.

The recursive least squares estimator has been proven very successful for linear systems. Because of its simple form, it is an attractive method. However, the assumption of uncorrelatedness of noise $\underline{\varepsilon}_n$ limited its use, since the failure of this condition generally result in biased estimates[9].

5.3 Recursive Instrumental Variable Technique

One of the identification techniques which is aimed at overcoming the problem caused by the correlated noise is the instrumental variable technique. Its basic idea is to replace the matrix X in the least squares method by a carefully built matrix Z. Matrix Z satisfies two conditions:

1. Z is closely related to X, that is $Z^T X$ should not be singular.
2. $Z^T Q$ tends to 0 with probability 1. That is the variables $\underline{z}$ consisting matrix Z are uncorrelated to the noise of $\underline{\varepsilon}_n$. Variable $\underline{z}$ is referred to as an *instrumental variable vector.*

Theoretically, the instrumental variable technique leads to better estimation results. But the results depend on the choice of the instrumental variables[20][16][22].

The recursive instrumental variable algorithm shown below is used for the identification of $\eta^{*'}s$.

$$\underline{\hat{\eta}}_k = \underline{\hat{\eta}}_{k-1} - P_{k-1}{}^* \underline{z}_k (\hat{Q} + \underline{z}_k{}^T P_{k-1}{}^* \underline{x}_k)^{-1} \underline{x}^T{}_k \underline{\hat{\eta}}_{k-1} - u_k \tag{5.17}$$

$$P_k{}^* = P_{k-1}{}^* - P_{k-1}{}^* \underline{z}_k (\hat{Q} + \underline{z}_k{}^T P_{k-1}{}^* \underline{x}_k)^{-1} \underline{x}_k{}^T P_{k-1}{}^* \tag{5.18}$$

where $\underline{z}$ is the instrumental variable vector:

$$\underline{z}_k = \begin{bmatrix} \hat{u}^2 \\ \hat{u}\hat{n} \\ \hat{n}^2 \end{bmatrix}_k$$

generated from

$$\Delta y_k = \underline{\hat{\eta}}^T{}_{k-1} \underline{z}_k \tag{5.19}$$

$\hat{n}$ is the filtered value of n from the measurement data. The instrumental variable method is as simple a technique as the least squares technique, but it can lead to improved estimation results. The appeal of this technique is that it does not require detailed a priori information of the noise statitics to yield consistent, asymptotically unbiased estimates.

Chapter 6

Results and Discussions

Based on the methodology developed in the previous chapters, the data measured onboard the tanker EXXON PHILADELPHIA on her voyage between Valdez, Alaska and San Francisco along the West Coast were processed in several steps. The whole process went through very smoothly. With EFK as the chosen identification technique, the obtained results indicated that the resistance coefficient C_R of the tanker was estimated accurately, and that the ship propeller thrust coefficients η_{s1}, η_{s2} and η_{s3}; the wake fraction w and the thrust deduction factor t were all estimated with satisfactary accuracy. To make this procedure clear, all the intermediate and final results are presented in this chapter. Moreover, the identification results of η_1^*, η_2^* and η_3^* by applying the recursive least squares technique and the recursive instrumental variable technique are also presented.

6.1 Results of System Identification

During the identification, the basic parameters of the system were as follows:

- Displacement of the tanker(m): 91,500 *long-ton* or 6.38×10^5 *slugs*
- Added-mass($-X_{\dot{u}}$): $0.0471m$—from MIT Radiation and Refraction Program.
- Overall lenghth(L): 763 *feet*
- Wetted surface area(S): $1.35 \times 10^5\ ft^2$
- Diameter of the ship propeller(D): 26.9 *feet*
- Model drag-thrust coefficient(η_{p1}): -0.1725
- Model associated drag-thrust coefficient(η_{p2}): -0.2415
- Model lift-thrust coefficient(η_{p3}): 0.3796
- Model wake fraction(w): 0.383
- Model thrust deduction factor(t): 0.216
- Water density(ρ): $1.9928\ slug/ft^3$

6.1.1 Result of estimated $\overline{C}_R$

$\overline{C}_R$ is one of the intermediate results of the whole process. It is estimated by applying the EKF technique with the data measured from the deceleration procedure. To avoid signals with low signal-to-noise ratio, only that part of the measurement data corresponding to the velocities changing from full speed to $\frac{2}{3}$ of the full speed were processed. Three figures are presented here to illustrate the identification procedure and its result. In *Fig.* 6.1, the filtering procedure of the EKF is displayed along with the input data u. *Fig.* 6.2 is the estimated $\overline{C}_R$ in the first iteration of identification. In that first iteration, the initial value of $\overline{C}_R$ is a rough guess. *Fig.* 6.3 represents $\overline{C}_R$ after the second iteration of identification. In this iteration, the initial value is based on the identification result from the first iteration. For coefficients in general to reach the final result, several iterations(usually less than 5 iterations) might be needed, until the estimate converges to a proper value. The validity of the identified results is checked through statistical hypothsis testing statistics.[12] As the final step, to find whether the estimated values of the coefficients proper or not, just bring them back into the system equations and see if the simulated results are consistent with the corresponding measured data.

The final result of the estimate is

$$\overline{C}_R = 0.00238$$

During the deceleration procedure, the ship propeller was kept wind-

milling as mentioned before, hence the apparent propeller advanced ratio $J_{awm} = \frac{u}{nD}$ is maintained constant. The identified apparent advanced ratio J_{awm} is presented in *Fig.* 6.4.

Once w is identified from the acceleration maneuver, the actual advanced ratio J_{wm} of the wind-milling propeller is obtained through the relation:

$$J_{wm} = \frac{u(1-w)}{nD}$$

The identified value of apparent advanced ratio is

$$J_{awm} = 1.36$$

and the advanced ratio for the ship propeller is

$$J_{wm} = 1.03$$

This value will be used later for deriving the ship resistance coefficient C_R and the thrust deduction factor t through working at the propeller thrust curve.(See Section 6.22)

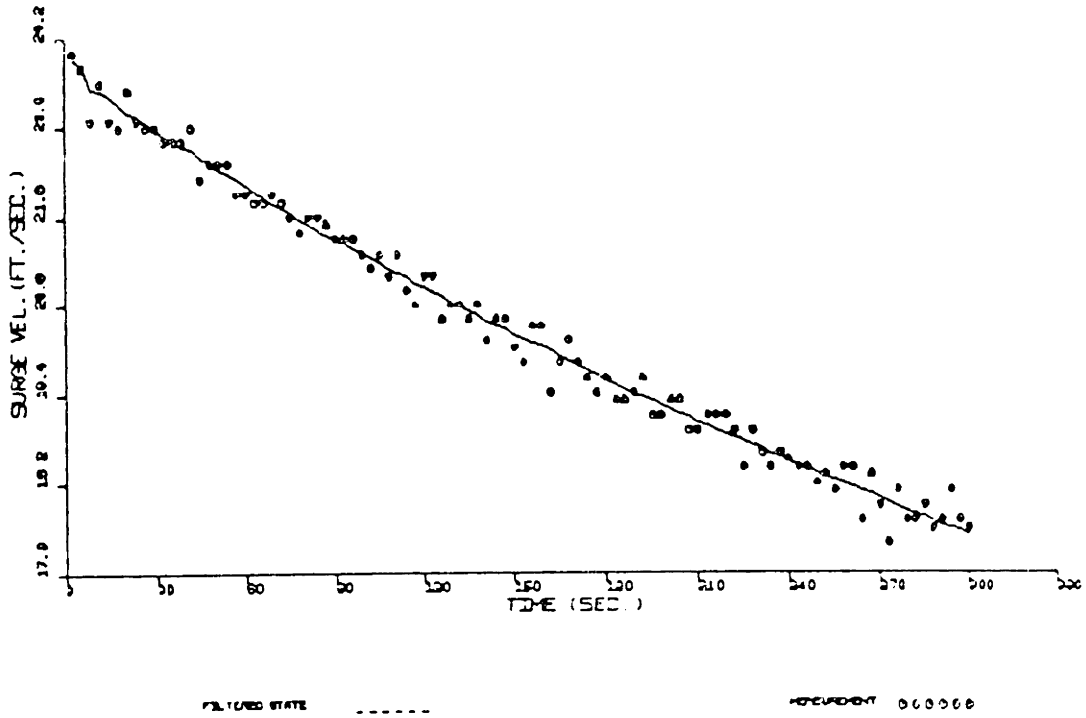

Figure 6.1: Measurement and Estimation of u during Identification

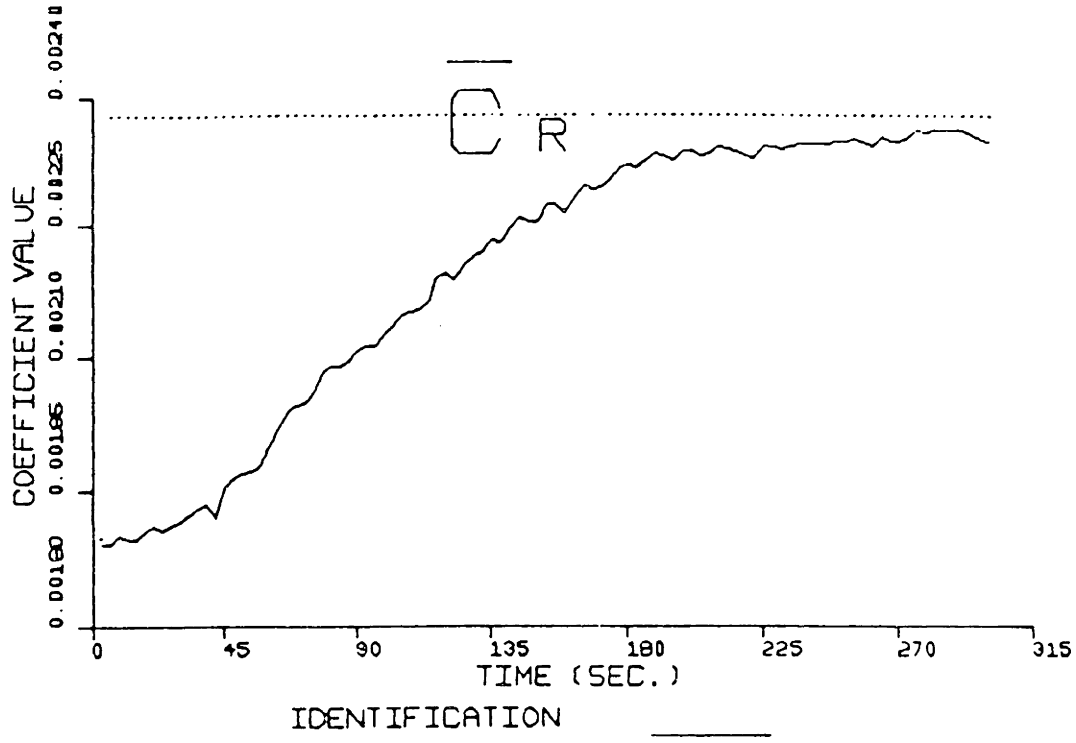

Figure 6.2: Estimate of $\overline{C}_R$ in Iteration One

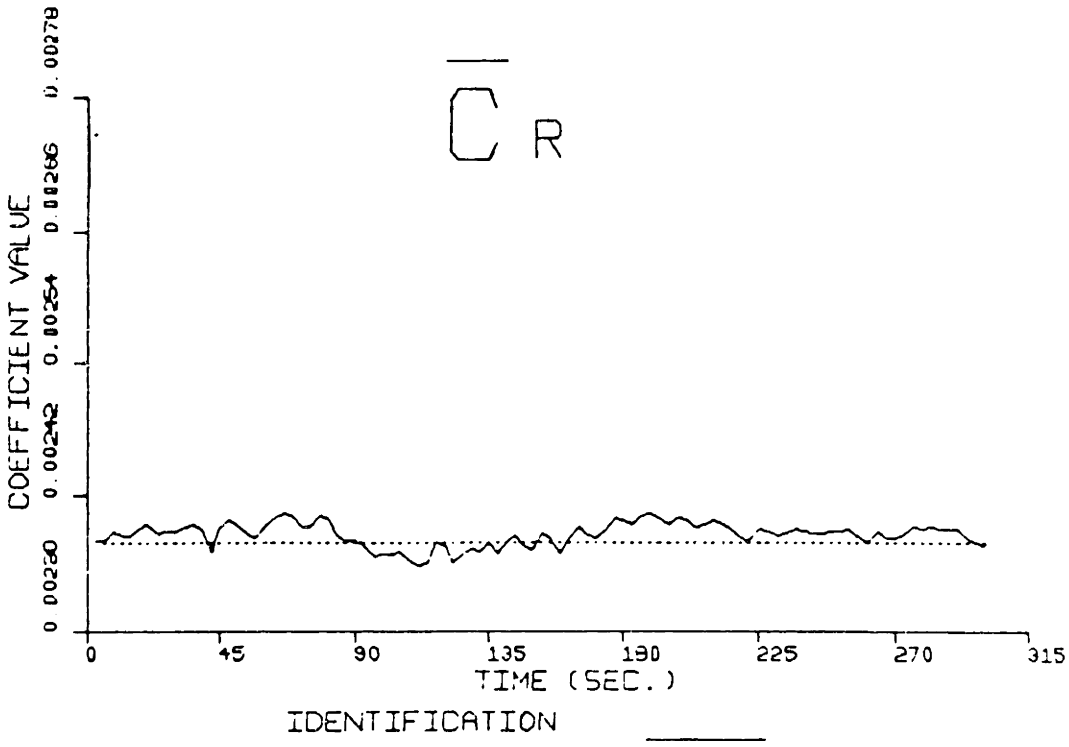

Figure 6.3: Estimate of $\overline{C}_R$ in Iteration Two

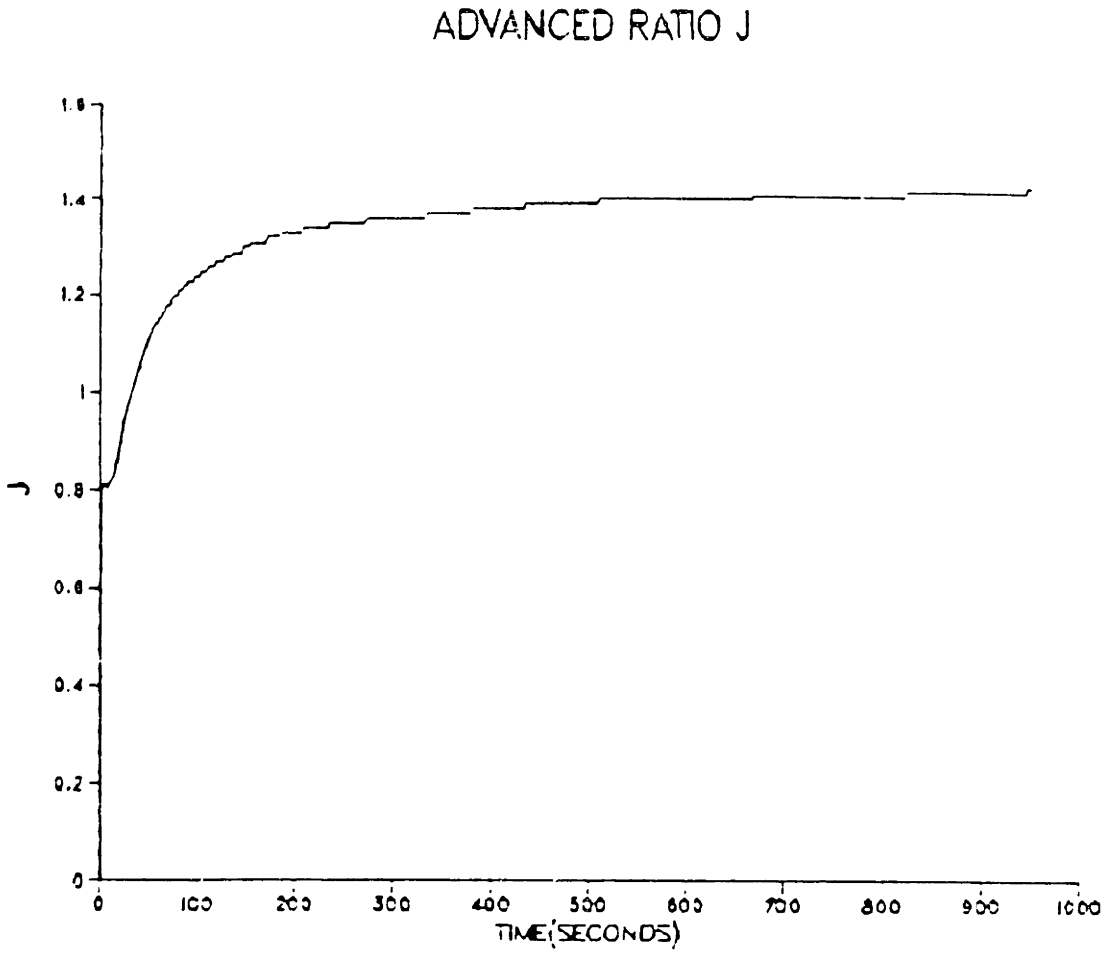

Figure 6.4: Estimated Apparent Advanced Ratio J_{awm}

6.1.2 Identified $\overline{\eta}_3$ at low J value

Identification of $\overline{\eta}_3$ at low J value region has two purposes as mentioned in Chapter 4. One is to use the estimated value of $\overline{\eta}_3$ in verifying the ship propeller condition. If there is evident difference between $\overline{\eta}_3$ and η_3, then investigation of the ship propeller condition is needed. The other is to use the estimated value of $\overline{\eta}_3$ in deriving the ship resistance coefficient C_R and the thrust deduction factor t, and the ship propeller thrust coefficients $\eta_s's$ together. $\overline{\eta}_3$ is used with both the direct comparison method and the recurrence method through slightly different procedures.

As in the identification of $\overline{C}_R$, in the procedure of identifying $\overline{\eta}_3$, the initial part of the measured data was omitted because of the low signal-to-noise ratio. At the same time, to avoid the influence of the increasing thrust deduction factor t during the estimation of $\overline{\eta}_3$, only the data ranging over 200 *seconds* are used in the range of slow speed. The curves of the estimated $\overline{\eta}_3$ for the first two iterations are shown in *Fig.* 6.5 and *Fig.* 6.6. Since the input data set is small, the result of estimation should be examined carefully.

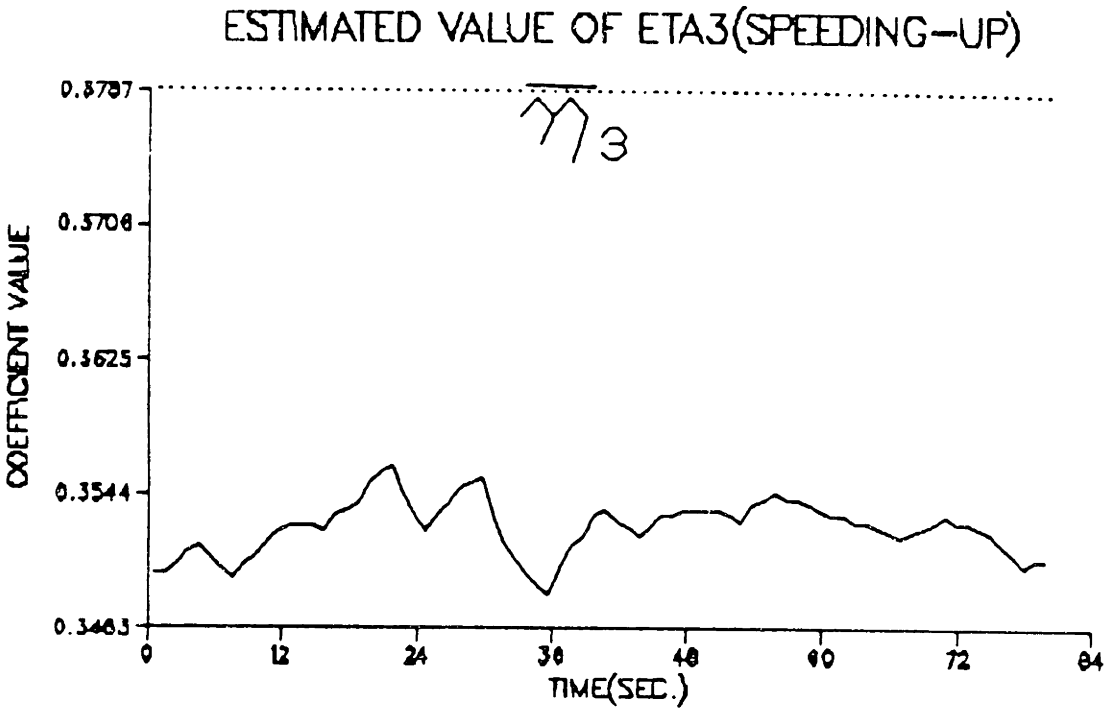

Figure 6.5: Estimation of $\overline{\eta}_3$ in Interation One

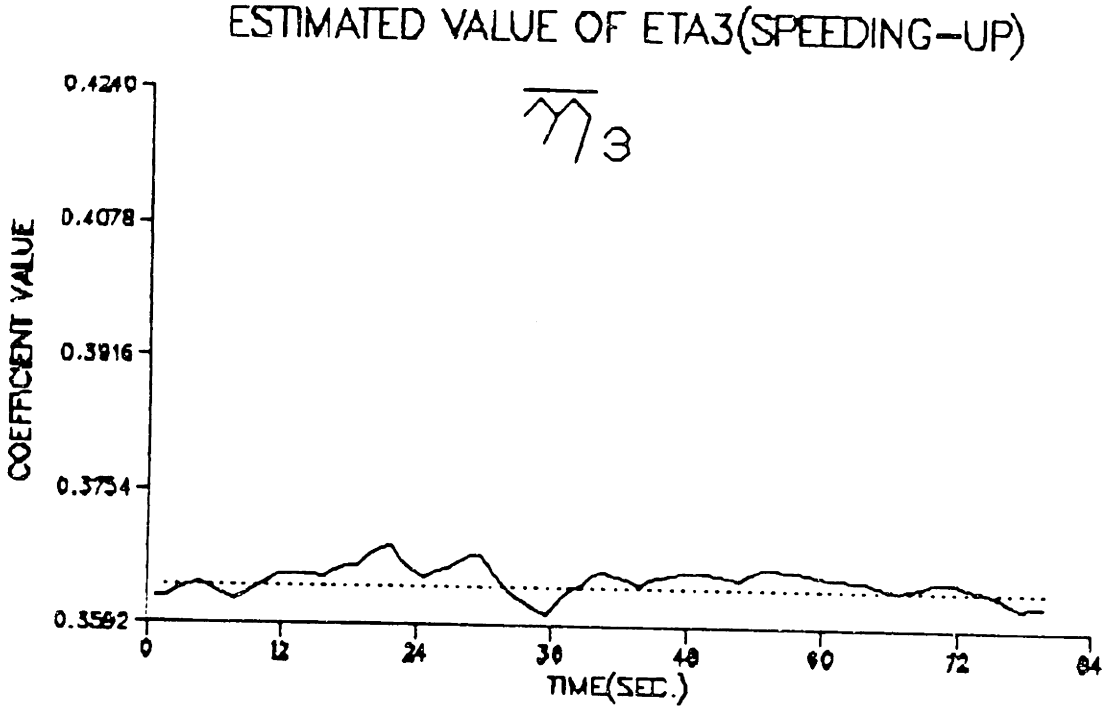

Figure 6.6: Estimation of $\overline{\eta}_3$ in Interation Two

6.1.3 Results of identified η_1^*, η_2^* and η_3^*

The results of identification of η_1^*, η_2^* and η_3^* are also intermediate results. The part of the measured data which covers the surge speed value from 19.8 ft/sec to 24.5 ft/sec is selected as the input data for the identification. To see the reason for doing so, the expressions for η_1^*, η_2^* and η_3^* in Equation(2.4) in Chapter 2 are recalled. From these relations, it is clear that each of these three coefficients has the thrust deduction factor t as a component. It is known that the thrust deduction factor t is initially defined as a constant in the equilibrium state of ships. However, when it is introduced into the ship surge motion equation, it becomes a variable. Its changing rate is much higher at small J values than at large J values. When the surge speed increases to the region near the equilibrium state, the thrust deduction factor t can then be assumed constant, and the variation of its value can be considered as a tolerable error(less than 1%). *Fig.s* 6.8 $\sim$ 6.10 are the curves of the estimated η_1^*, η_2^* and η_3^* obtained by the EKF technique for a recursive time interval of 1 *second*. *Fig.s* 6.12 $\sim$ 6.14 show the estimation through the EKF technique with the time-interval increased to 2 *seconds*. The results make it clear that the difference in the time interval causes little difference in the results. Since the computer time is not a big issue in this problem, a 1 *second* time-interval is recommended.

The results of the estimation are:

$$\begin{cases} \eta_1^* &= -0.285 \\ \eta_2^* &= -0.135 \\ \eta_3^* &= 0.279 \end{cases}$$

The results are very good judging from the order of magnitude and the parity. For example, η_3^* is positive and less than the value of η_{p3}, because it is the product of η_{p3} and the positive factor $(1-t)$ which is less than *one*.

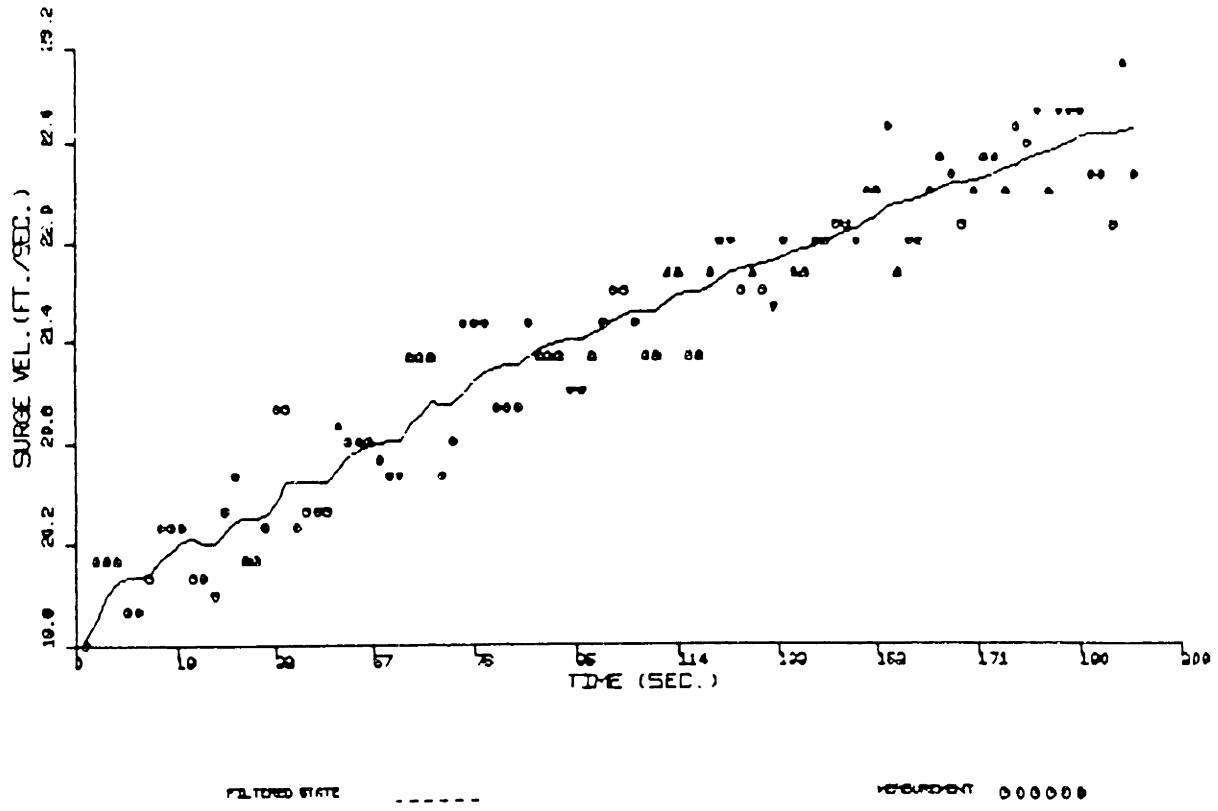

Figure 6.7: Measurement and Estimated u(1 Second Time-Interval)

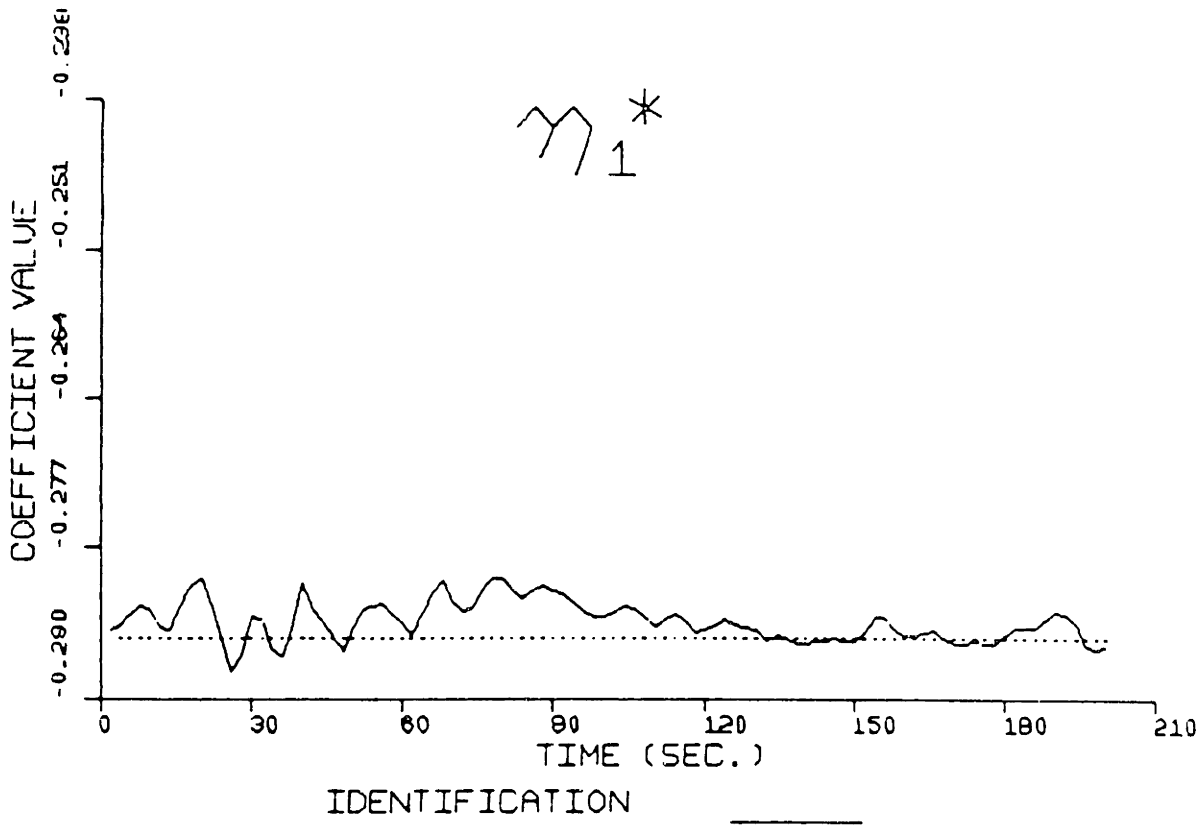

Figure 6.8: Estimation of η_1^* by EKF(1 Second Time-Interval)

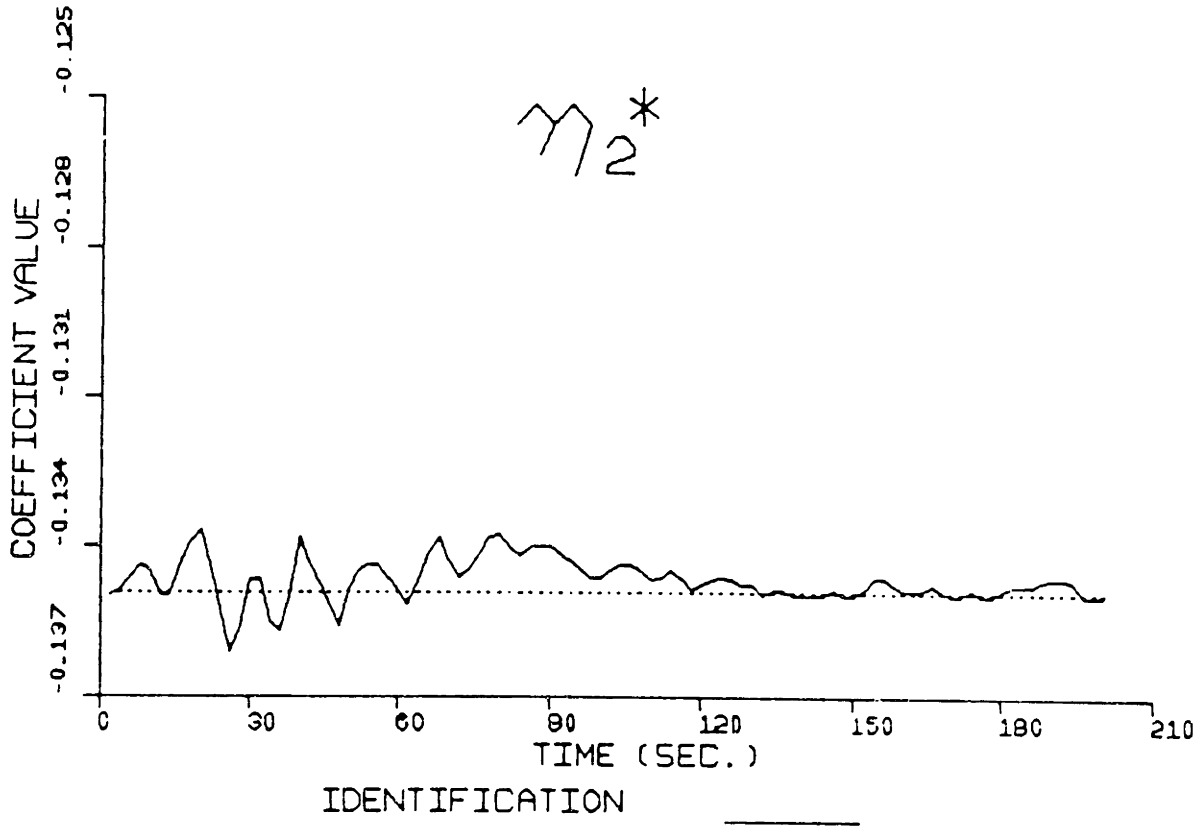

Figure 6.9: Estimation of η_2^* by EKF(1 Second Time-Interval)

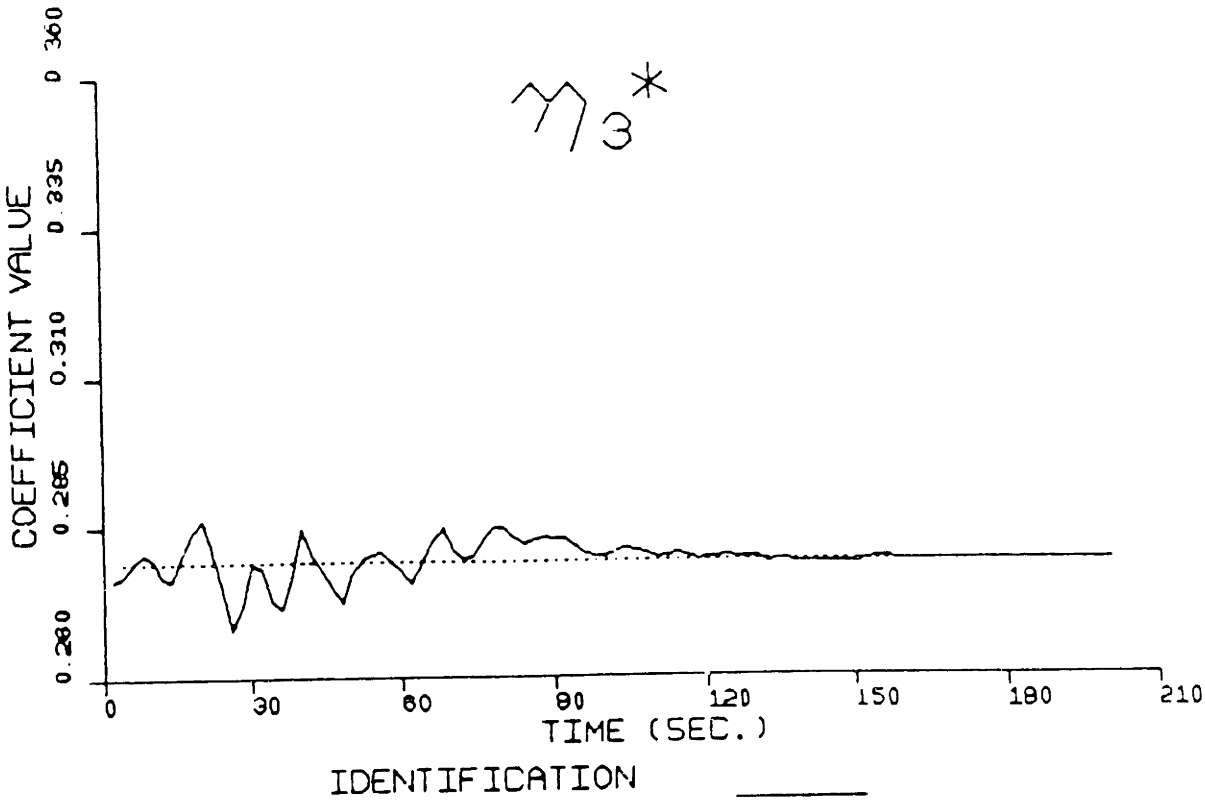

Figure 6.10: Estimation of η_3^* by EKF(1 Second Time-Interval)

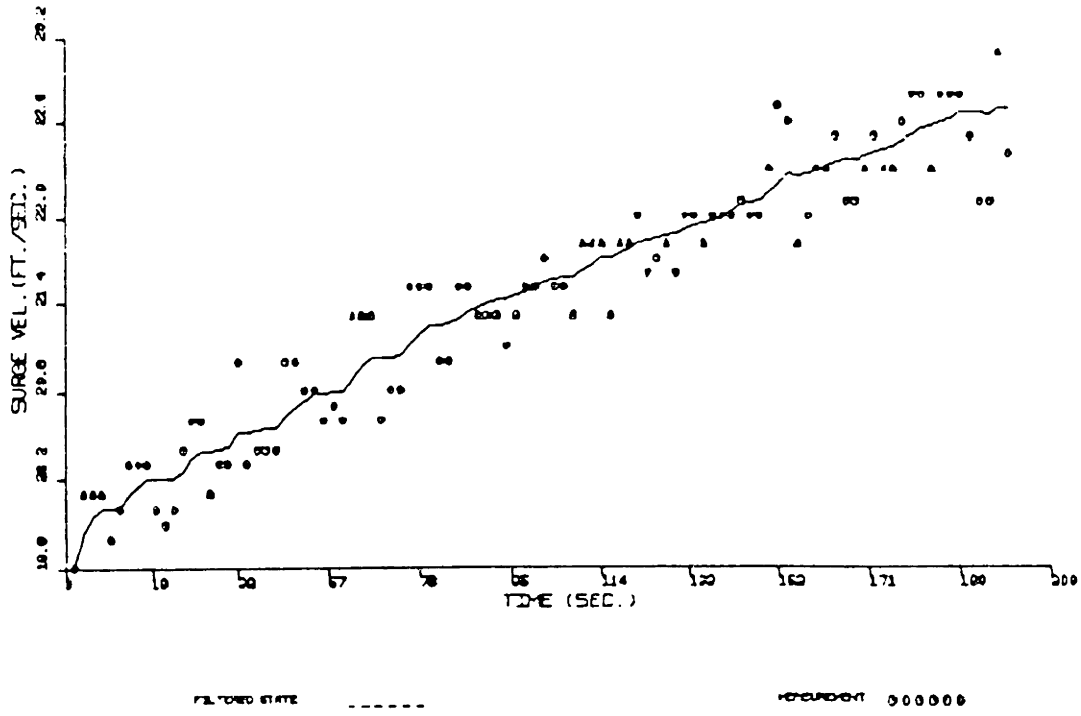

Figure 6.11: Measurement and Estimated u(2 Second Time-Interval)

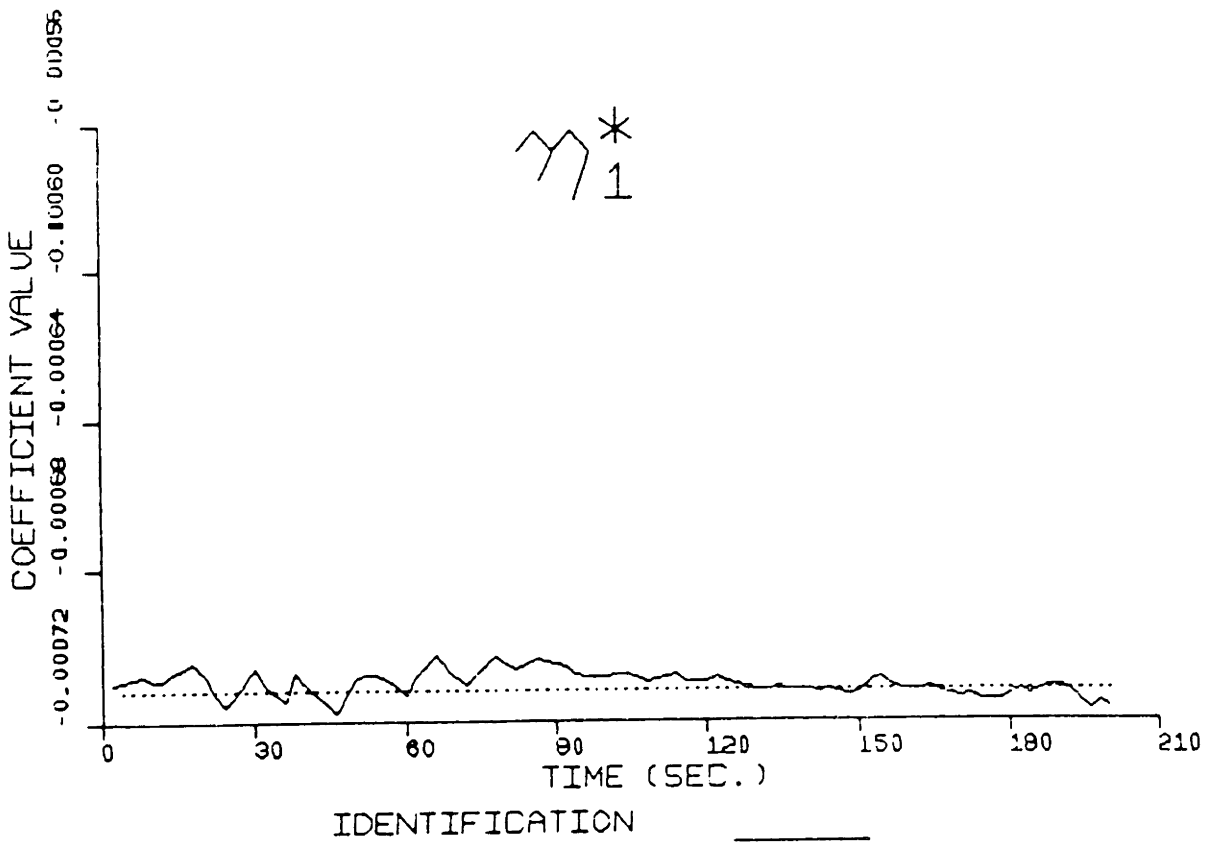

Figure 6.12: Estimation of η_1^* by EKF(2 Second Time-Interval)

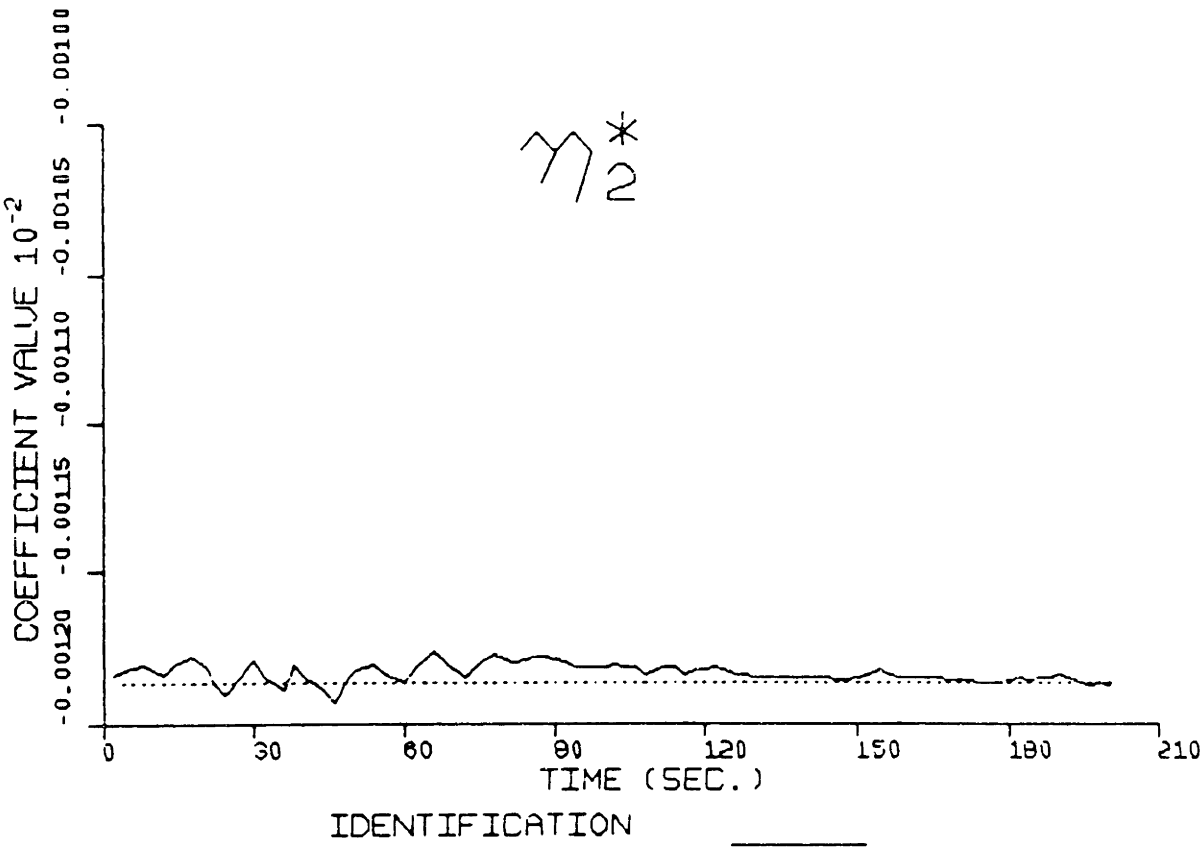

Figure 6.13: Estimation of η_2^* by EKF(2 Second Time-Interval)

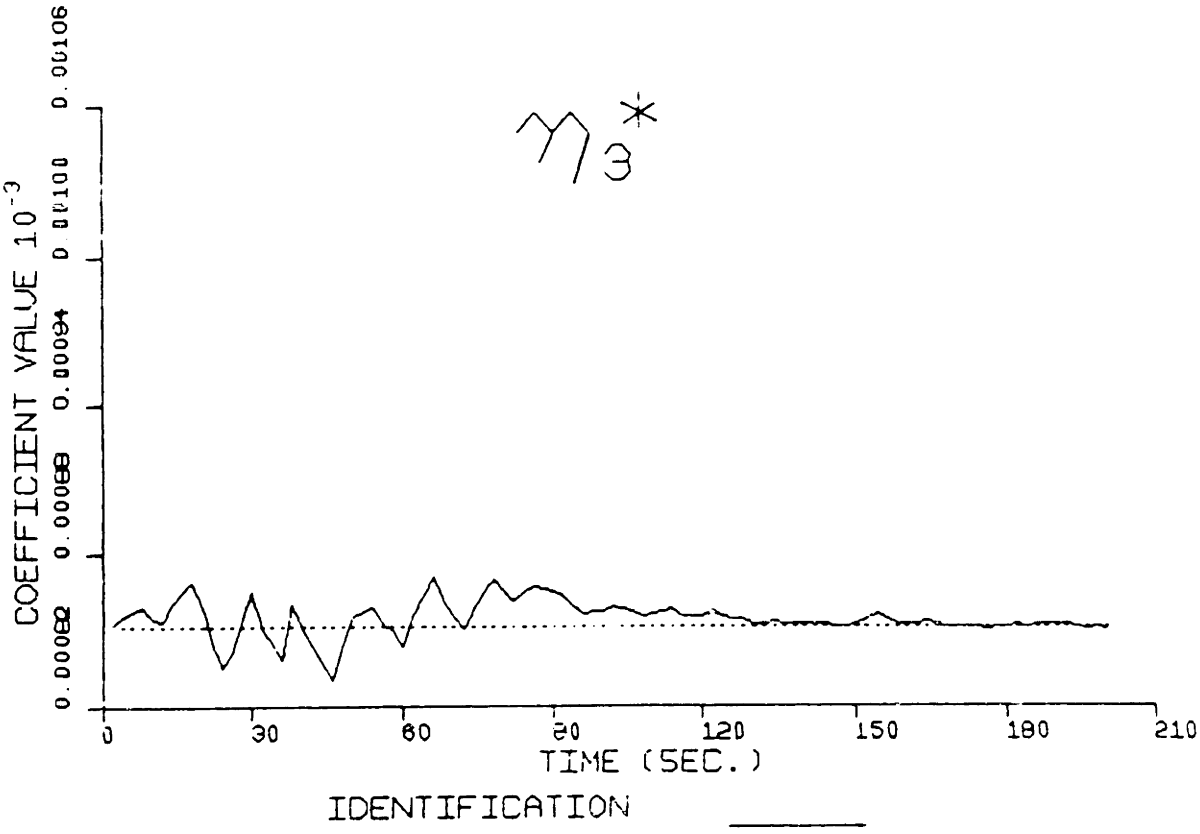

Figure 6.14: Estimation of η_3^* by EKF(2 Second Time-Interval)

6.2 Derived Coefficients Values

6.2.1 C_R by direct comparison method

Calculation

Since the value of $\overline{\eta}_3$ is 0.359 and the value of η_{p3} obtained from the open water test of the model propeller is 0.379, the difference is 0.020, therefore the assumption that the ship propeller is in good condition holds. Consequently the following steps are carried out:

1. According to Equation(4.2)

$$1 - t = \frac{\eta_3{}^*}{\eta_{p3}}$$

then

$$\begin{aligned} t &= 1 - \frac{0.279}{0.3796} \\ &= 0.265 \end{aligned}$$

2. From

$$1 - w = \frac{\eta_2{}^* \eta_{p3}}{\eta_3{}^* \eta_{p2}}$$

then

$$\begin{aligned} w &= 1 - \frac{-0.135 \times 0.3796}{-0.2415 \times 0.279} \\ &= 0.239 \end{aligned}$$

3. From the propeller model test K_t curve,

$$\eta_{p1} = -0.1725$$

Consequently, the corresponding coefficient $\eta_{\dagger 1}$ is

$$\begin{aligned} \eta_{\dagger 1} &= \eta_{p1}(1-w)^2(1-t) \\ &= -0.0734 \end{aligned}$$

4. Since

$$C_R = \frac{\eta_{\dagger 1} - \eta_1^*}{\frac{S}{2D^2}}$$

the ship resistance coefficient should be

$$C_R = 0.00227$$

Judging from marine hydrodynamics, the figure for C_R is realistic.

Adjustment of t_e and K_t curve

1. From the preceding calculation and the model propeller K_t curve, one has

$$\begin{aligned} 1 - t_e &= 0.735 \\ K_{te} &= 0.186 \end{aligned}$$

The updated a_e and κ are then obtained

$$a_e = \frac{1}{1-a_e} - 1$$

$$= 0.3605$$

$$\kappa = \frac{a_c}{2(1-w)(\sqrt{1+\frac{8K_{tc}}{\pi J_c{}^2}}-1)}$$
$$= 0.4179$$

2. From the model test propeller K_t curve,

$$\overline{K}_t = 0.332$$

The values of $\bar{a}$ and $\bar{t}$ corresponding to $\overline{\eta}_3$ can now be obtained through calculation.

$$\bar{a} = 2\kappa(1-w)(\sqrt{1+\frac{8\overline{K}_t}{\pi \overline{J}_p{}^2}}-1)$$
$$= 2.8211$$
$$\bar{t} = \frac{SC_R\overline{J}_p{}^2}{2D^2\overline{K}_t(1-w)^2}\bar{a}$$
$$= 0.085$$

3. The adjusted η_{s3} is then

$$\eta_{s3} = \frac{\overline{\eta}_3}{1-\bar{t}}$$
$$= 0.3923$$

This value is then used to calculate the updated $1-t_c$:

$$1-t_c = \frac{\eta_3{}^*}{\eta_{s3}}$$
$$= 0.7112$$

η_{s1} and η_{s2} are updated immediately:

$$\begin{aligned}\eta_{s1} &= \frac{\eta_1^* + \frac{SC_R}{2D^2}}{(1-t_e)(1-w)} \\ &= -0.178 \\ \eta_{s2} &= \frac{\eta_2^*}{(1-t_e)(1-w)} \\ &= -0.249\end{aligned}$$

Since the value of $1 - t_e$ changed during the adjustment, another iteration is needed. Then the following calculations are carried out.

4. The updated a_e, $\overline{K}_t$, K_{te} and κ are then:

$$\begin{aligned}a_e &= 0.4061 \\ \overline{K}_t &= 0.3442 \\ K_{te} &= 0.192 \\ \kappa &= 0.4587\end{aligned}$$

One is now ready for the next iteration. After the third iteration, $1 - t_e$ converges to a constant, so the adjustment is finished. The final results are

$$\begin{aligned}1 - t_e &= 0.704 \\ \eta_{s1} &= -0.180 \\ \eta_{s2} &= -0.252 \\ \eta_{s3} &= 0.396\end{aligned}$$

6.2.2 C_R by recurrence method

The following shows how to obtain the ship resistance coefficient C_R by the recurrence method.

1. The value of $\overline{C}_R$ is 0.00238

2. The value of the estimated apparent advanced ratio J_{awm} during the deceleration process is

$$J_{awm} = 1.36$$

   The value of the corresponding propeller advanced ratio J_{wm} is

$$J_{wm} = 1.03$$

3. After the estimated $\overline{\eta}_3$ is obtained through EKF, compare it with η_{p3} from the model propeller K_t curve to see if the ship propeller is damaged. If not, as a first approximation the model propeller K_t curve can be used for the ship propeller in deriving C_R. Then the ship propeller thrust coefficient of wind-milling state K_{twm} is found:

$$K_{twm} = -0.058$$

4. From the identified $\overline{\eta}_3$ and the η_{p3} obtained from the preceding step, get the value of t corresponding to the equilibrium state. Then get the corresponding value of the resistance augmentation fraction a. Plugging this value into Equation(4.9), the constant κ is determined.

$$\kappa = 0.4179$$

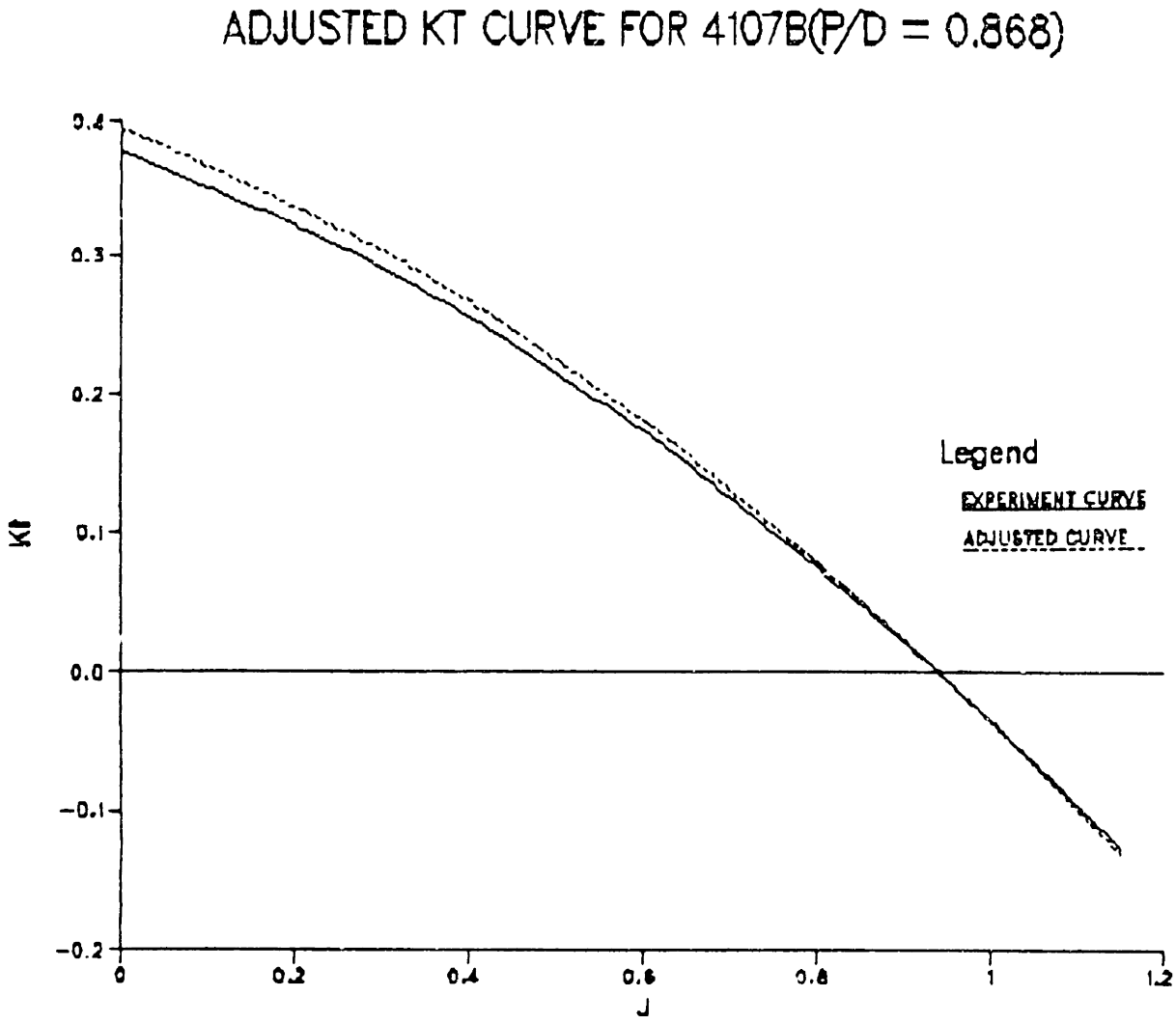

Figure 6.15: Derived K_t Curve for the Ship Propeller

5. Plugging κ and K_{twm} into Equation(4.7), the value of a in the propeller wind-millling state a_{wm}, will be determined:

$$a_{wm} = -0.0459$$

6. Inserting a_{wm}, $\overline{C}_R$ and K_{twm} into Equation(4.12), the ship resistance coefficient C_R is obtained.

$$\begin{aligned} C_R &= \frac{1}{1+a_{wm}}(\overline{C}_R + \frac{2D^2 K_{twm}}{S{J_{wm}}^2}) \\ &= 0.00214 \end{aligned}$$

The result from this whole procedure is not yet the final result, since the ship propeller K_t curve has not been adjusted. Starting from the adjusted ship propeller K_t curve, the updated C_R value is obtained through the following steps:(*Fig.* 6.15)

1. Using the value of C_R just obtained as input, insert it into the following relation to solve for $\bar{t}$ which is the thrust deduction factor of the ship propeller corresponding to $\overline{\eta}_3$.

$$\begin{aligned} \bar{t} &= \frac{SC_R{\overline{J}_p}^2}{2D^2\overline{K}_t(1-w)^2}\overline{a} \\ &= 0.0308\overline{a} \end{aligned}$$

and $\overline{a}$ can be calculated as

$$\begin{aligned} \overline{a} &= 2\kappa(1-w)(\sqrt{1+\frac{8\overline{K}_t}{\pi{\overline{J}_p}^2}}-1) \\ &= 2.8211 \end{aligned}$$

Therefore,

$$\bar{t} = 0.087$$

2. With this result, the ship propeller lift-thrust coefficient η_{s3} is obtained:

$$\begin{aligned} \eta_{s3} &= \frac{\overline{\eta}_3}{1-\bar{t}} \\ &= 0.3932 \end{aligned}$$

3. The thrust deduction factor of equilibrium t_e is also obtained:

$$\begin{aligned} 1-t_e &= \frac{\eta_3^*}{\eta_{s3}} \\ &= 0.7099 \end{aligned}$$

4. Hence, the other two thrust coefficients of the ship propeller can also be calculated based on the already obtained results.

$$\begin{aligned} \eta_{s1} &= \frac{\eta_1^* + \frac{SC_R}{2D^2}}{(1-w)^2(1-t_e)} \\ &= -0.2077 \end{aligned}$$

and

$$\begin{aligned} \eta_{s2} &= \frac{\eta_2^*}{(1-w)(1-t_e)} \\ &= -0.2497 \end{aligned}$$

5. Now the ship propeller K_t curve can be adjusted and the updated $\overline{K_t}$, K_{twm} and K_{te} are as follows:

$$\overline{K_t} = 0.3441$$

$$K_{twm} = -0.048$$

$$K_{te} = 0.196$$

6. Also the updated a_{wm} is calculated through the following steps:

$$\begin{aligned} a_e &= \frac{1}{1-t_e} - 1 \\ &= 0.4086 \\ \kappa &= \frac{a_e}{2(1-w)(\sqrt{1+\frac{8K_{te}}{\pi J_e^2}}-1)} \\ &= 0.4538 \\ a_{wm} &= 2\kappa(1-w)(\sqrt{1+\frac{8K_{twm}}{\pi J_{wm}{}^2}}-1) \\ &= -0.041 \end{aligned}$$

7. The updated value of C_R then is

$$\begin{aligned} C_R &= \frac{1}{1+a_{wm}}(\overline{C}_R + \frac{2D^2K_{twm}(1-w)^2}{SJ_{wm}{}^2}) \\ &= 0.00219 \end{aligned}$$

After the new value of C_R is obtained, the same updating and adjusting procedure will be repeated, until the C_R value converges to a constant. For the tanker EXXON PHILADELPHIA, the final value of C_R after four iterations by the recurrence method is

$$C_R = 0.00221$$

As this value is compared with the result obtained from direct comparison method, the difference is less than 3% of 0.00227, so the result is accurate.

Furthermore, considering the fact that when the ship propeller is wind-milling, the wake fraction w_{wm} is different from that in the acceleration procedure. According to Kerwin,[13] the flow into a propeller is not the same as it would be if the propeller were not there and is altered by the presence of the propeller. This altered flow field is termed the *effective wake*. When a ship is being accelerated as EXXON PHILADELPHIA did, the wake flow in front of the propeller is of this kind. The contrary term is the *nominal wake* which exists in the absence of the propeller. When the ship propeller is wind-milling, the wake flow in front of the propeller is very close to the nominal wake. Therefore, the wake fraction w_{wm} in the wind-milling state should be larger than that in the acceleration procedure. Adjustment in the value of w_{wm} will improve the result of the ship resistance coefficient C_R. For example, if an adjustment is made by referring to the curves given by Huang & Groves [11], the final result of C_R will be obtained as follows: (note: since the curves is corresponding to the case of a propeller operating behind an axisymmetric body, not exactly the same as surface ships, this adjustment may not be accurate.)

1. The ratio of $1-w_{ef}$ to $1-w_n$ corresponding to the apparent advanced ration $J_{awm} = 1.36$ is

$$\frac{1-w_n}{1-w_{ef}} = 0.9778$$

where w_{ef} is the *effective wake fraction* and w_n is the *nominal wake fraction.*

2. Then, there will be

$$\begin{aligned} 1 - w_n &= 0.744 \\ J_{wm} &= 1.01 \\ K_{twm} &= -0.033 \\ \kappa &= 0.4782 \\ a_{wm} &= -0.0299 \end{aligned}$$

3. Then, the updated value of C_R is

$$C_R = 0.00226$$

This value will make the difference of C_R between the direct comparison method and the recurrence method less than 1% of 0.00227.

Simulation and discussions

To check the results of identification, the identified coefficients are plugged into the ship surge motion equation to simulate the surge motion. With the measured *rps* as input data, the surge motion of the tanker EXXON PHILADELPHIA is simulated. Simutaneously, the data of the measured surge speed u are compared with the simulated results. In the presented figures of simulation, the curves are the simulated results and the scattered points as the background are the measured data.

Fig. 6.16 is the simulation of the surge motion for EXXON PHILADELPHIA in the deceleration procedure with the propeller wind-milling. The

simulated surge speed curve is compared with the measured u. From *Fig.* 6.16, the simulated data are very consistent to the measured data, hence the identified parameter values are considered accurate.

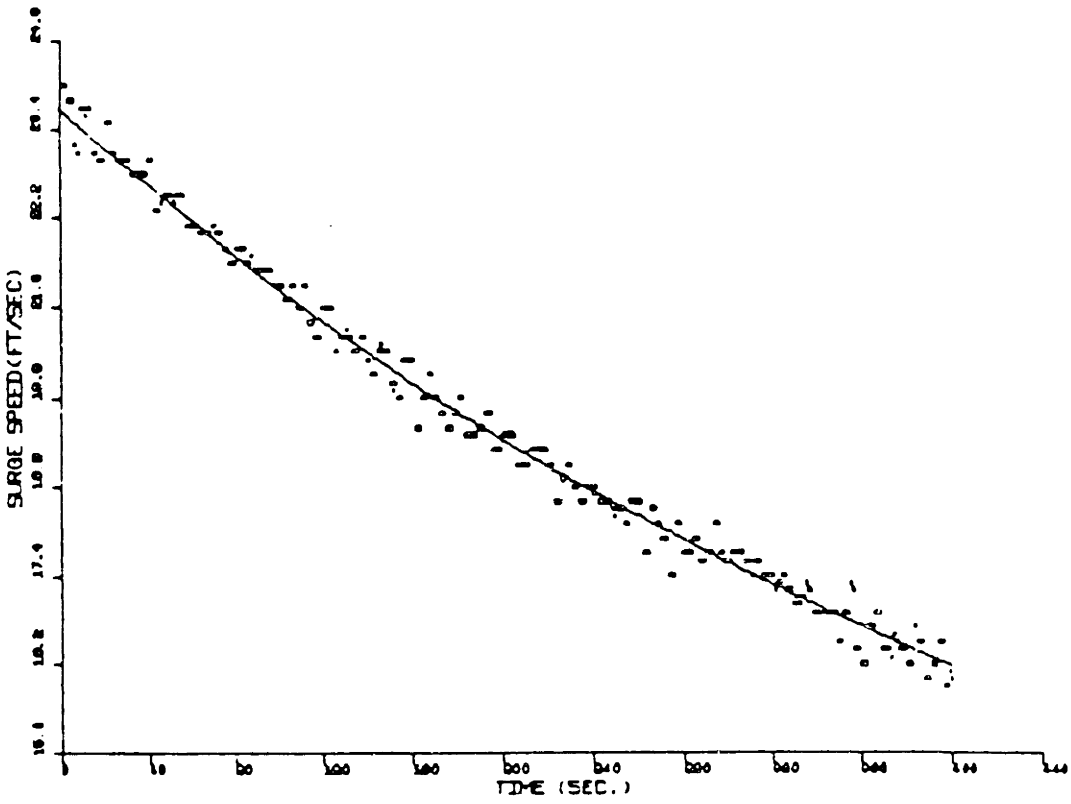

Figure 6.16: Simulation of Deceleration Procedure

Fig. 6.17 is the simulation of the acceleration of EXXON PHILADELPHIA with the surge speed extending from 19.8 ft/sec to 24.5 ft/sec. The

comparison between the simulation and the measured surge speed u shows good consistency. However, using the same estimated parameter values and simulating the same acceleration procedure, when the surge speed ranging from $0.0\,ft/sec$ to $24.5\,ft/sec$, the simulation drifts away from the measured data at the low speed region(See *Fig.* 6.18). It is not because of the inaccuracy of the estimation of the parameters, it is because of the variation of the value of t. The results of the simulation shows:

1. The thrust deduction really varies with the advanced ratio J. During the deceleration procedure, the consistency of the simulation with the measured data is because of the thrust deduction factor being constant while the ship propeller wind-milling. Under that condition, the advanced ratio J_{wm} keeps constant. The consistency of the simulation with the measured data in Fig. 6.17 is because of that part of the acceleration procedure corresponding to the region in which the change of t is very small.

2. The variation rate of t is much higher at low J than that at high J. Therefore, at the early stage of the acceleration procedure, t can not be treated as a constant. Simulation with t as a constant caused the inconsistency between the simulation and the measured data.

This strongly agrees with the analysis on the property of t. As mentioned before, t is a variable and when the advanced ratio is low it changes drastically. Also, the resistance coefficient C_R changes with the Reynolds' num-

ber. Therefore, while simulating the acceleration procedure of the ship surge motion, the variation of t and C_R has to be reckoned with.

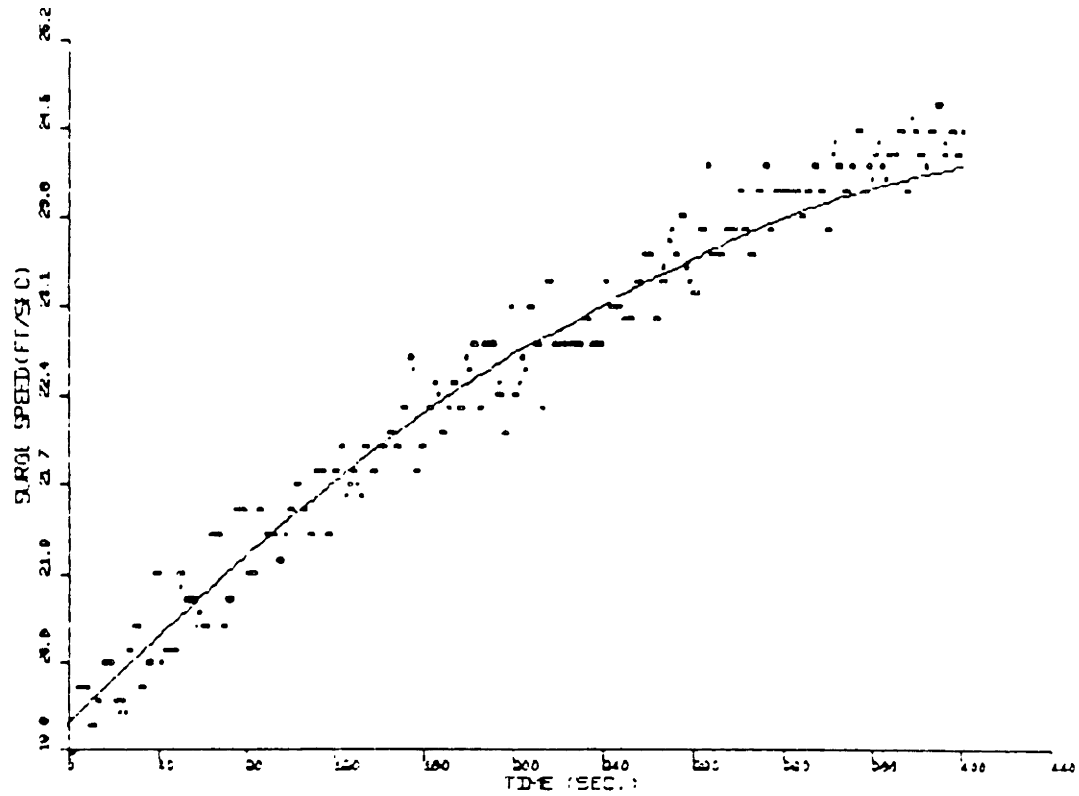

Figure 6.17: Simulation of Acceleration Near Equilibrium State

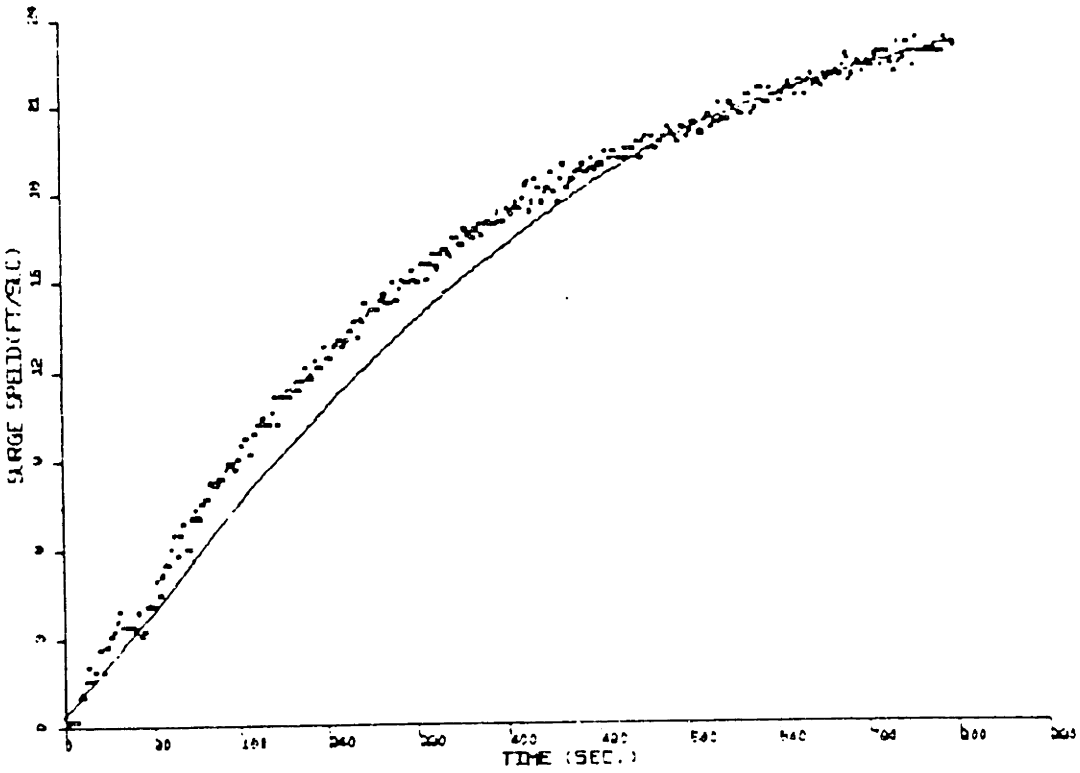

Figure 6.18: Simulation of Whole Acceleration Procedure

Taking $(1-t)$ as a variable, using Equation(4.8) as the expression of it in the simulation program, at the same time considering the change of C_R with the Reynolds' number, the surge motion of EXXON PHILADELPHIA is simulated. The comparison between the simulated surge speed curve and the measured surge speed data is shown in *Fig.* 6.19. The simulated surge motion is the acceleration procedure. The κ value in the simulation is

$$\kappa = 0.4705$$

The simulation is clearly consistent with the measured data. Consequently, it shows that the estimated values of the coefficients are accurate.

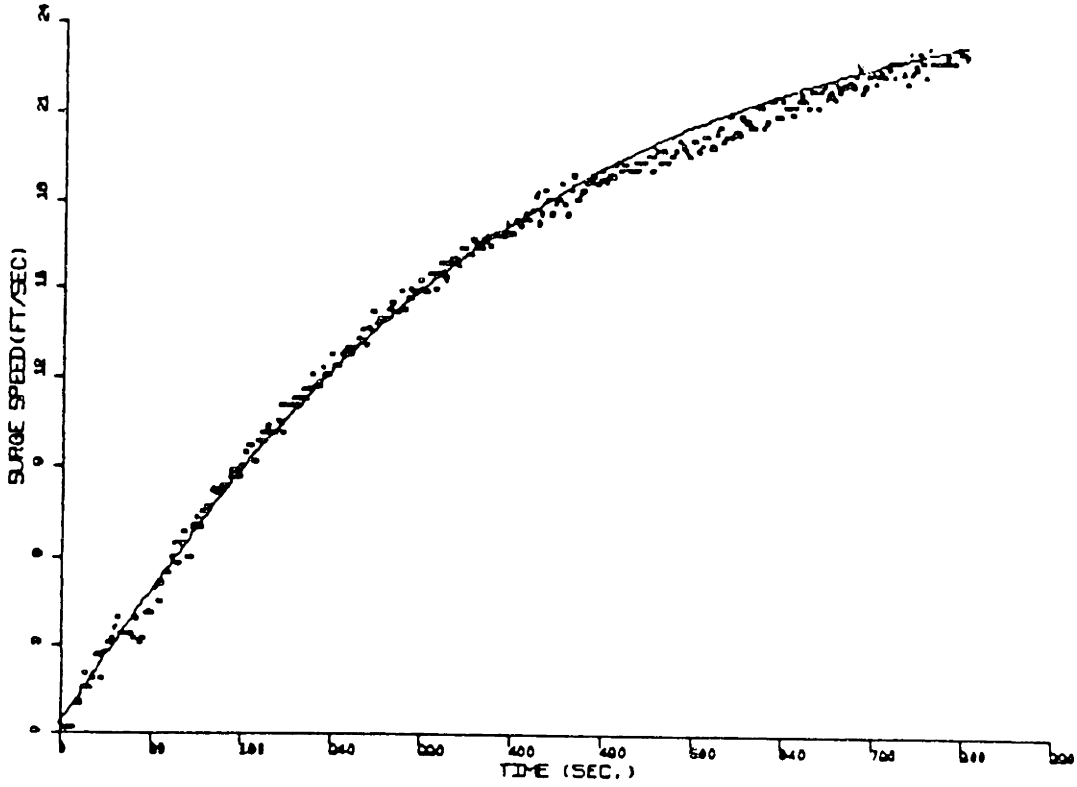

Figure 6.19: Measurement and Simulation ($t = f(J)$)

6.3 The Least Squares Technique

The identified values of η_1^*, η_2^* and η_3^* obtained by processing the measured data in the acceleration maneuver with the recursive least squares technique are presented in *Figs.* 6.20 $\sim$ 6.22. The curves show that the identification results by the least squares technique converge to steady values but the estimated values are biased. This phenomenon for a linear system can explained as caused by the correlated noise of the system. For the system being studied here, the reason may also be the direct application of the linear theory to a nonlinear system. Further study based on the present results may lead to better results, however it is beyond this thesis.

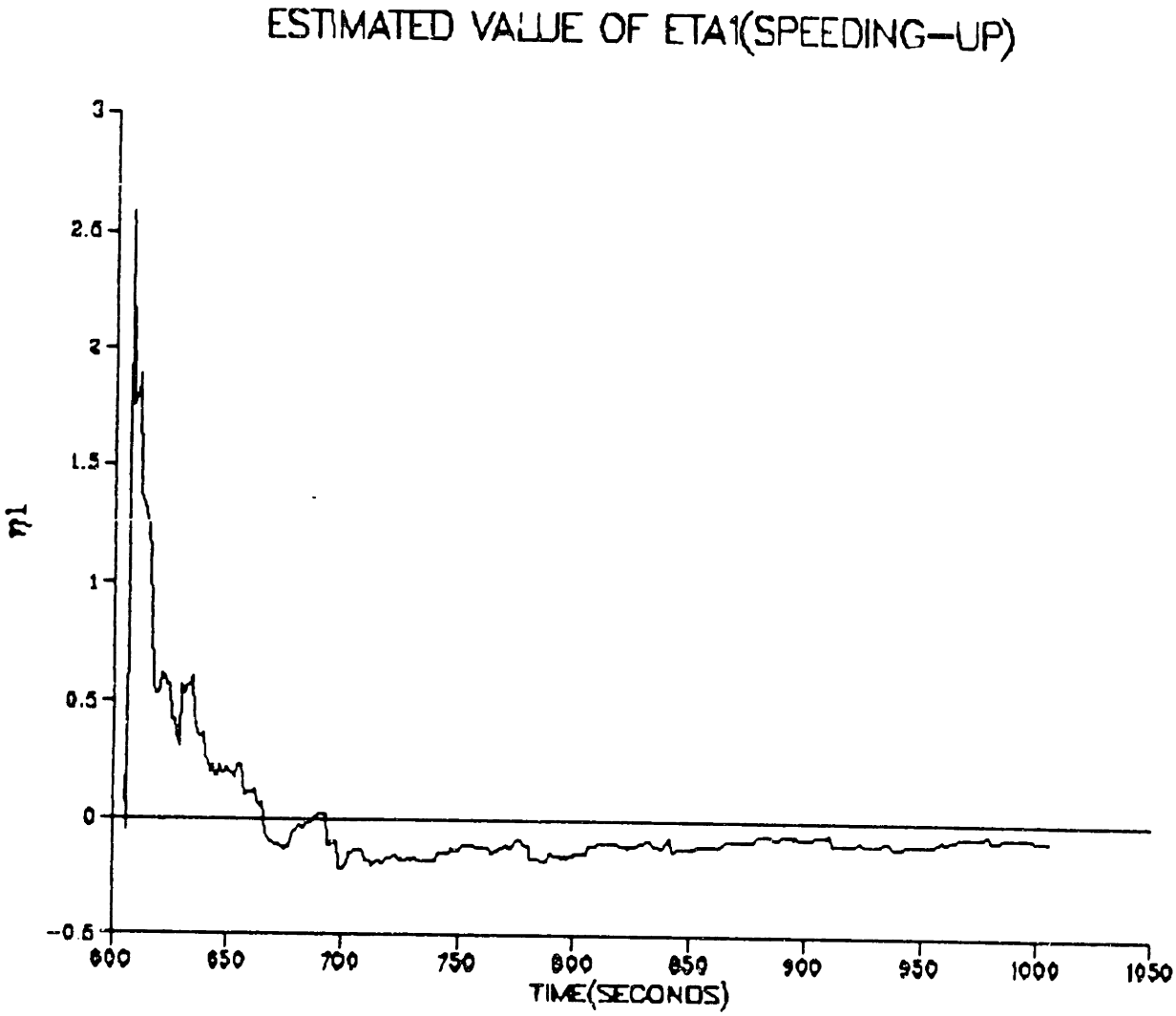

Figure 6.20: Estimation of η_1^*, Least Squares Method

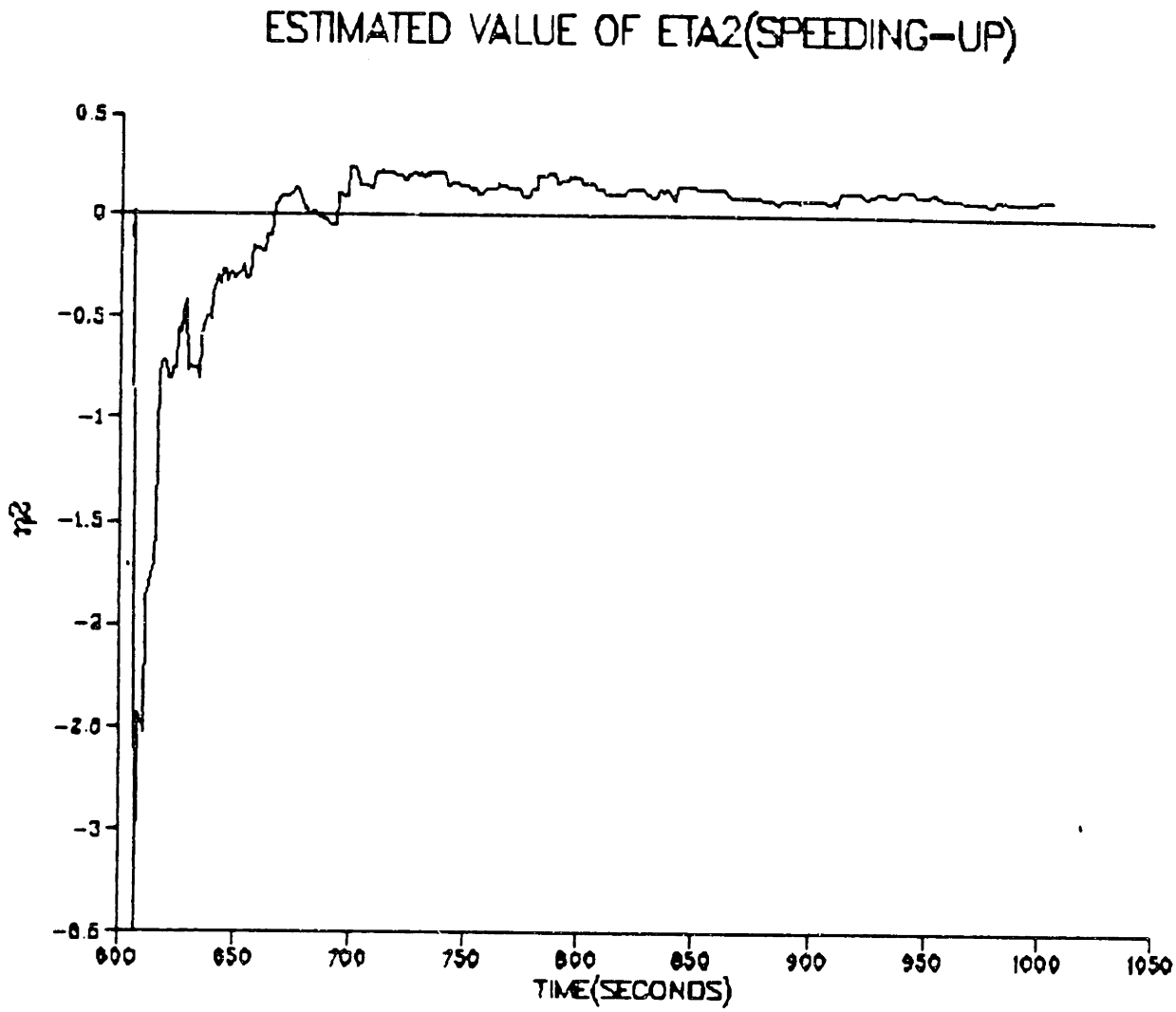

Figure 6.21: Estimation of η_2^*, Least Squares Method

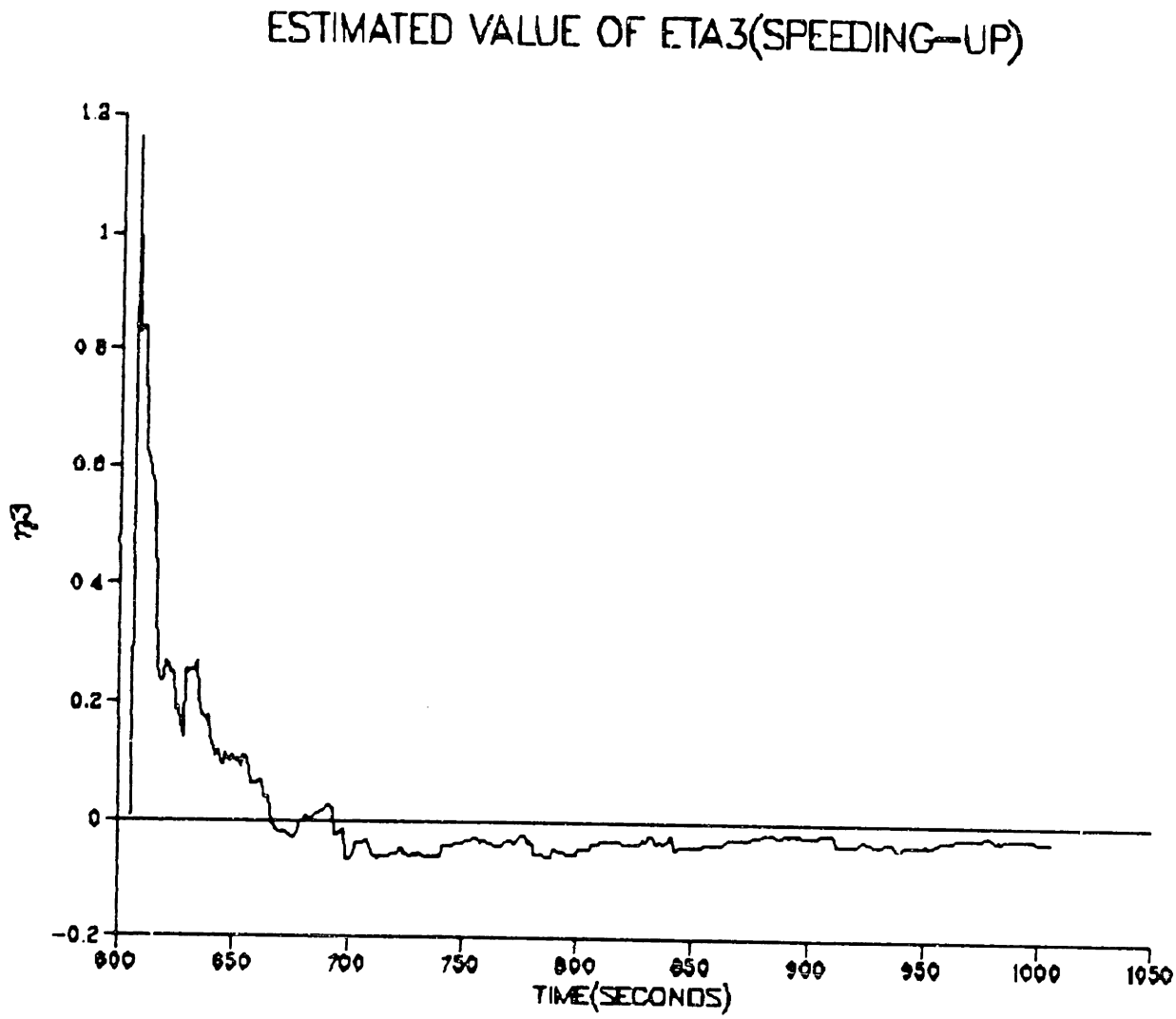

Figure 6.22: Estimation of η_3^*, Least Squares Method

6.4 The Instrumental Variable Technique

The identified results of η_1^*, η_2^* and η_3^* by processing the measured data in the acceleration process with the recursive instrumental variable technique are presented in *Figs.* 6.23 $\sim$ 6.25. The instrumental variables are chosen to be u^2, un and n^2 in which n is the filtered value of rps from the measurements, and u is generated by solving the deterministic ship surge motion equation. (i.e. ignoring the noise in the system equation). The resulting curves show that the recursive instrumental technique fails to give a satisfactory result. This does not mean that the recursive instrumental variable technique developed for linear systems cannot be used in the estimation part of this problem. However, it shows that to apply the intrumental variable technique, the critical part is to choose the instrumental variables appropriately, which is a difficult task.

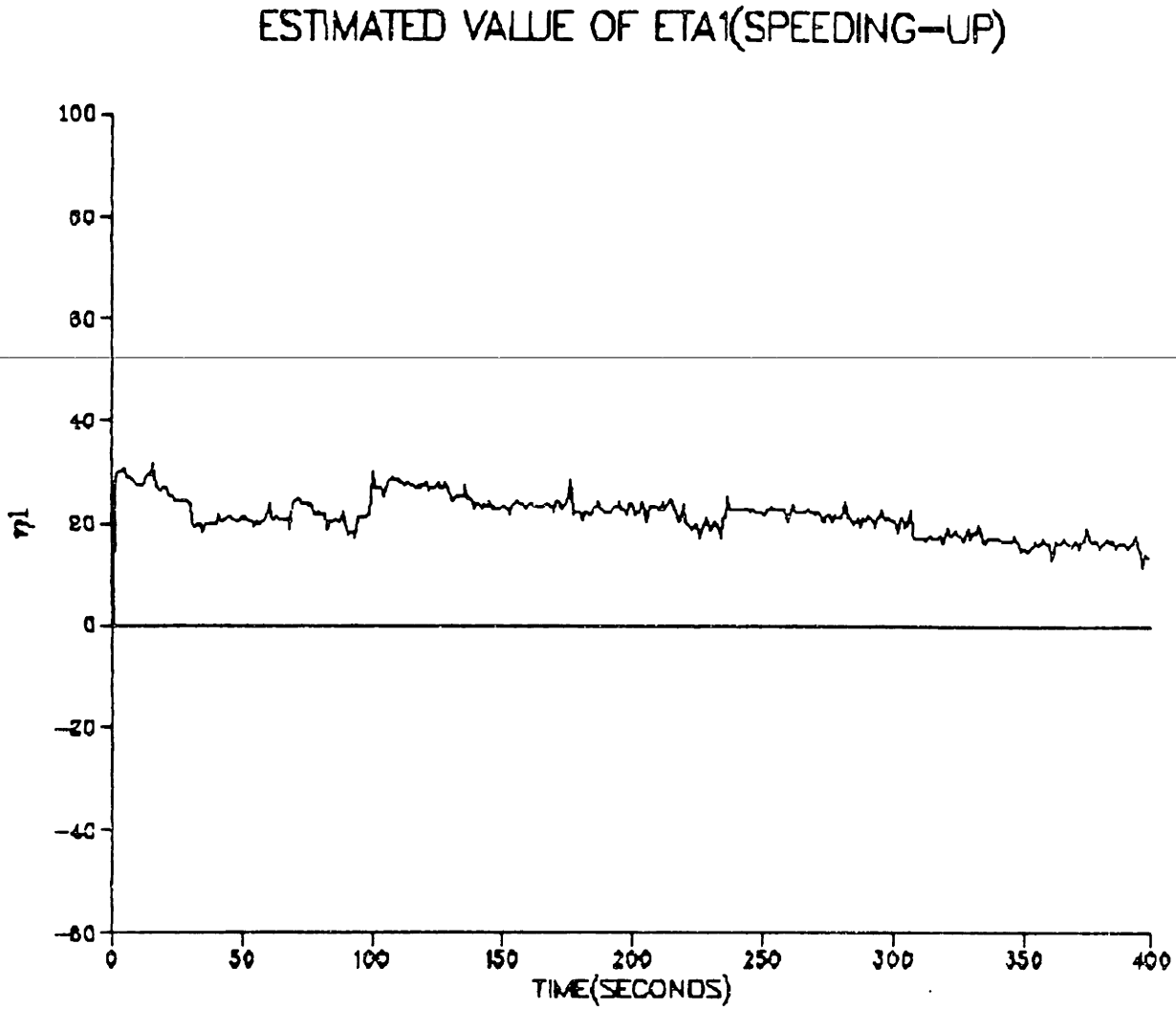

Figure 6.23: Estimation of $\eta_1{}^*$, Instrumental Variable Method

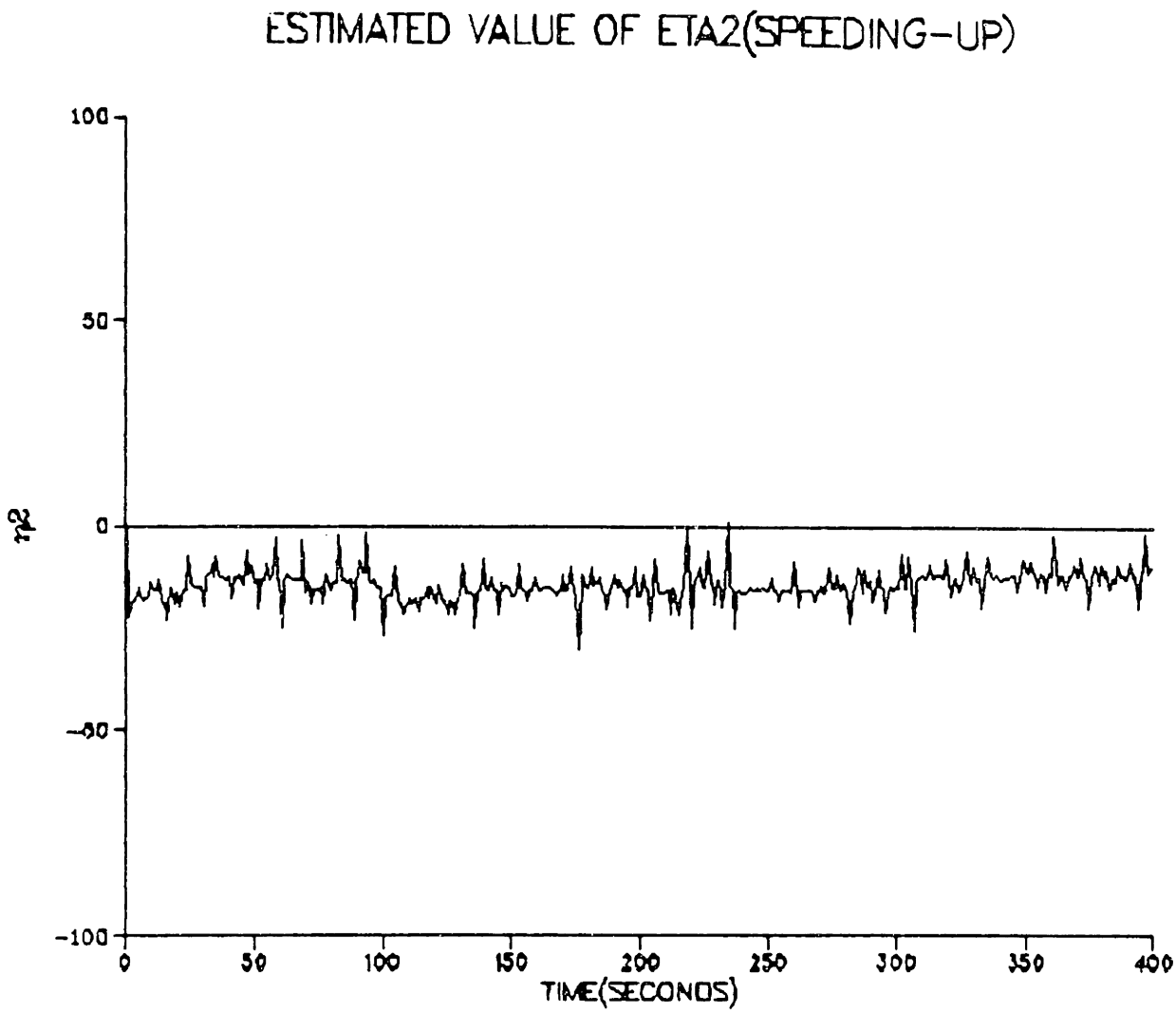

Figure 6.24: Estimation of $\eta_2{}^*$, Instrumental Variable Method

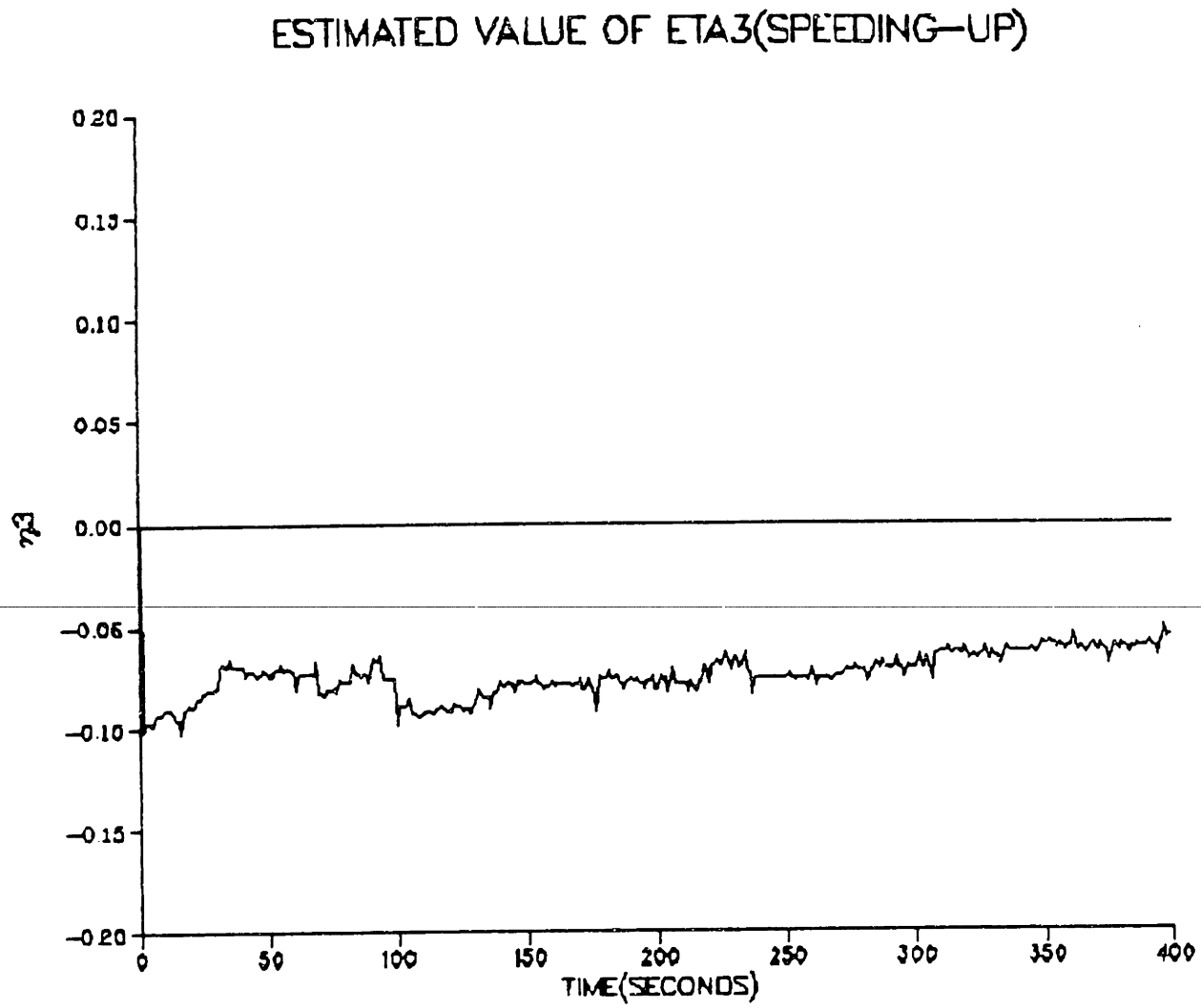

Figure 6.25: Estimation of $\eta_3{}^*$, Instrumental Variable Method

Chapter 7

Conclusions and Recommendations

This thesis has been concerned with the measurement of the ship resistance coefficient through simple maneuvers during a regular ship voyage, which constitutes a first in marine hydrodynamics. The research work includes setting up the system model, establishing the strategies for determining the ship resistance coefficient C_R and other hydrodynamic coefficients, testing them with simulated noisy data, collecting data, applying identification techniques to the ship surge motion system and deriving the ship resistance coefficient and other hydrodynamic coefficients from the identified parameters. The research work has been completed successfully. Not only was the ship resistance coefficient derived from the measured data in a simply conducted sea trial, but also the wake fraction w, the thrust deduction

factor t and the K_t curve of the ship propeller were derived from the same data set. This is also a first in ship hydrodynamic research.

7.1 Conclusions

1. The surge motion equation of ships derived in Chapter 2 is proven to be a correct model for the research of the dynamics of ship resistance. The approximation of the propeller K_t curve with the polynomials of the advanced ratio J simplifies the equation and maintains the excellent accuracy of the K_t value.(The error is less than 1%)

2. The added-mass of the ship is calculated through numerically solving the Green theorem by using the MIT Radiation and Refraction Program. The calculation result is accurate for use in the ship surge motion equation.

3. Using the PC-based datalogger and the instruments already onboard, the data collection was successful. The measurement took less than 35 *minutes* with the ship heading in to the desired direction of the voyage and no complicated technique was involved. Because of the short time required relative to the duration of a voyage, it is not difficult to find a calm sea state with negligible wind to make the measurements with little noise. This is a very important asset for this method and should result in extensive use on ships in the future.

4. To get informative data for the identification, the sea trial pattern is simple. The results presented in this thesis show that the acceleration process of a ship from *zero* speed to *full* speed is sufficient for providing necessary data to the estimation. The deceleration process with the propeller wind-milling independently provides a measure of the resistance and certainly helps in assuring the accuracy of the results. However it is not a necessary process for deriving the ship resistance coefficient. The confirmation of this conclusion allows for a wider application of this method, since not all ships can wind-mill their propellers when they slow down.

5. In estimating η_1^*, η_2^*, η_3^* and $\overline{C}_R$, the EKF technique is a good choice. It gives accurate estimation, and since the system model for ship surge motion is in a very simple form, computing time is not a burden. The recursive least squares technique introduced bias in the estimation, when it was tried. The application of the recursive instrumental variable technique requires very careful choice of the instrumental variables which are very critical to the success of the identification.

6. Through solving for the resistance coefficient, the wake fraction w and the value of the thrust deduction factor t at the equilibrium state can also be obtained at the same time. The thrust deduction factor t, with an extended definition, is a function of the advanced ratio J.

This relation can be established during the procedure for estimating the ship resistance coefficient. The results obtained for w and t are excellent and this new method of obtaining w and t from sea trial data on a full scale ship should contribute to hydrodynamic research, particularly for research on high Reynolds number flow. It should also be very useful in the design of ship propellers.

7. The comparison of the results of this research with the model test is as follows:

   - The model test value of the ship resistance coefficient is

     $$C_{Rm} = 0.00391$$

     and the estimated value for the ship based on present extrapolation methods is

     $$C_{Rs} = 0.00260$$

   - The identified value of the ship resistance coefficient is

     $$C_R = 0.00227$$

It shows that there is significant "scale effect" in the present extrapolation procedures for estimating C_R of the ship. Furthermore, if the effect of fouling and wind is considered, the "scale effect" would be more serious. Also the comparison of t, w and ηs between ship and ship model shows the "scale effect" in these parameters, among them the large "scale effect" of w is conspicuous.

7.2 Recommendations

1. In light of the success of the measurement of the ship resistance coefficient of the tanker EXXON PHILADELPHIA, it should be useful to conduct the same kind of sea trials on different types of ships. A data bank can be obtained through which better methods of extrapolating model test results can be achieved.

2. A specially designed compact data collecting and processing device which is based on a micro computer and can interface with the instruments onboard ship should be developed along with a software package to collect and process the sea trial data in real time, so that the results are available shortly after the testing.

3. Further research on the wake fraction w and the thrust deduction factor t should be carried out. The better understanding of the characteristics of these two parameters, will not only help the design of ship propellers, but also help the improvement of the estimation of the ship resistance. One possibility is to bring Equation(4.7) into the identification program and directly estimate the value of κ. If this is successful, the ship propeller K_t curve can be determined with better accuracy, and hence improve the estimates of all the hydrodynamic coefficients involved in the surge motion of the ship.

Appendix A

Propeller Thrust Coefficients

There are several kinds of propulsion devices available for ships, such as propellers, jet propulsion systems, paddle wheels, vertical-axis propellers, etc. The most commonly used one is the screw propeller. In this thesis, the discussion is limited to screw propellers.

The function of a screw propeller is to establish a difference of hydrodynamic pressure between the front surface and the back surface of each blade; or if the whole screw propeller is seen as a disk, to produce a hydrodynamic pressure difference between the front end and the back end while it is rotating. This pressure difference provides the thrust force on the ship.

The mutual action between the propeller and the water is very complicated, due to the complex geometric form of the screw propeller and the distribution of the fluid field around it. To simplify the analysis, two different kinds of models are available. One is to model the whole propeller as a

disk, called the actuator disk. With this method, only the global relation between the velocities and the hydrodynamic forces are analysed, while the details inside the disk are ignored. The other is to analyse the hydrodynamic forces on the blade of the propeller. The basic idea is that each blade of the propeller can be regarded as a *helix-formed lifting surface*, then *lifting surface theory* can be applied with proper modifications.

Here, the purpose of the analyses is to find the relationship between the thrust and the rotating rate of the propeller and the ship surge speed. This relation will be useful in setting up the ship surge motion equation, although it does not give explicit formulae for the parameter calculations.

A.1 Representative Section of Blades

For a screw propeller with q blades, the total thrust produced by the propeller is

$$T_{total} = T_q q \tag{A.1}$$

To get the thrust force on the whole propeller, it is only necessary to work on a single blade.

It is known that each blade can be expanded into a helix surface consisting of infinite helix curves at different r. At each r, the section of the blade forms an infinitesimal element of a wing and the inflow of the water will produce a lift force dL and a resistance force dD on this element. The component of the resultant force of dL and dD along the propeller axial

direction is the thrust force dT provided to the ship by that element of the propeller blade. The integration of dT along r is the thrust force T_q provided by a single blade of the propeller. It is clear that the thrust force T_q on a blade of a screw propeller is not uniformly distributed along the radius r, in other words, dT is a function of r. The reason is that the geometric form of the blade section varies along r. Experimental results show that, the load on the propeller reaches its maximum at $r \approx 0.7\,\Re$ with the distribution of the load is as shown in *Fig.* A.1[6]. In the figure, $\frac{dT_q}{dr}$ as a function of r varies in the interval from r_b to $\Re$, where r_b is the *radius* of the hub of the propeller and $\Re$ is the *radius* of the propeller disk. It is clear that the area under the $\frac{dT_q}{dr}$ curve equals T_q—the thrust force provided by one single propeller blade, so T_q can always be written as

$$T_q = (\frac{dT_q}{dr})_{r^*}(\Re - r_b) \tag{A.2}$$

where $\Re > r^* > 0.7\,\Re$.

Since $(\Re - r_b)$ is constant, the problem is reduced to considering a piece of wing with the span of $(\Re - r_b)$ and a section similar to that at r^*. That is, only the forces on the blade section at r^* need to be studied.

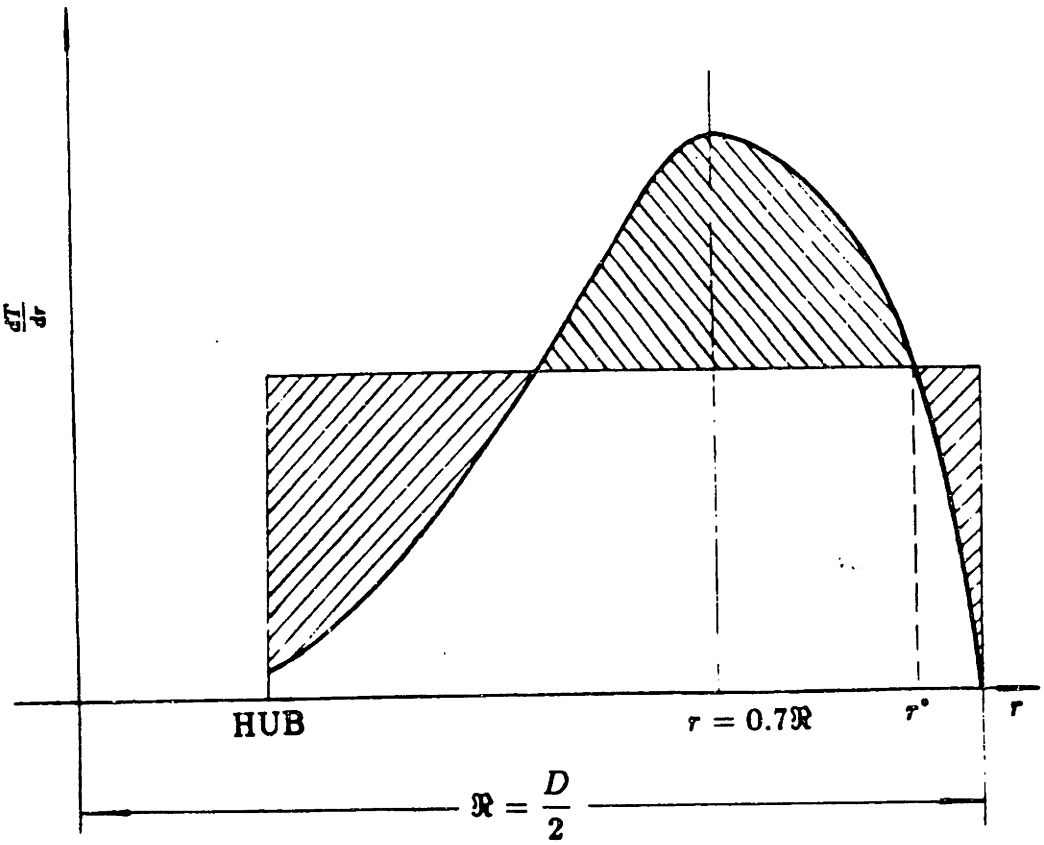

Figure A.1: Load Distribution on Propeller Blade

The forces on the wing section are described in *Fig. A.2*, where U is the axial velocity of the inflow, n is the rotating rate of the propeller, U_t is the resultant velocity of these two velocities, u_a is the ***axial induced velocity*** at the propeller disk, and u_t is the ***tangential induced velocity*** at the propeller disk. U_t which is the resultant velocity of U, $2\pi nr$, u_a and u_t, is the ***incident velocity*** to the wing section.

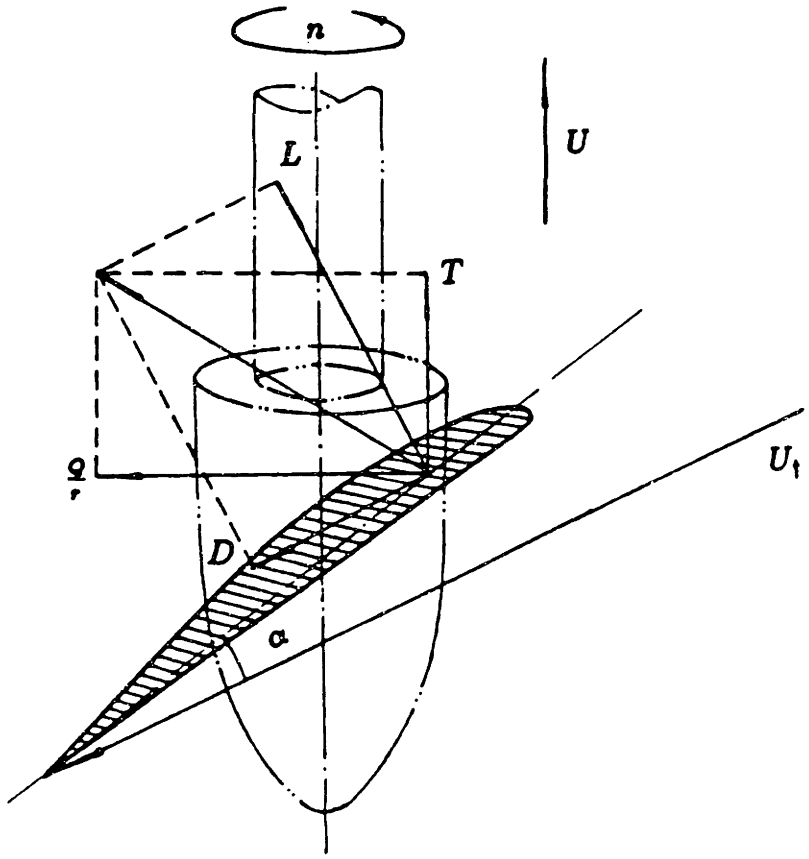

Figure A.2: Hydrodynamic Forces on a Propeller Blade Section

A.2 Induced Velocities

The induced velocities are the critical factors in this study. For a given screw propeller, the geometric characteristics are known, so are the lift coefficients C_L and the drag coefficient C_D of the expanded wing section. To calculate the forces on the wing section, the only unknown is the incident angle α. While to find the incident angle, for each given couple of u and n, the only unknowns are the induced velocities u_a and u_t. So the whole problem of calculating the thrust force boils down to be the calculation of the induced velocities.

A.2.1 Axial and tangential induced velocity

To find the induced velocities, both the momentum theory and the circulation theory are applied in the analysis. First, by applying the momentum theory, the relationship between the two components of induced velocity u_a and u_t is derived. Then, through the application of the circulation theory a new equation is established, which gives the explicit relation between the induced velocities and the known parameters, the surge velocity u and the propeller rotating rate n.

According to the momentum theory, the propeller is regarded as a circular disk consisting of infinite small blades which are uniformly located on the hub of the propeller. The disk is called an actuator disk. By using the principle of relative motion, the actuator disk is still and the fluid particles

form a steady flow passing through it. The following assumptions are made before the analyses is started:

1. The flow is ideal flow, i.e. friction is ignored.
2. The flow velocity fields including the surge velocity field and the angular velocity field are uniformly distributed on the disk, and so are the forces.
3. There is an unlimited inflow of water to the propeller.

Under these assumptions, the flow through the disk and the distribution of the hydrodynamic pressure in the flow is just as shown in *Fig.* A.3[6].

At the far front of the actuator disk, the flow has a linear velocity U parallel to the axis of the disk and a rotating velocity ω about the same axis. When the flow passes through the disk, the fluid particles are accelerated in both the axial direction and the tangential direction. In the axial direction, the sternward velocity component is greater than U, and in the area far behind the disk, the axial velocity will be $U + u_a$, where u_a is called the induced velocity in the axial direction. By applying the momentum theory, it can be shown that the axial induced velocity at the disk is $\frac{u_a}{2}$. The axial induced velocity is assumed uniformly distributed on the actuator disk.

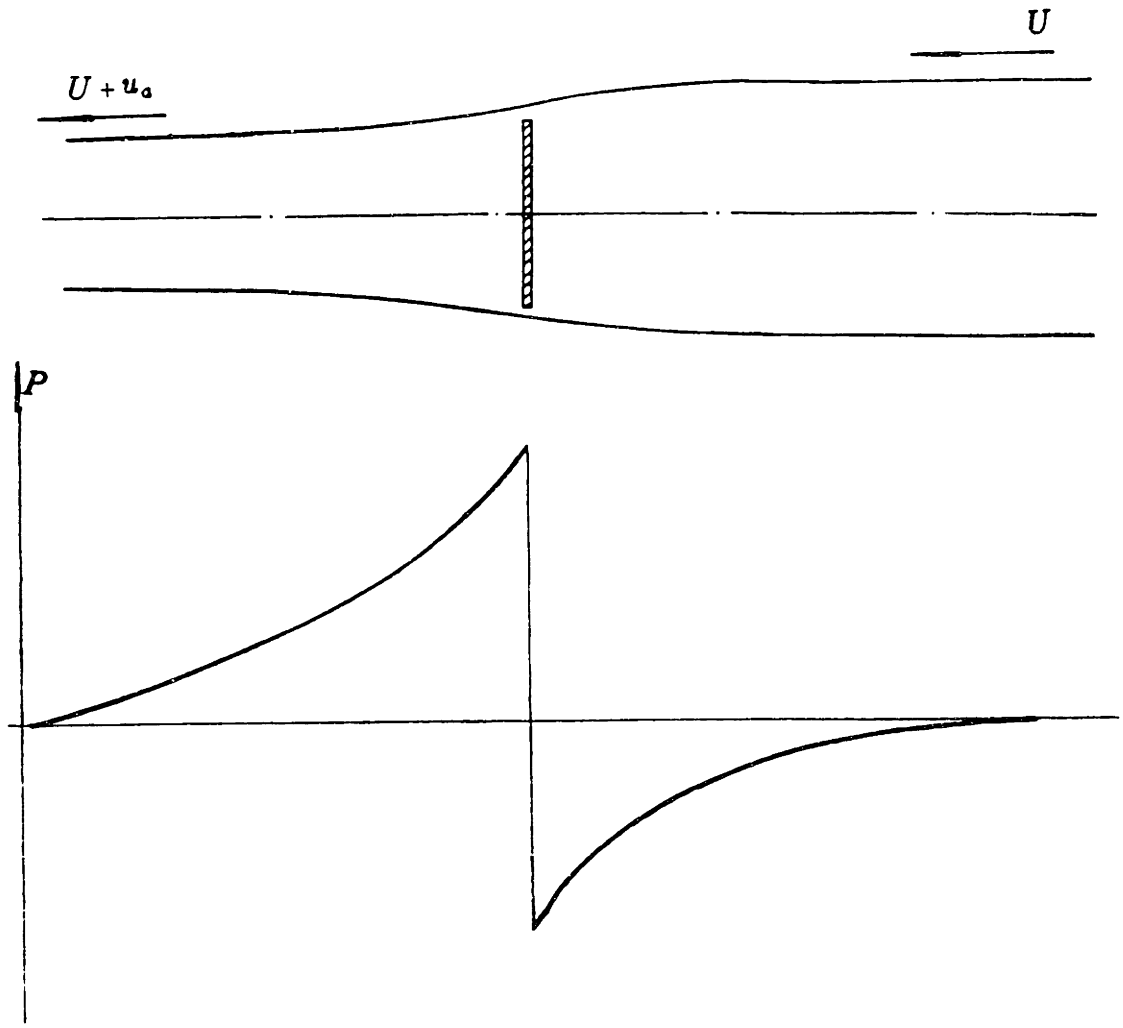

Figure A.3: Distribution of Hydrodynamic Pressure

In the tangential direction, in front of the disk, the relative angular velocity of the flow about the disk axis is ω, Far behind the disk, the angular velocity is $\omega - \omega_i$, where ω_i is the *induced angular velocity.* By applying the angular momentum theory, it is shown that at the disk, the value of the induced angular velocity is $\frac{\omega_i}{2}$. So when considering the flow

element at radius r from the disk axis, and taking the tangential induced velocity in the area far behind the disk as u_t, the tangential induced velocity at the disk would be $\frac{u_t}{2}$.

From *Bernoulli's theorem*, at any r,

$$\frac{p_1}{\rho} + \frac{(u+u_a)^2 + (\omega r - u_t)^2}{2} = \frac{p_2}{\rho} + \frac{u^2 + (\omega r)^2}{2} \tag{A.3}$$

Since $p_1 = p_2$, it follows that

$$u_a(u + \frac{u_a}{2}) - u_t(\omega r - \frac{u_t}{2}) = 0 \tag{A.4}$$

(Strictly speaking, $p_1 < p_2$, because of the existence of a centrifugal force caused by the induced angular velocity.) And

$$\frac{u_a}{u_t} = \frac{\omega r - \frac{u_t}{2}}{u + \frac{u_a}{2}} \tag{A.5}$$

This relation is important in the analysis of the forces at the propeller blade, when the lifting surface theory is applied.

A.2.2 Relation between circulation and induced velocity

In *Fig. A.4*, an imaginary column of radius r is shown, the surface of which has cross sections with the blades of the propeller[24].

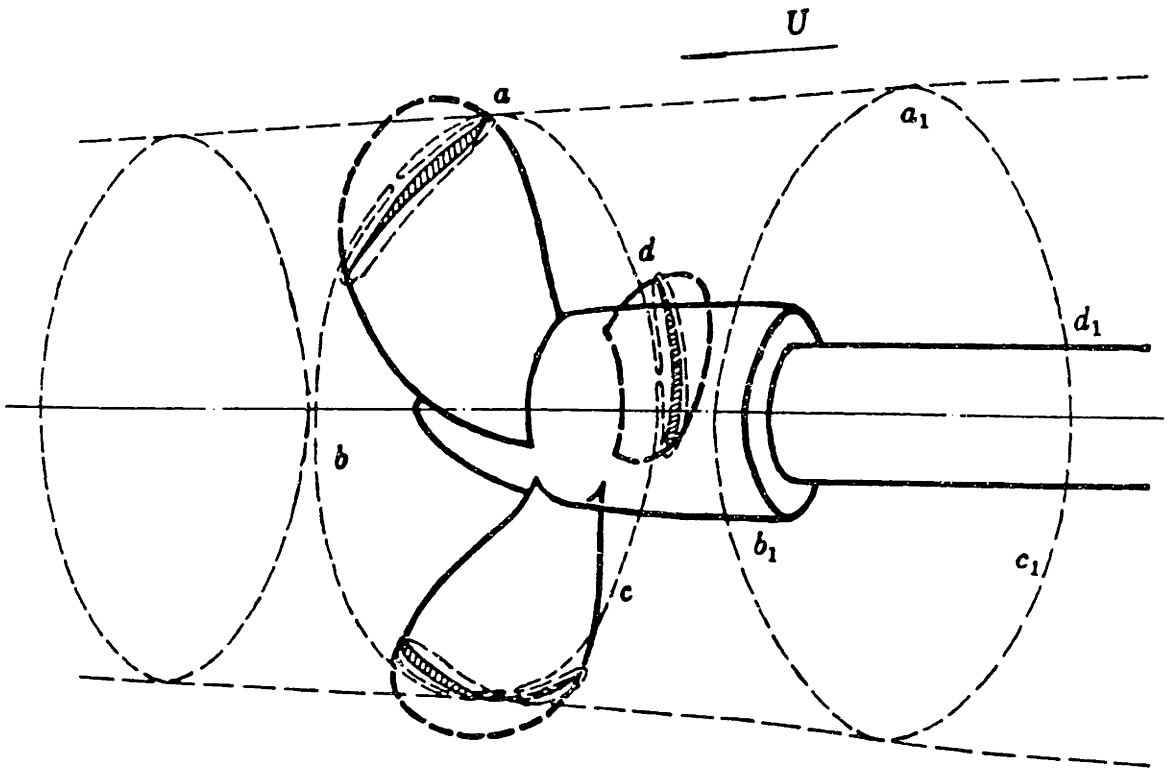

Figure A.4: Induced Velocity Analysis Through Circulation

The circulation along the closed loop *abcd* should be the circulation of the circle $a_1b_1c_1d_1$ of r at the immediate front of the propeller disk. Because there is no circulation in front of the propeller disk, hence

$$\Gamma_{abcd} = 0$$

While at the same time, the circulation of loop *abcd*

$$\Gamma_{abcd} = \Gamma_1 + q\Gamma_q$$

where Γ_1 is the circulation along the closed loop of the circle immediately behind the propeller disk. So

$$\Gamma_1 = 2\pi r u_t$$

and

$$\Gamma_q = \frac{2\pi r u_t}{q} \tag{A.6}$$

That is the relation between the unit circulation of the propeller blade and the tangential induced velocity.

A.3 Thrust Force Analysis

The analysis of the thrust force acting on the propeller blade can now proceed. As mentioned in *A*.1, each propeller blade is considered as a wing

whose cross section is the same as that of the blade at $r = r^*$. The incident angle and flow velocities are shown in *Fig. A.5*.

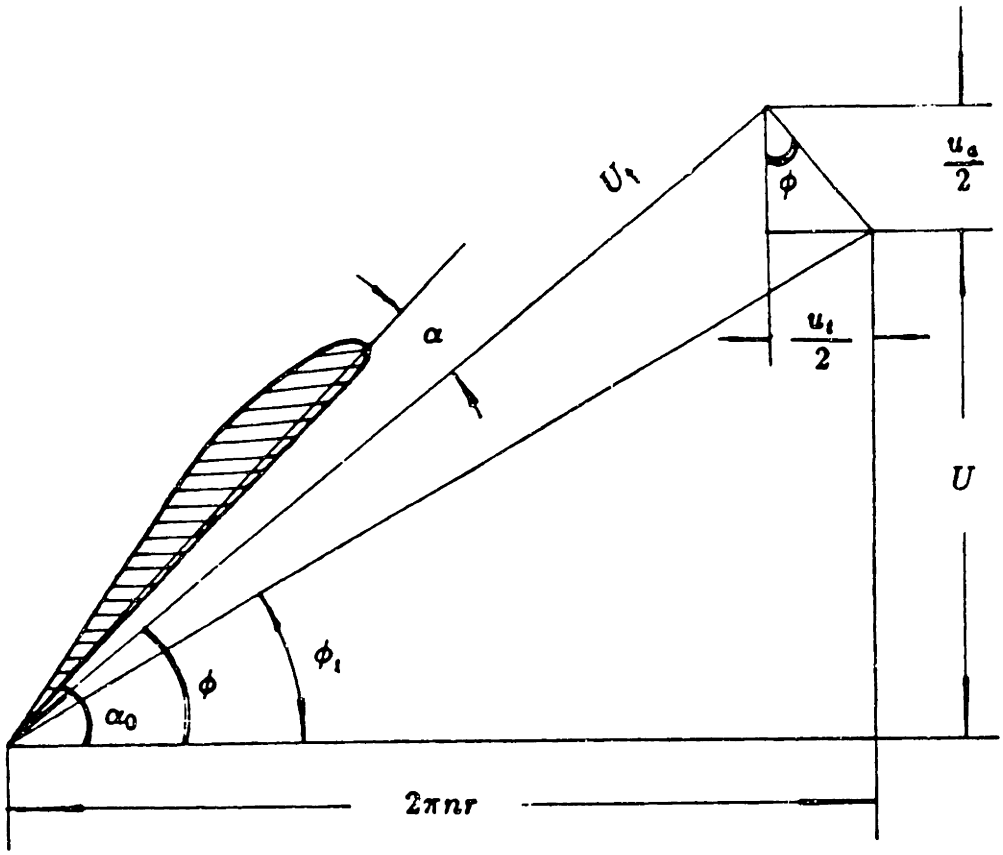

Figure A.5: Incident Flow and Attacking Angle

According to Schlichting et al[19] for a moderate incident angle the following relations hold:

$$C_L = (\frac{\partial C_L}{\partial \alpha})(\alpha - \alpha_0) \tag{A.7}$$

$$C_D = C_{D_0} + K_1 C_l + K_2 {C_L}^2 \tag{A.8}$$

where C_{D_0} is the drag coefficient of the wing at *zero* lift, K_1, K_2 depend mainly on the geometry of the wing. Here, C_D includes both parts for *profile drag* and *induced drag* of the wing.

The thrust force on one blade of the propeller is then

$$\begin{aligned} T_q &= L\cos\phi - D\sin\phi \\ &= \frac{1}{2}\rho {U_t}^2 (C_L\cos\phi - (C_{D_0} + K_1 C_L + K_2 {C_L}^2)\sin\phi) \end{aligned} \tag{A.9}$$

From the lifting surface theory, we know that at radius r of a propeller, the circulation should be

$$\Gamma = \frac{1}{2} C_L b U_t \tag{A.10}$$

where b is the *blade section chord* at radius r.

Comparing it with the result from Equation(A.6), we have

$$\frac{2\pi r u_t}{q} = \frac{1}{2} C_L b U_t \tag{A.11}$$

Introducing the relationships:

$$a_1 = \frac{\frac{u_a}{2}}{u}$$

$$a_2 = \frac{\frac{u_t}{2}}{2\pi rn}$$

then,

$$U_t = 2\pi rn(1 - a_2)\sqrt{1 + \tan^2\phi} \tag{A.12}$$

$$\frac{a_2}{1 - a_2} = \frac{qbC_L}{8\pi r}\sqrt{1 + \tan^2\phi} \tag{A.13}$$

Recalling the relation between u_a and u_t established in Equation(A.5),

$$u_t = u_a \tan\phi \tag{A.14}$$

Then, a_1 can be expressed as:

$$\frac{a_1}{1 + a_1} = \frac{qbC_L}{8\pi r}\frac{\cos\phi}{\sin^2\phi} \tag{A.15}$$

And it follows that

$$a_1 = \frac{\frac{qb^*C_L\cos\phi}{8\pi r^*\sin\phi^2}}{1 - \frac{qb^*C_L\cos\phi}{8\pi r^*\sin\phi^2}} \tag{A.16}$$

$$a_2 = \frac{\frac{qb^*C_L}{8\pi r^*\cos\phi}}{1 + \frac{qb^*C_L}{8\pi r^*\cos\phi}} \tag{A.17}$$

Substituting in equation(A.14), one obtains

$$\begin{aligned} \tan\phi &= \frac{u_t}{u_a} \\ &= \frac{\tan^2\phi(1 - \frac{qb^*C_L\cos\phi}{8\pi r^*\sin\phi^2})}{J_*(1 + \frac{qb^*C_L}{8\pi r^*\cos\phi})} \end{aligned} \tag{A.18}$$

where $J_* = \frac{u}{2\pi r^*}$.

Comparing with the definition of the advanced ratio of the propeller:

$$J = \frac{u}{nd}$$

It is clear that $J_* = \frac{\Re}{\pi r^*} J$. After algebraic operations on Equation $(A.18)$, the relation between the lifting coefficient C_L and $\tan\phi$ is established as follows:

$$C_L = \frac{\sin\phi(\tan\phi - J_*)}{A(1 + J_*\tan\phi)} \tag{A.19}$$

For succinctness, a constant $A = \frac{qb^*}{8\pi\Re r^*}$ is introduced. Then from Equation $(A.19)$ one gets

$$\alpha_0 - \phi = \frac{\sin\phi(\tan\phi - J_*)}{A(\frac{\partial C_L}{\partial\alpha})(1 + J_*\tan\phi)} \tag{A.20}$$

Since ϕ and J_* are the only variables in Equation $(A.20)$, ϕ or $\tan\phi$ can be expressed approximately as a function of J_*.

Now considering two cases:

a. $\phi \approx \tan\phi$

Then,

$$\begin{aligned}(\frac{\partial C_L}{\partial\alpha})(\alpha_0 - \phi) &\approx \frac{\tan\phi(\tan\phi - J_*)}{A(1 + J_*\tan\phi)} \\ &\approx \frac{\tan\phi(\tan\phi - J_*)}{A}\end{aligned} \tag{A.21}$$

This yields

$$\frac{\tan\phi^2}{A} + \frac{A(\frac{\partial C_L}{\partial\alpha}) - J_*}{A}\tan\phi - (\frac{\partial C_L}{\partial\alpha})\alpha_0 = 0 \tag{A.22}$$

and

$$\tan\phi = \frac{-A(\frac{\partial C_L}{\partial\alpha}) - J_* \pm \sqrt{A(\frac{\partial C_L}{\partial\alpha}) - J_*^2 + 4A(\frac{\partial C_L}{\partial\alpha})\alpha_0}}{2} \tag{A.23}$$

For ship propellers, $\tan\phi > 0$. Notice that in all the above steps, the unit of angle ϕ is implicitly in *radians*, so that $(\frac{\partial C_L}{\partial \alpha})$ corresponding to the very small values of ϕ is large. Therefore,

$$\begin{aligned}
\tan\phi &\approx \frac{\sqrt{(\frac{\partial C_L}{\partial \alpha})(A(\frac{\partial C_L}{\partial \alpha})-2J_*)A} - A(\frac{\partial C_L}{\partial \alpha}) - J_*}{2} \\
&\approx \frac{\sqrt{A(\frac{\partial C_L}{\partial \alpha})(A(\frac{\partial C_L}{\partial \alpha})+4\alpha_0)(1-\frac{2J_*}{A(\frac{\partial C_L}{\partial \alpha})+4\alpha_0})} - A(\frac{\partial C_L}{\partial \alpha}) - J_*}{2} \\
&\approx A_1 + A_2 J_* + A_3 J_*^2 \qquad \text{(A.24)}
\end{aligned}$$

$$\begin{aligned}
\text{where } A_1 &= \frac{2\alpha_0 A(\frac{\partial C_L}{\partial \alpha})}{A(\frac{\partial C_L}{\partial \alpha}) + \sqrt{A(\frac{\partial C_L}{\partial \alpha})^2 + 4A(\frac{\partial C_L}{\partial \alpha})\alpha_0}} \\
A_2 &= \frac{\sqrt{A(\frac{\partial C_L}{\partial \alpha})^2 + 4A(\frac{\partial C_L}{\partial \alpha})\alpha_0} - A(\frac{\partial C_L}{\partial \alpha})}{2\sqrt{A(\frac{\partial C_L}{\partial \alpha})^2 + 4A(\frac{\partial C_L}{\partial \alpha})\alpha_0}} \\
A_3 &= \frac{A(\frac{\partial C_L}{\partial \alpha})\alpha_0}{(\sqrt{A(\frac{\partial C_L}{\partial \alpha})^2 + 4A(\frac{\partial C_L}{\partial \alpha})\alpha_0})^3}
\end{aligned}$$

With these results, the thrust force can be expressed as a function of the advanced ratio J. Based on this result, the relation between $C_D\tan\phi$ and the advanced ratio J is

$$\begin{aligned}
C_D\tan\phi &= (C_{D_0} + K_1 A_1^2 + K_2 A_1^4) A_1 \\
&\quad + ((K_1 + 2K_2 A_1^2(2A_2 - 1)A_1^2 + (C_{D_0} + K_1 A_1^2 \\
&\quad + K_2 A_1^4) A_2)) J_* + (A_1 K_1 (2A_1 A_3 + A_2(A_2 - 1)) \\
&\quad + A_1 K_2 (A_1^2 (2A_2 - 1)^2 + 4A_1^3 A_3 + 2A_1^2 A_2 (A_2 - 1)) \\
&\quad + (C_{D_0} + K_1 A_1^2 + K_2 A_1^4) A_3) J_*^2
\end{aligned}$$

$$
\begin{aligned}
C_L - C_D\tan\phi &= A_1(A_1 - (C_{D_0} + K_1 A_1^2 + K_2 A_1^4)) \\
&\quad +(A_1(2A_2 - 1)(1 - A_1^2(K_1 + 2K_2 A_1^2)) \\
&\quad -A_2(C_{D_0} + K_1 A_1^2 + K_2 A_1^4))J_* \\
&\quad +(2A_1A_3 + A_2(A_2 - 1))(1 - A_1K_1) \\
&\quad -A_1^3K_2((2A_2 - 1)^2 + 4A_1A_3 + 2A_2(A_2 - 1)) \\
&\quad -A_3(C_{D_0} + K_1A_1^2 + K_2A_1^4)))J_*^2 \qquad \text{(A.25)}
\end{aligned}
$$

Since $\phi \ll 1$, the propeller thrust coefficient K_t can be expressed as:

$$
\begin{aligned}
K_t &= \frac{qb^*}{8\Re r^*}\pi^2(1-a^2)^2\sqrt{1+\tan^2\phi}(C_L - C_D\tan\phi) \\
&\approx \frac{qb^*\pi^2}{8\Re r^*}(C_L - C_D\tan\phi) \\
&= \eta_1 J^2 + \eta_2 J + \eta_3 \qquad \text{(A.26)}
\end{aligned}
$$

where

$$
\begin{aligned}
\eta_1 &= \frac{qb^*\Re}{8r^{*3}}((2A_1A_3 + A_2(A_2-1))(1 - A_1K_1 - A_1^3K_2((2A_2-1)^2 \\
&\quad +4A_1A_3 + 2A_2(A_2-1)) - A_3(C_{D_0} + K_1A_1^2 + K_2A_1^4)) \\
\eta_2 &= \frac{qb^*\pi}{8r^{*2}}(A_1(2A_2-1)(1 - A_1^2(K_1 + 2K_2A_1^2)) - A_2(C_{D_0} + \\
&\quad K_1A_1^2 + K_2A_1^4)) \\
\eta_3 &= \frac{qb^*\pi^2}{8r^*\Re}A_1(A_1 - (C_{D_0} + K_1A_1^2 + K_2A_1^4))
\end{aligned}
$$

Now, the sign of each of the above three coefficients can be checked, based on the previous discussions.

1. According to the data from the "Theory of Wing Section" [2] by Abbot et al, C_{D_0} and K_2 are small and positive, while K_1 is negative and its absolute value is even smaller. For example:

   For wing section "NACA 0009",

$$\begin{aligned} C_{D_0} &= 0.009 \\ K_1 &= -0.00067 \\ K_2 &= 0.0133 \end{aligned}$$

   For wing section "NACA 63-206",

$$\begin{aligned} C_{D_0} &= 0.009 \\ K_1 &= -0.0066 \\ K_2 &= 0.0156 \end{aligned}$$

   It follows that $A_1 > C_{D_0} + K_1 {A_1}^2 + K_2 {A_1}^4 > 0$ always holds, that is, η_3 always positive.

2. $$2A_2 - 1 = -\frac{A(\frac{\partial C_L}{\partial \alpha})}{\sqrt{A(\frac{\partial C_L}{\partial \alpha})^2 + 4A(\frac{\partial C_L}{\partial \alpha})\alpha_0}} < 0$$

$$0 < {A_1}^2 < 1$$

$$0 < (K_1 + 2K_2 {A_1}^2) < 1$$

There follows

$$A_1(2A_2-1)(1-{A_1}^2(K_1+2K_2{A_1}^2)) \quad < \quad 0$$

$$A_2(C_{D_0}+K_1{A_1}^2+K_2{A_1}^4) \quad > \quad 0$$

Therefore η_2 is always less than *zero.*

3. $1-A_1K_1>0$

$$2A_1A_3+A_2(A_2-1)=-\frac{A(\frac{\partial C_L}{\partial \alpha})^2\alpha_0}{(\sqrt{A(\frac{\partial C_L}{\partial \alpha})^2+4A(\frac{\partial C_L}{\partial \alpha})\alpha_0})^3}<0$$

$${A_1}^3K_2((2A_2-1)^2+4A_1A_3+2A_2(A_2-1))>0$$

So η_1 is always negative.

b. $\alpha_0-\phi \approx \tan\alpha_0-\phi$:

In this case,

$$\begin{aligned}(\frac{\partial C_L}{\partial \alpha})(\alpha_0-\phi) &\approx (\frac{\partial C_L}{\partial \alpha})\tan(\alpha_0-\phi)\\ &\approx \tan\alpha\cos\alpha_0\tan(\phi-\phi_1) \qquad \text{(A.27)}\end{aligned}$$

where $\tan\phi_1=J_*$.

This relation is the same as

$$\tan\phi=\frac{A(\frac{\partial C_L}{\partial \alpha})\tan(\alpha_0-\phi)}{\cos\alpha_0\tan(\phi-\phi_1)} \qquad \text{(A.28)}$$

Introducing $B=\frac{A(\frac{\partial C_L}{\partial \alpha})}{\cos\alpha_0}$, we get

$$\begin{aligned}\tan\phi &= B(\frac{\sin(\alpha_0-\phi_1)}{\sin(\phi-\phi_1)}-1)\\ &\approx B(\frac{\tan\alpha_0-J_*}{\tan\phi-J_*}-1) \qquad \text{(A.29)}\end{aligned}$$

It follows that

$$\tan^2\phi + (B - J_*)\tan\phi - B\tan\alpha_0 = 0 \tag{A.30}$$

And using the same procedure as in the first case, there follows

$$\tan\phi = B_1 + B_2 J_* + B_3 {J_*}^2 \tag{A.31}$$

And finally, K_t can be expressed as

$$K_t = \eta_1' J^2 + \eta_2' J + \eta_3' \tag{A.32}$$

and

$$\begin{aligned} \eta_1' &< 0 \\ \eta_2' &< 0 \\ \eta_3' &> 0 \end{aligned}$$

In this section it is shown that the K_t curve of the propeller can be approximated by a *second order* curve. It is known that the *pitch ratio* of a propeller P/D is generally less than 1.4, and in most cases, it is less than 1. The pitch angle corresponding to the pitch ratio 1.4 is 24°. Then angle ϕ in case *a* and angle $\alpha - \phi$ in case *b* are both less than 12°, and this means that the assumptions that $\tan\phi \approx \phi$ or $\tan(\alpha - \phi) \approx (\alpha - \phi)$ are reasonable. In the next section it will be shown that at least for 4-*blade* and 5-*blade* B-screw series propeller, the whole K_t curve can be very smoothly approximated by a single *second order* curve.

A.4 Curve Fitting for B-Screw Series Propellers

Van Lammeren et al,[21] have pointed out that for the 4-*blade* and 5-*blade* B-screw series propellers, the K_t curves can be expressed as a *third order* polynomial of the advanced ratio J, with the higher powers of J negligible. To see whether the *second order* polynomial approximation is proper and to assess the difference between it and the *third order* polynomial approximation, the K_t curves of B-screw series propellers published in the above paper are examined. The coordinates of J and K_t for each thrust coefficient curve are picked as input values into the curve fitting packages to find the coefficients corresponding to the *second order* polynomials. The residue between the input K_t and that from the calculation through the polynomial at each J is also calculated. And the curve of calculated values is drawn and compared with the original curve. The results show that the approximation is very good for representing the thrust force in the surge equation of the ship.

In *Fig. A.6*, as an example, a $B4$-55 propeller($P/D = 1.2$) is chosen, its K_t curve is approximated by both the *second order* polynomial and the *third order* polynomial. Little improvement for the third order polynomial approximation can be seen.

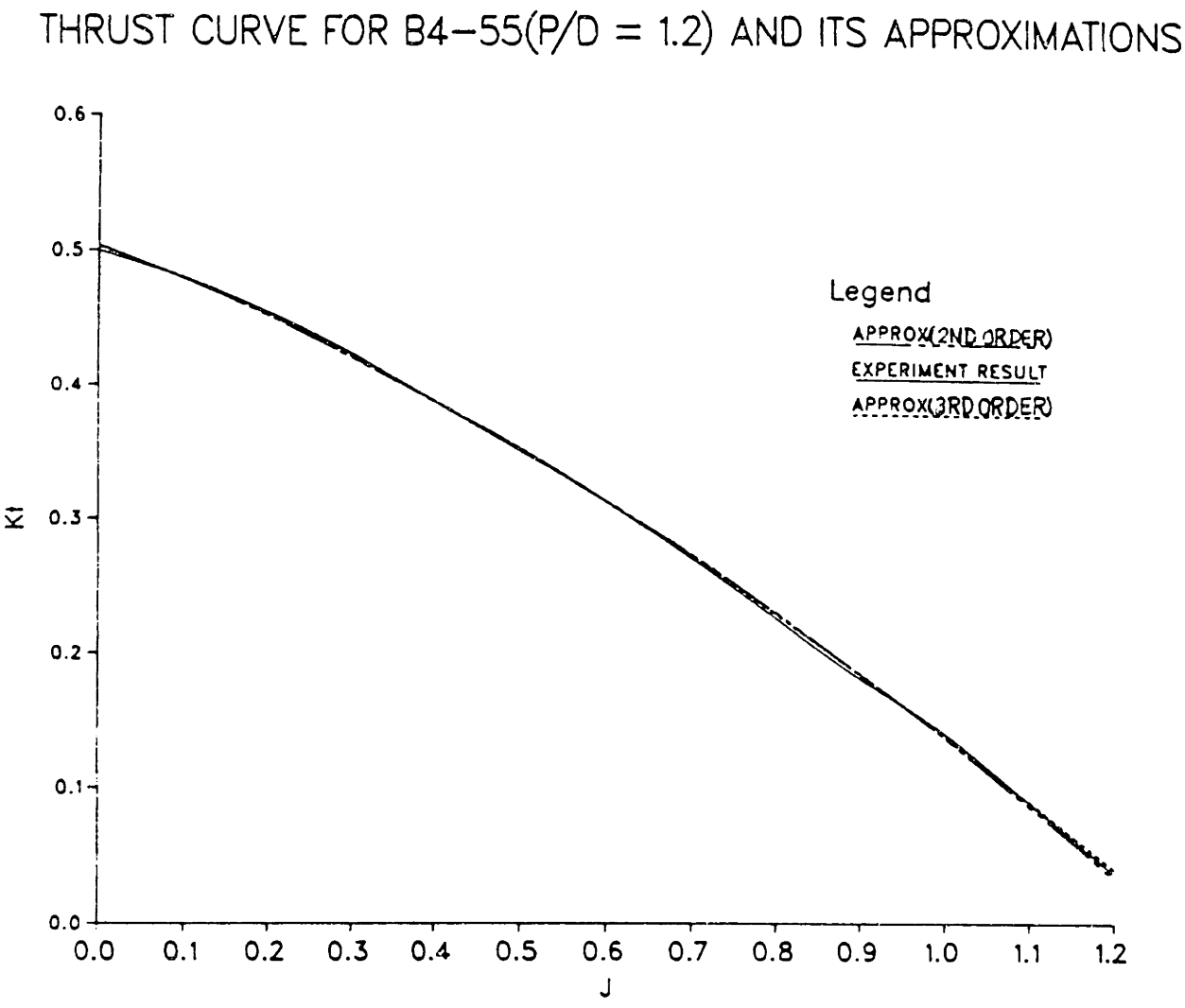

Figure A.6: Model Test K_t Curve for B4-55 and Its Approximation

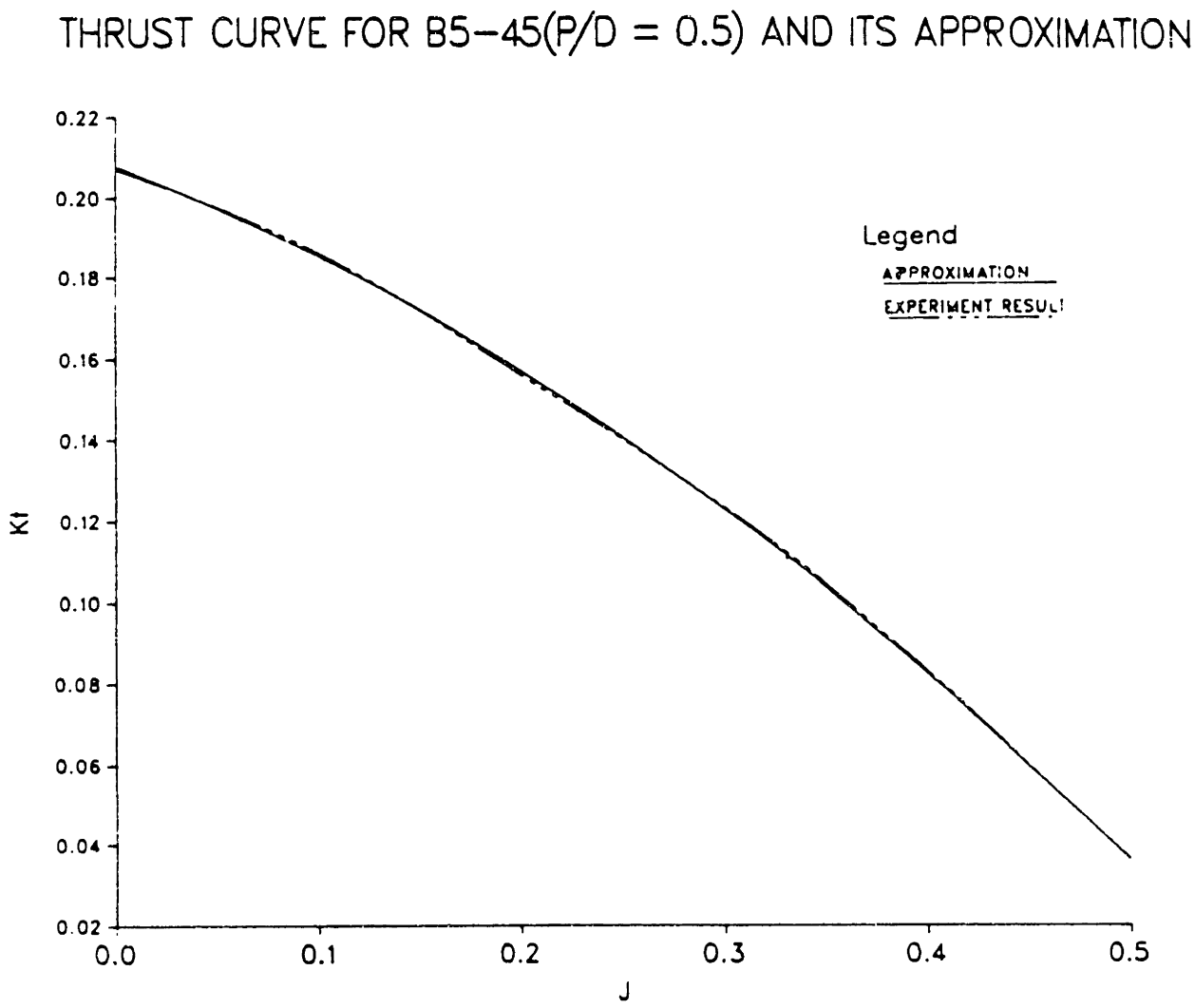

Figure A.7: Model Test K_t Curve for B5-45 and Its Approximation

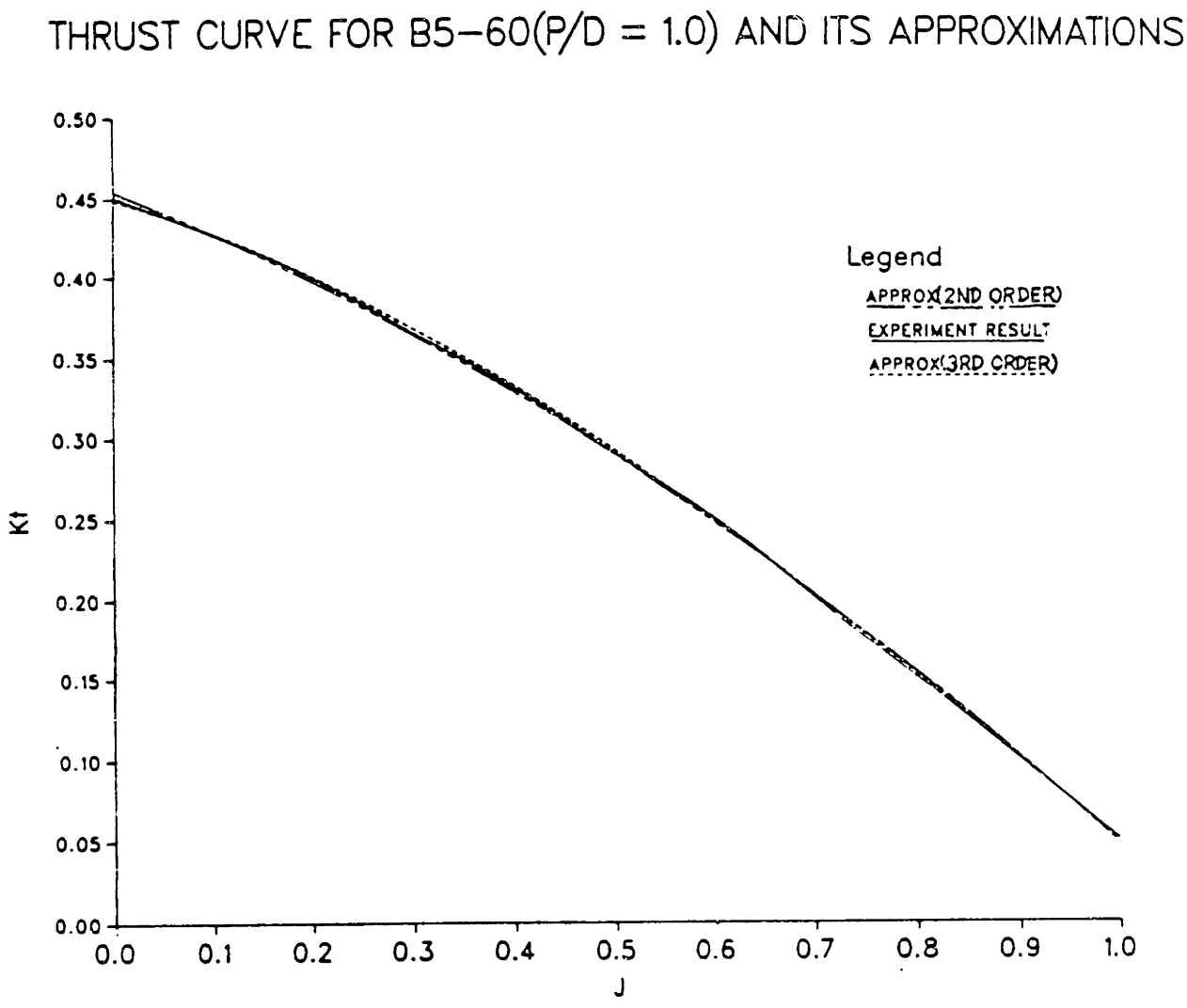

Figure A.8: Model Test K_t Curve for B5-60 and Its Approximation

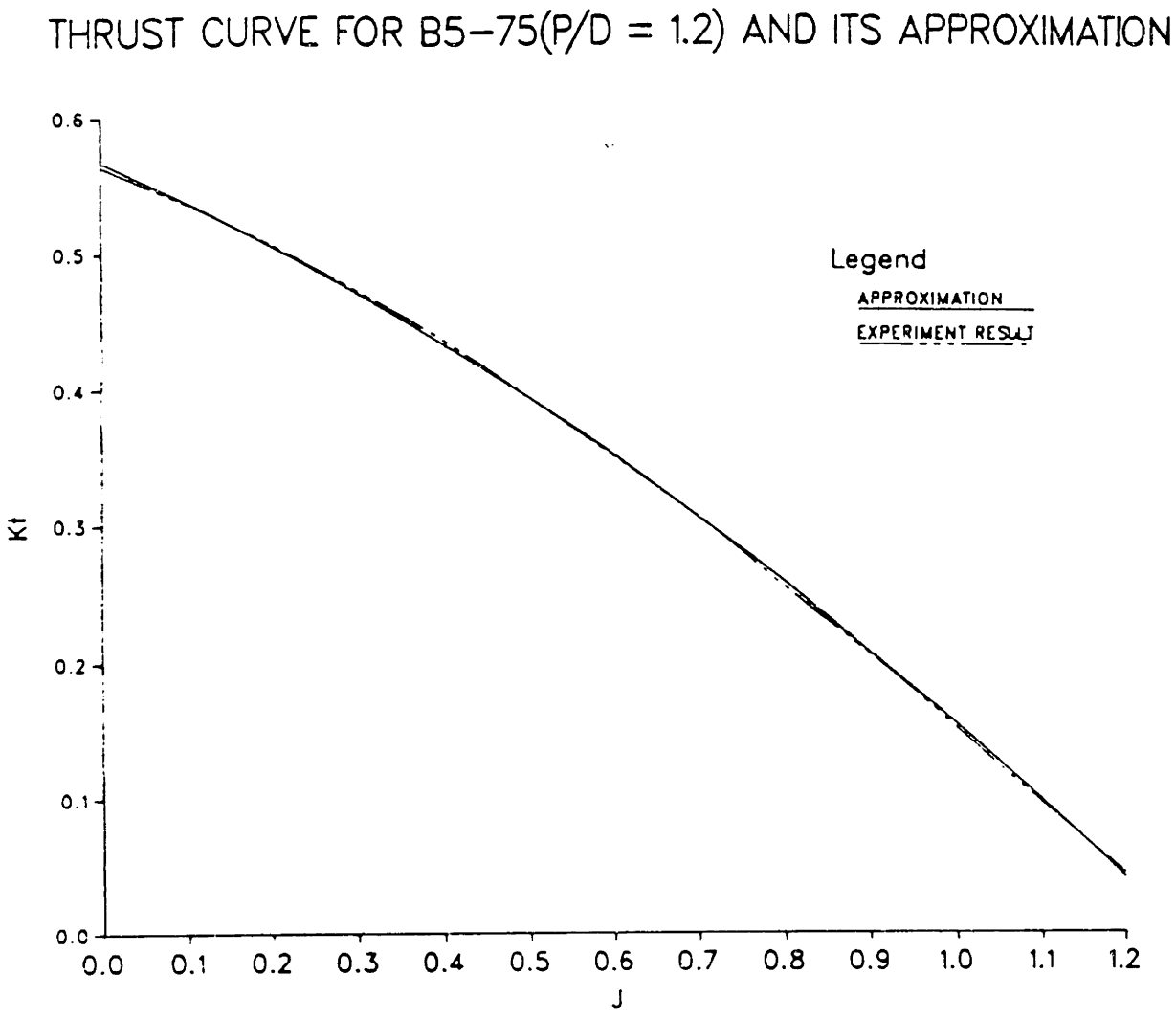

Figure A.9: Model Test K_t Curve for B5-75 and Its Approximation

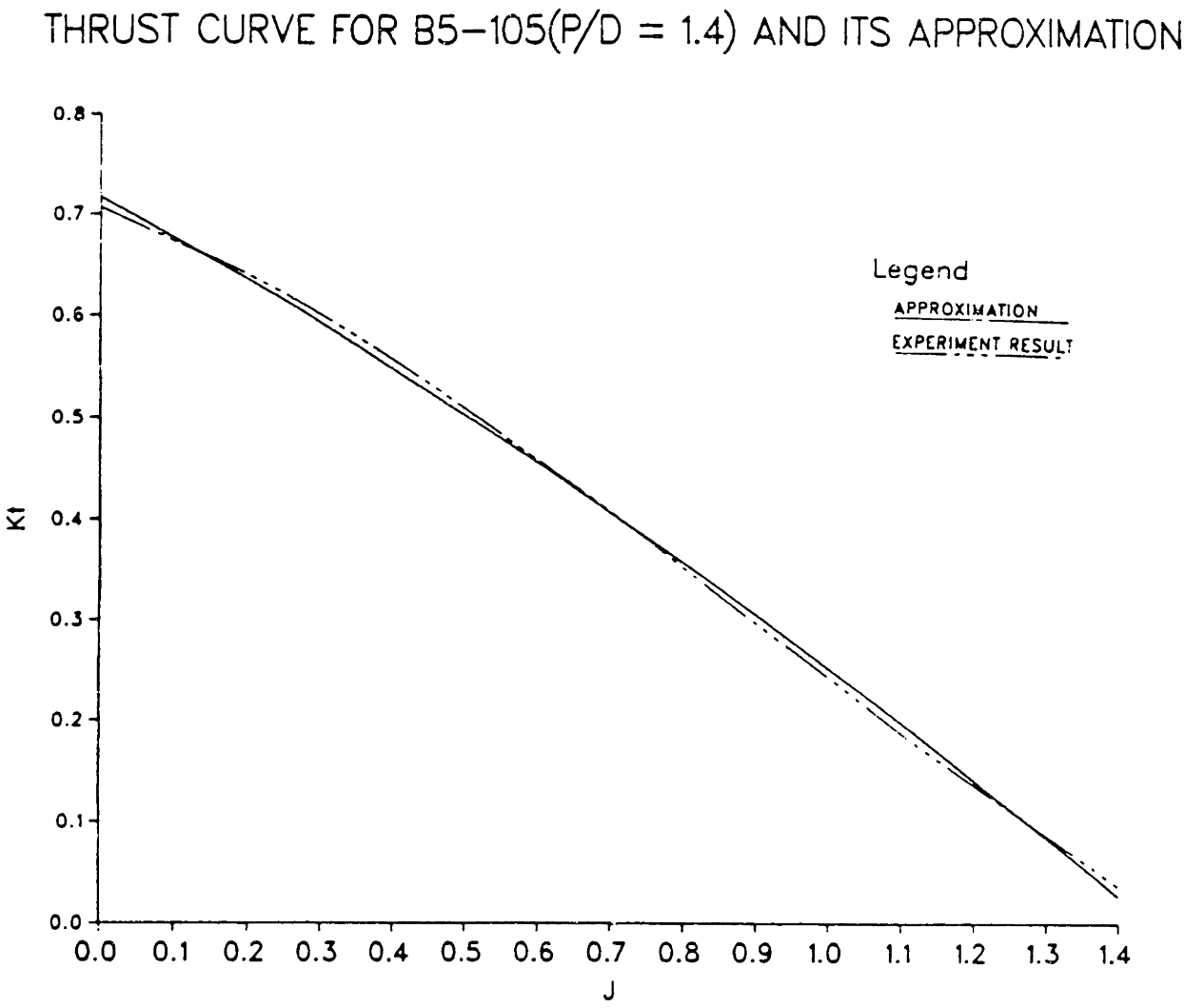

Figure A.10: Model Test K_t Curve for B4-105 and Its Approximation

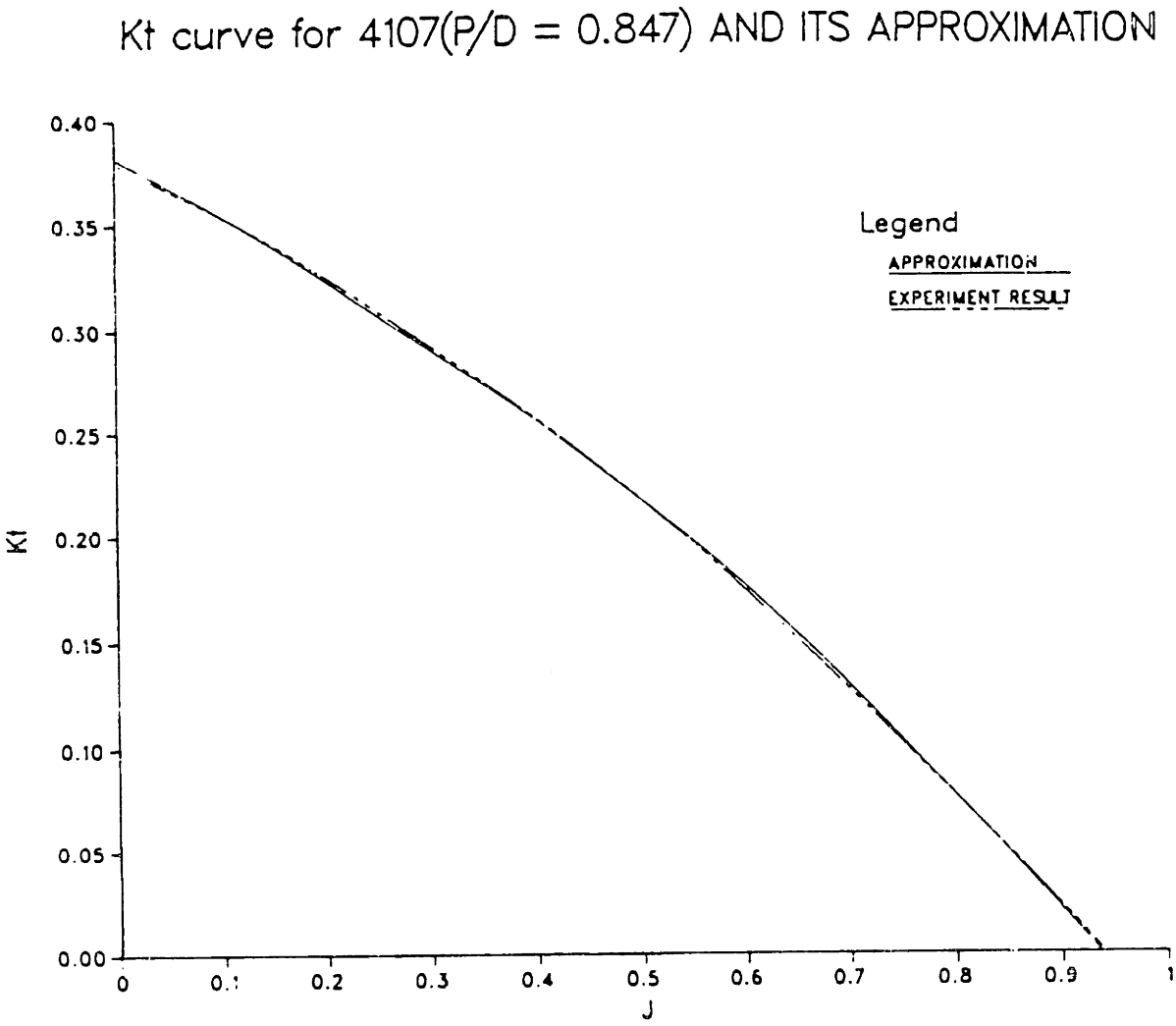

Figure A.11: Model Test K_t Curve for 4017 and Its Approximation

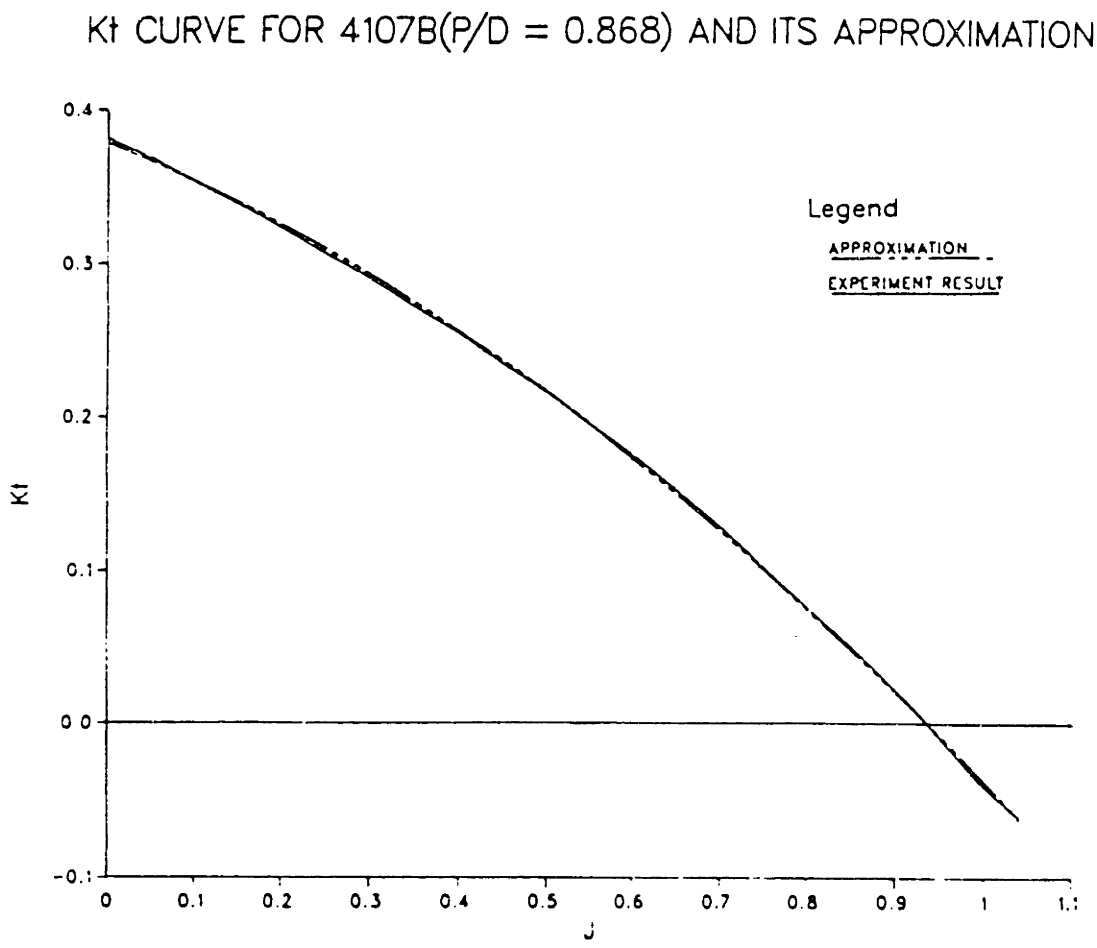

Figure A.12: Model test K_t Curve for 4017B and Its Approximation

Appendix B

Time Constant of Surge Motion System

The time constant is a characteristic constant for a linear system. However, because of the particular features of the equation of ship surge motion, a pseudo time constant is used following the definition extended from the linear system. The pseudo time constant for the tanker EXXON PHILADELPHIA can be obtained in two ways:

1. Analysis method.

   It is considered that the tanker is accelerated from the still state by the propeller rotating at cruising $rps = n_f$ which is the value of the rps when the tanker is in the equilibrium state at cruising speed.

Under this condition, the equation of the surge motion becomes

$$\dot{u} = \frac{\eta_1{}^* u^2 + \eta_2{}^* u n_f + \eta_3{}^* {n_f}^2}{m - X_{\dot{u}}} \tag{B.1}$$

Then bring in the values of all the parameters related to the tanker together with $n_f = 1.167\,rps$, there follows

$$\begin{aligned} \dot{u} &= -0.0000587u^2 - 0.000831u + 0.0665 \\ &= -0.0000587(u^2 + 14.157u) + 0.0665 \\ &= -0.0000587(u + 7.079)^2 + 0.0694 \end{aligned}$$

Introducing $u_1 = u + 7.079$

$$\dot{u_1} = -0.0000587{u_1}^2 + 0.0694$$

$$\begin{aligned} \frac{du_1}{0.0694 - 0.0000587{u_1}^2} &= dt \\ \frac{du_1}{1 - 0.000846{u_1}^2} &= 0.0694dt \end{aligned}$$

Introducing $u_2 = 0.0291u_1$, the equation becomes

$$\frac{du_2}{0.0291(1 - u_2)^2} = 0.0694dt$$

The solution of this differential equation is

$$\frac{1}{2}\ln\left|\frac{1 + u_2}{1 - u_2}\right| = \frac{1}{2}\ln\left|\frac{1 + u_2}{1 - u_2}\right|_{u_{20}} + 0.00202 \tag{B.2}$$

$t = 0, u_0 = 0 \implies u_{20} = 0.206$

Therefore, the solution for u_2 is

$$u_2 = \frac{1.519e^{0.00404t} - 1}{1.519e^{0.00404t} + 1} \tag{B.3}$$

And the solution for u is

$$u = 27.285 - \frac{68.728}{1.519e^{0.00404t} + 1} \tag{B.4}$$

The derivative of u to t at time $t = 0$ is then

$$K = \left(\frac{du}{dt}\right)_{t=0} = 0.0665$$

The pseudo time constant τ is therefore

$$\begin{aligned} \tau &= \frac{u_e}{K} \\ &= \frac{27.285}{0.0665} \\ &= 410.5(sec) \end{aligned} \tag{B.5}$$

where u_e is the surge speed of the tanker in the equilibrium state.

2. Simulation Method.

The other method is to use n_f as the input to simulate the surge motion of the tanker, and to find the slope of the velocity curve at the initial time and then the time constant as shown in *Fig. B.1*. From the figure, it is clear, the pseudo time constant is the same as that obtained by the previous method.

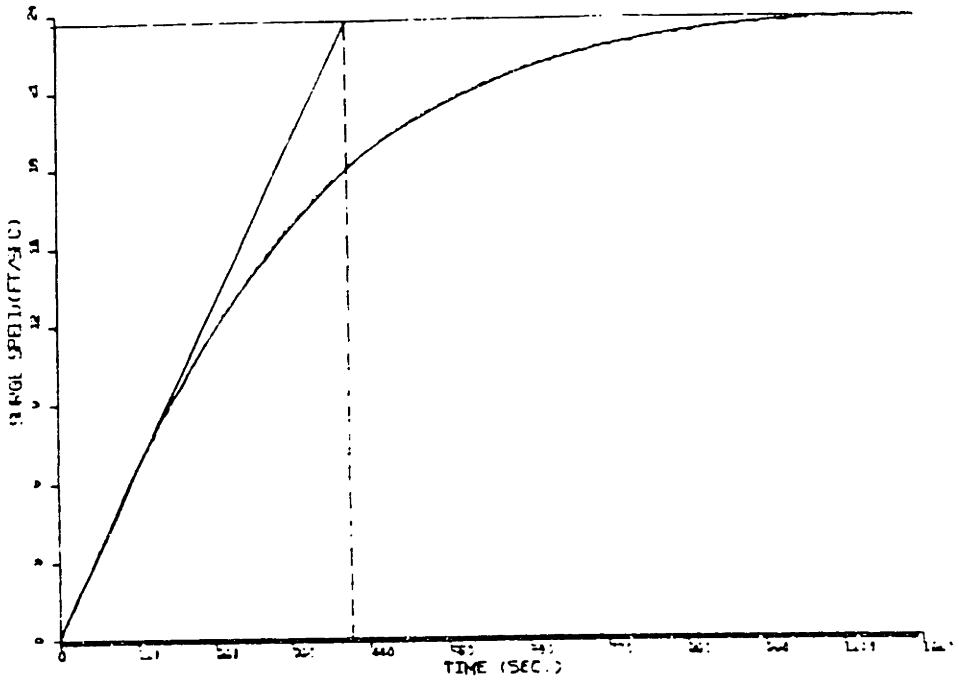

Figure B.1: Pseudo Time Constant from Simulation Curve

Appendix C

Noise Analysis of Data

After the collection of the measured data, the noise level of each measured variable is analysed. The results of these analyses are useful in the identification. The analyses were carried out by applying the *time series theory* developed by Box and Jenkins[5]. Briefly, the idea is as follows:

The measured data set of each variable is taken as a *time series*. This time series is represented by an *autoregressive integrated moving average*(ARIMA) model, If the variable is taken as χ_t, then the ARIMA model is defined as

$$\nabla^d \chi_t - \varsigma = \gamma_t \tag{C.1}$$

where $\nabla^d \chi_t$ is the result of applying differencing of order d to the series χ_t. Scalar ς is the expected value of the differenced series. Series γ_t follows a zero-mean stationary *autoregressive moving average*(ARMA) model de-

fined by

$$\gamma_t = \vartheta_1\gamma_{t-1} + \vartheta_2\gamma_{t-2} + \ldots + \vartheta_i\gamma_{t-i} + \epsilon_t - \xi_1\epsilon_{t-1} - \xi_2\epsilon_{t-2} - \ldots - \xi_j\epsilon_{t-j} \quad \text{(C.2)}$$

where ϵ_t is an uncorrelated series.

The program in the NAG library based on this theory can fit an ARIMA model to an observed time series by using a non-linear least squares procedure. As a result, parameters in the model are estimated together with appropriate standard errors, and the residual series is produced. These results give the noise level of the measured data, and it will help in applying identification techniques to the surge motion model.

Fig.s $C.1 \sim C.8$ are plots of the residuals of surge speed u and propeller rotating rate n for the deceleration procedure and for the acceleration procedure respectively.

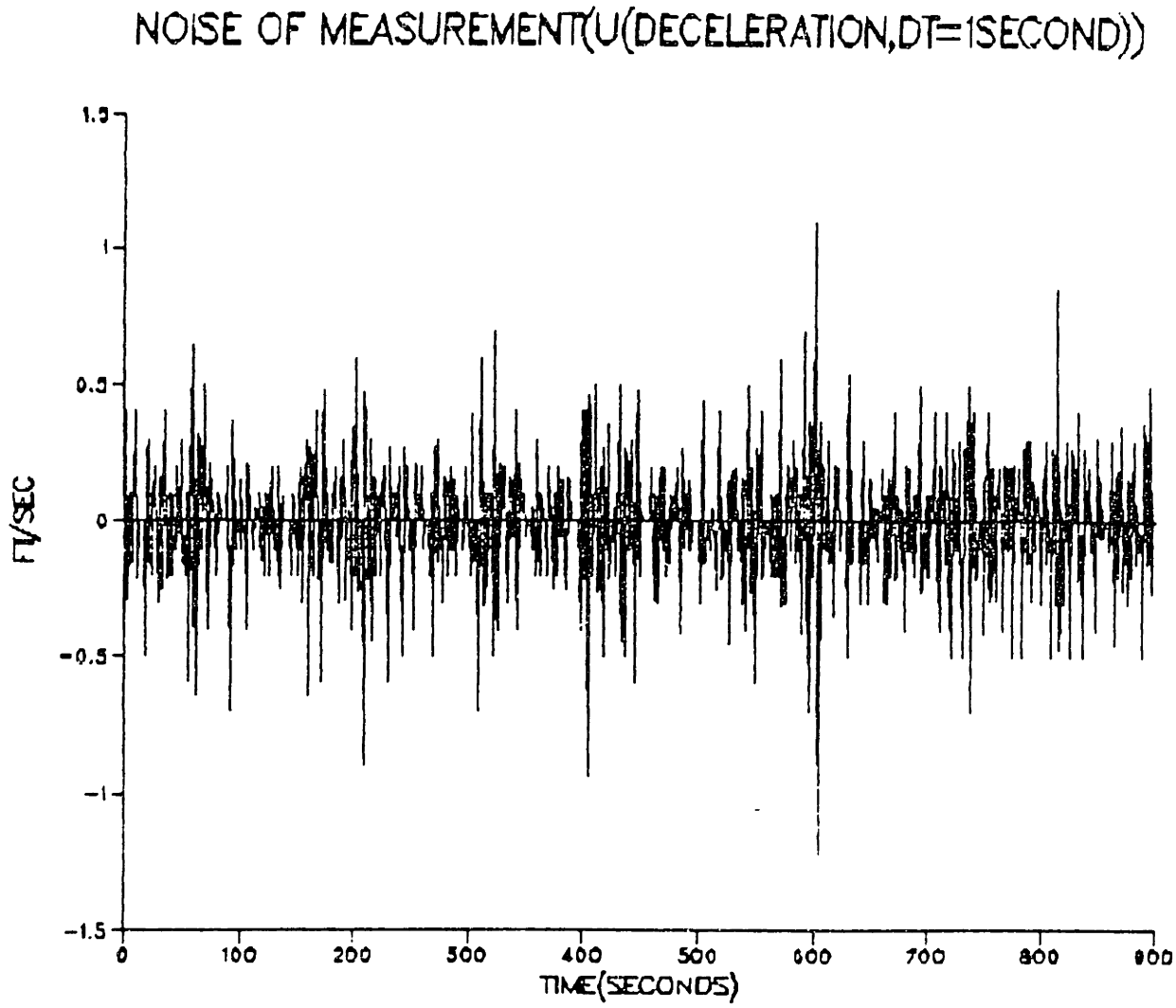

Figure C.1: Measurement Noise of u during Deceleration(1)

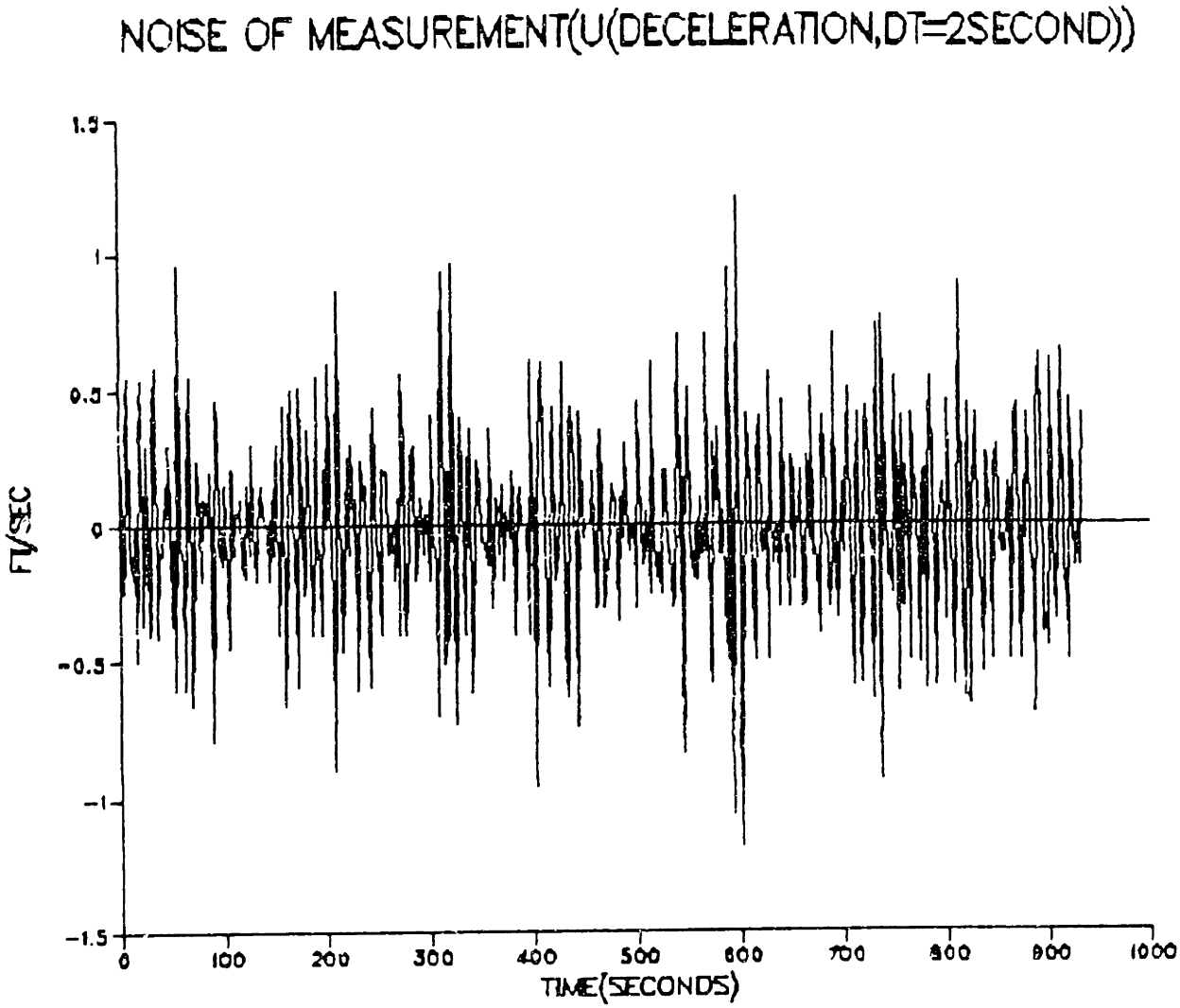

Figure C.2: Measurement Noise of u during Deceleration(2)

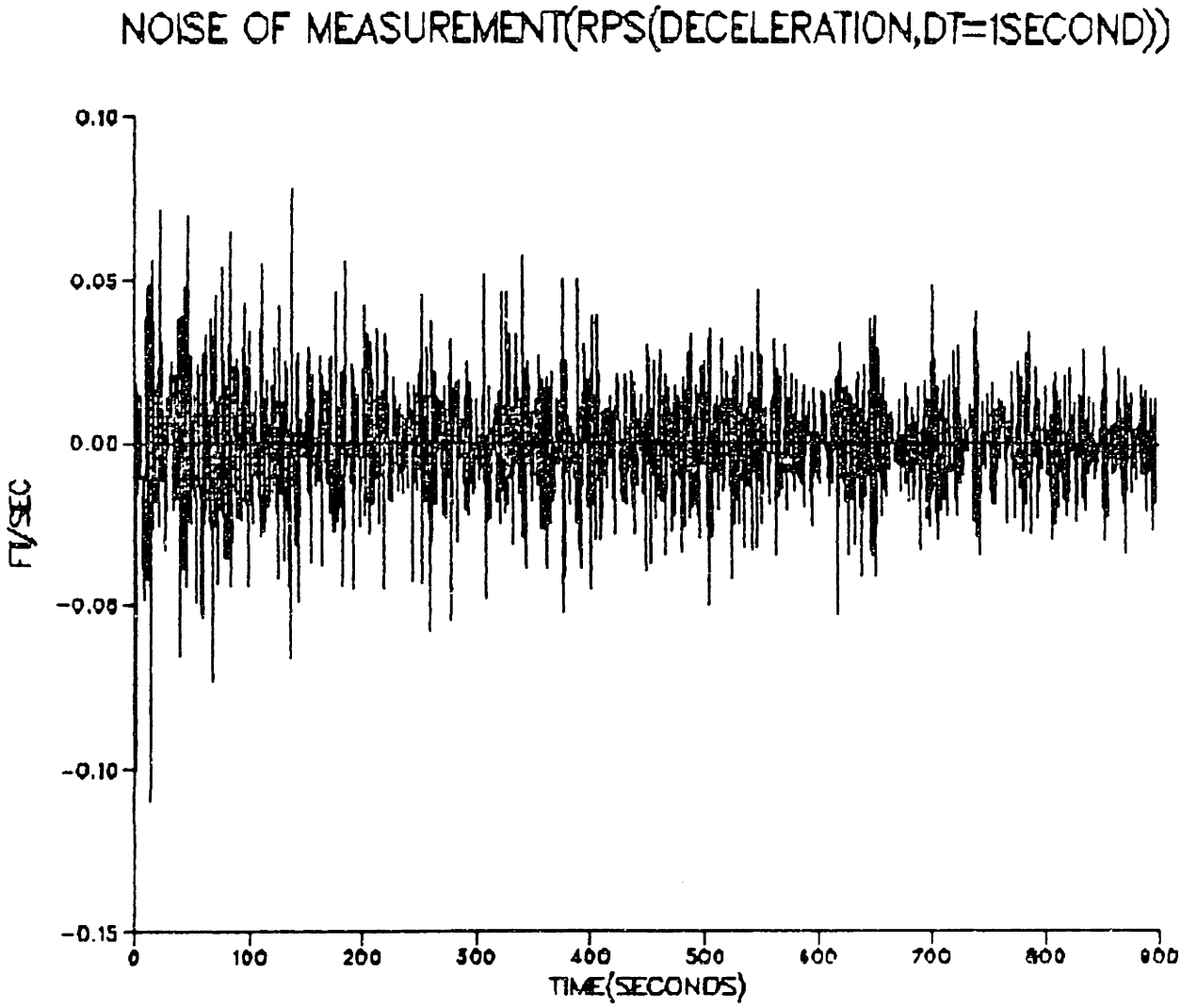

Figure C.3: Measurement Noise of n during Deceleration(1)

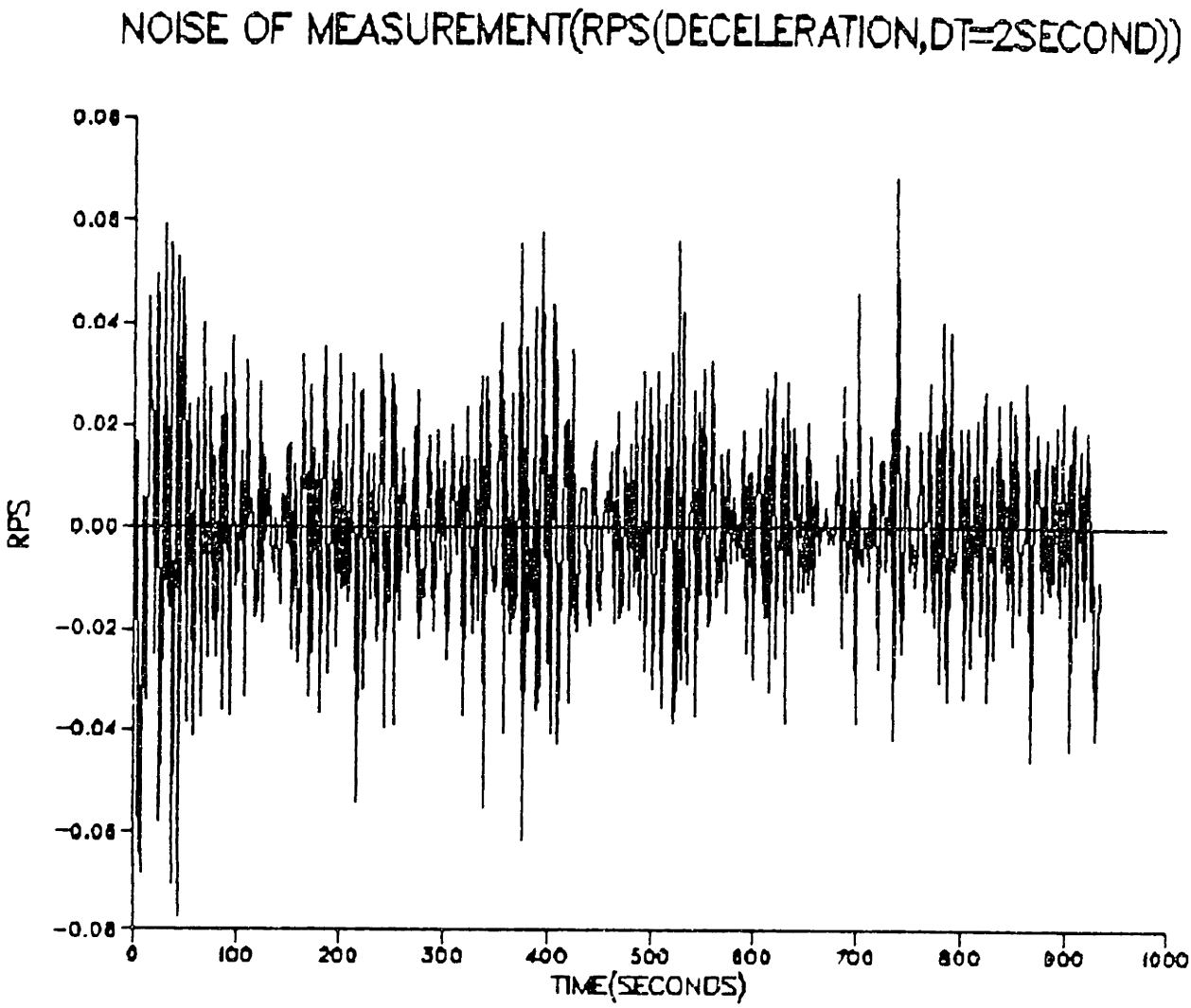

Figure C.4: Measurement Noise of n during Deceleration(2)

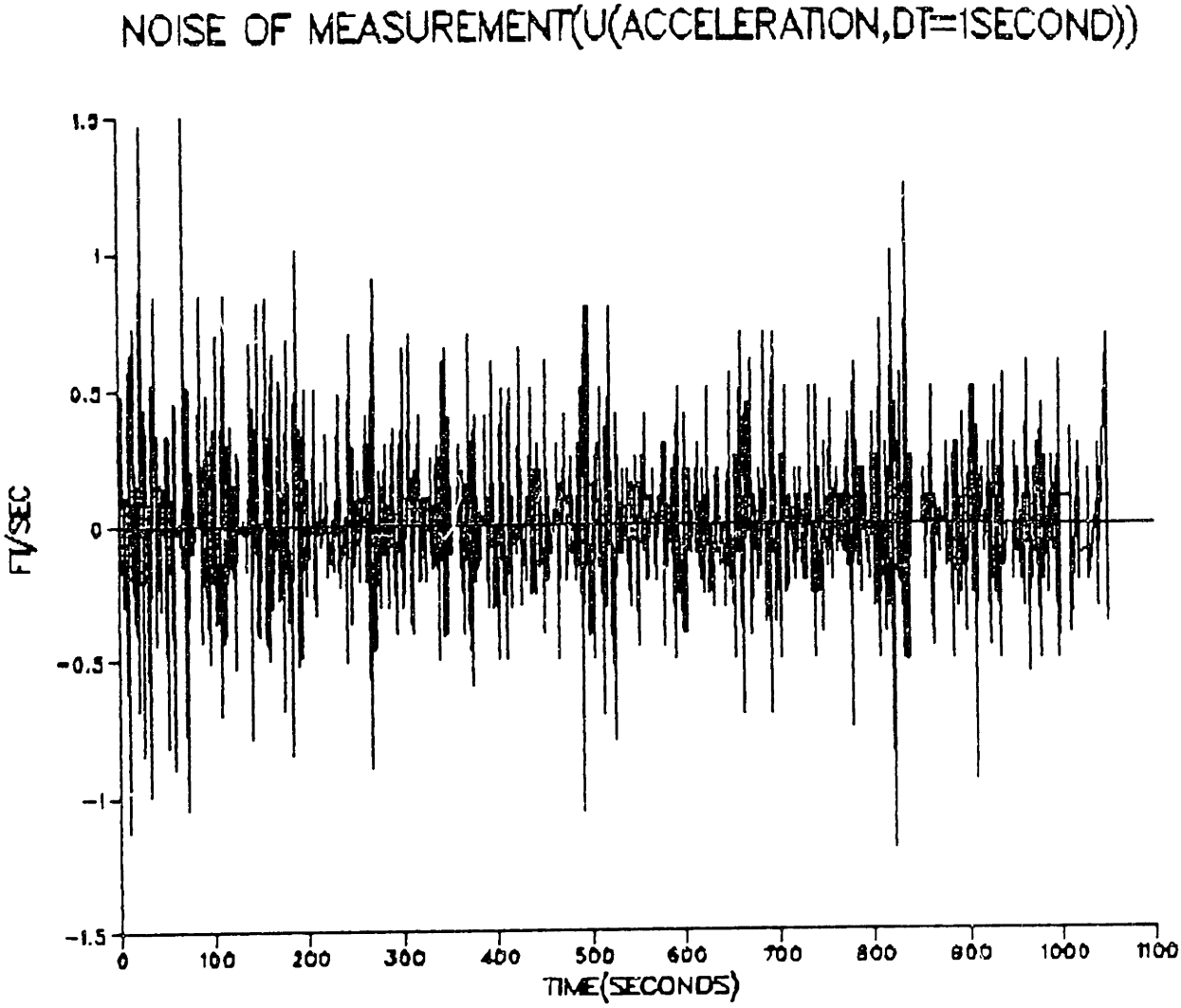

Figure C.5: Measurement Noise of u during Acceleration(1)

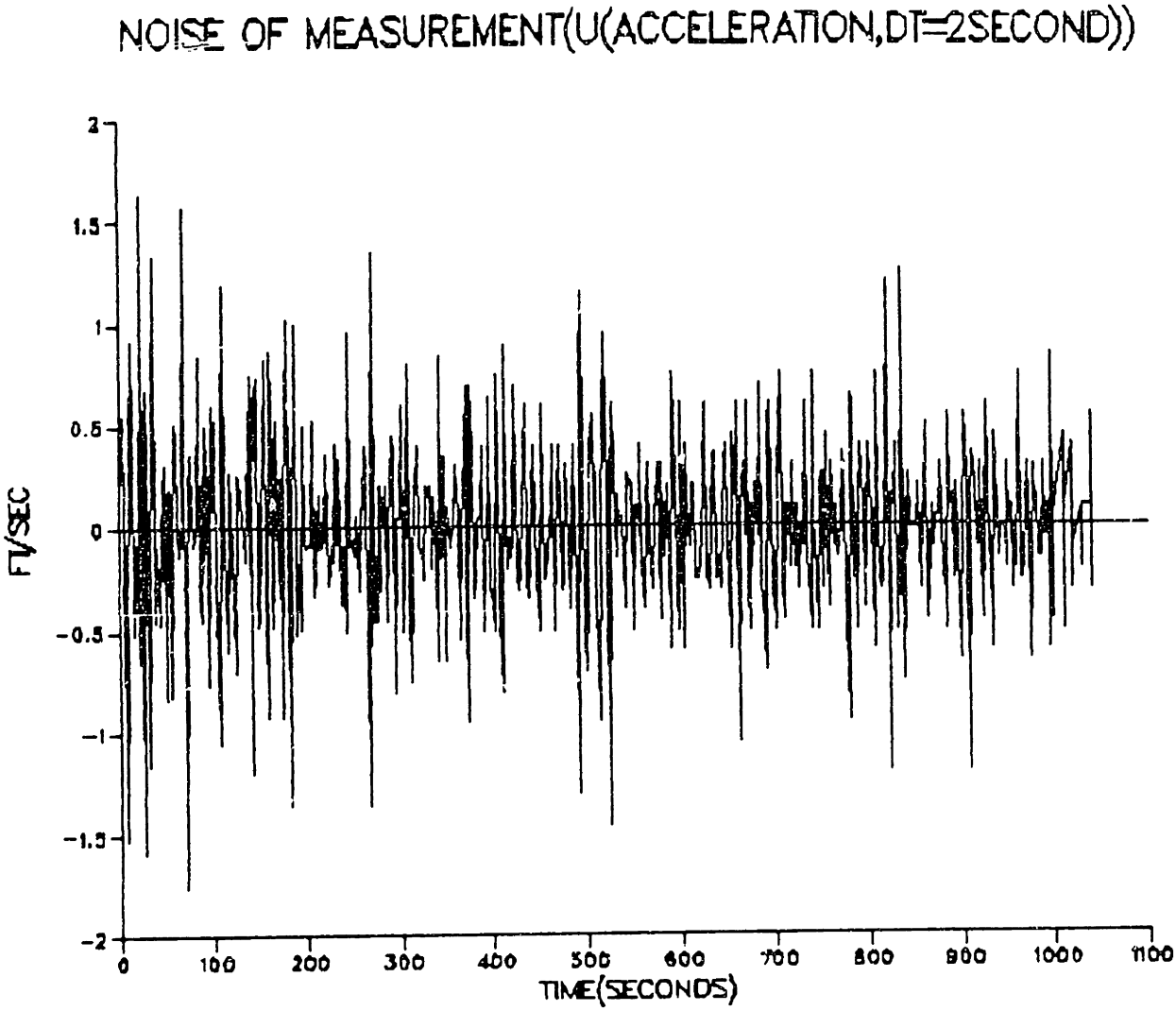

Figure C.6: Measurement Noise of u during Acceleration(2)

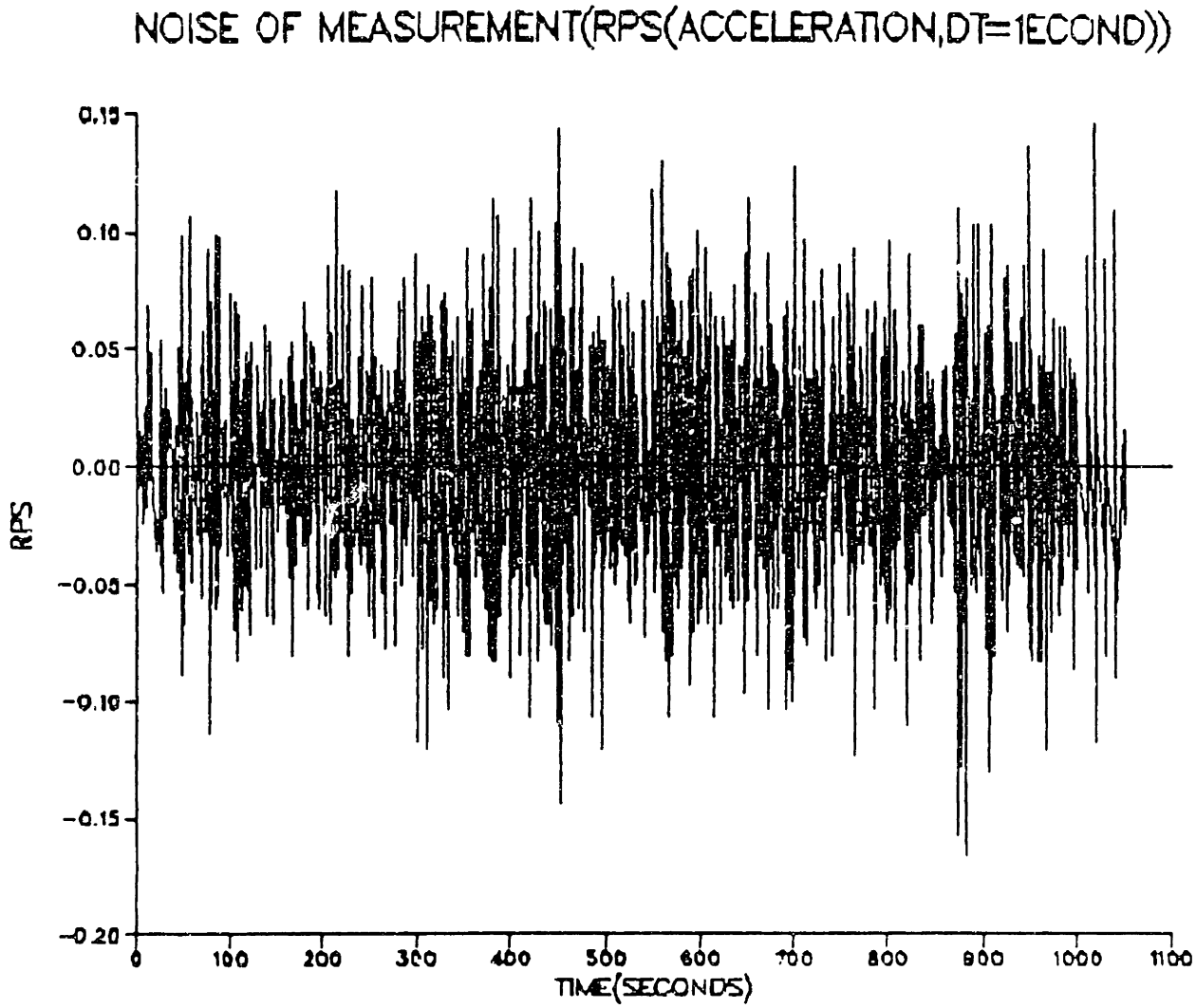

Figure C.7: Measurement Noise of n during Acceleration(1)

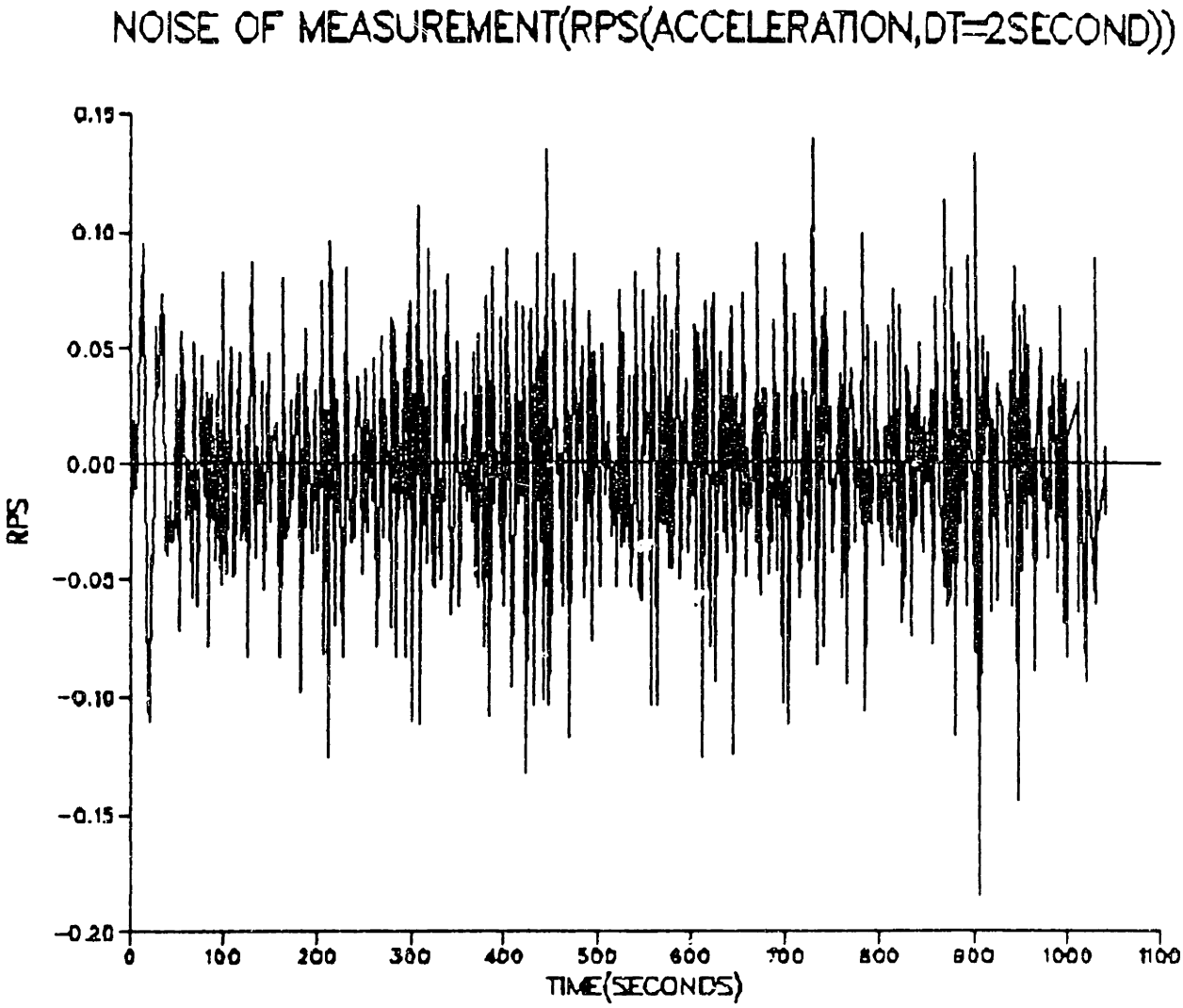

Figure C.8: Measurement Noise of n during Acceleration(2)

Bibliography

[1] K.J. Åstrom. *Intruduction to Stochastic Control Theory.* Academic Press, New York, 1970.

[2] I. H. Abbott and A.E. von Doenhoff. *Theory of Wing Section, Including a Summary of Airfoil data.* Dover, New York, 1959.

[3] M. A. Abkowitz. *Measurement of Hydrodynamic Characteristic from Ship Maneuvering Trials by System Identification.* it Transaction SNAME, pages 283–318, 1980.

[4] M. A. Abkowitz. *Thrust Deduction Factor during Acceleration.* Proc. ITTC, 18th, pages 151–152, 1987.

[5] G. E. P. Box and G. M. Jenkins. *Time-Series Analysis: forcasting and control.* Holden Day Inc., San Francisco, California, 1976.

[6] J. P. Comstock, editor. *Principle of Naval Architecture*, chapter VII, Resistance and Propulsion. The Society of Naval Architects and Marine Engineers, New York, 1967.

[7] A. Gelb. *Applied Optimal Estimation.* The M.I.T.Press, Cambridge Massachusetts, 1974.

[8] G. C. Goodwin. *Optimal Input Signals for Nonlinear-System Identification.* Proceeding IEE, 118:922–926, 1971.

[9] G.C. Goodwin and R.L. Payne. *Dynamic System Identificatrion: Experiment Design and Data Analysis.* Academic Press, New York, 1977.

[10] I. Gustavsson. *Survey of Applications of Identification in Chemical and Physical Processes.* Automatica, 11:3–24, 1975.

[11] T. Huang and N. Groves. *Effective Wake: Theory and Experiment.* Proc. Symp. Nav. Hydrodyn., 13th, pages 651–673, 1980.

[12] W. Y. Hwang. *Application of System Identification to Ship Maneuvering.* PhD thesis, M.I.T., 1980.

[13] J. E. Kerwin. *Marine Propellers.* Annual Review Fluid Mechanics, 18:367–403, 1986.

[14] F. L. Lewis. *Optimal Estimation with an Introduction to Stochastic Control Theory.* John Wiley & Sons, Inc., New York, 1986.

[15] G. Liu. *Identification of Ship Hydrodynamic Coefficients from Simple Trial Maneuvers during Regular Operations.* Master's thesis, M.I.T., 1984.

[16] L. Ljung. *System Identification: Theory for the User.* Prentice-Hall Inc., Englewood Cliffs, New Jersey, 1987.

[17] L. Ljung and Söderström. T. *Theory and Practice of Recursive Identification.* The MIT Press, Cambridge, Massachusetts, 1983.

[18] J. N. Newman. *Marine Hydrodynamics.* The M.I.T. press, Cambridge, Massachusetts, 1977.

[19] H. Schlichting and E. Truckenbrodt. *Aerodynamics of the Airplane.* McGraw-Hill International Book Company, New York, 1979.

[20] T. Söderström and P. Stoica. *Instrumental Variable Methods for Systems Identificaton.* Springer-Verlag, Berlin Heidelberg, New York, Tokyo, 1983.

[21] J.D. van Manen W.P.A. van Lammeren and M.W.C. Oosterveld. *The Wageningen B-Screw Series.* Transaction SNAME, pages 269–317, 1969.

[22] P. Young. *Recursive Estimation and Time-Series Analysis, An Introduction.* Springer-Verlag, Berlin Heidelberg New York Tokyo, 1984.

[23] M. B. Zarrop. *Optimal Experiment Design for Dynamic Systems Identificaton.* Springer-Verlag, Berlin Heidelberg, New York, Tokyo, 1974.

[24] Sheng Zhen-bang. *Ship Propulsion.* Beijing Science and Education, Beijing, 1963.